Title
Genetic and Cell Biological Dissection of Alpha-Synuclein Trafficking Defects in Yeast and Mammalian Cells

Author
Lee, Ching Fern Sue-Ann

Publication Date
2010

Peer reviewed|Thesis/dissertation

GENETIC AND CELL BIOLOGICAL DISSECTION OF ALPHA-SYNUCLEIN TRAFFICKING DEFECTS IN YEAST AND MAMMALIAN CELLS

by

CHING FERN SUE-ANN LEE

DISSERTATION

Submitted in partial satisfaction of the requirements for the degree of

DOCTOR OF PHILOSOPHY

in

BIOMEDICAL SCIENCES

in the

GRADUATE DIVISION

of the

UNIVERSITY OF CALIFORNIA, SAN FRANCISCO

Dedication

To my parents Lee Lip Nyean and Tan Geok Bee:
Thank you for everything.

ACKNOWLEDMENTS

I would like to give thanks to everybody who helped me along the long winding road of graduate school and made the journey so much better than the ordeal it could have been.

I really appreciate the freedom and independence in carrying out my research given to me by my supervisor, Dr. Paul Muchowski, and whose guidance and advice was never more than an open office door away. His enthusiasm for science and breadth of knowledge will always be inspirational to me. If not for his encouragement and insistence on learning to multitask, doubtless the last leg of this journey would have been infinitely more stressful.

A very special thank you goes to Dr. Vicente Sancenon, whom I had the good fortune to have worked closely with the first few years of graduate school. I will forever be grateful for his patience, mentorship and unstinting support all these years, and for the fond memories of our many impromptu language lessons.

I would also like to thank the members of my lab for creating such a fun, friendly environment to work in. Truly, the lab was my home away from home and I will always remember the hilarious lunch time conversations, Girls' Nights Out and the meaningful one on one interactions.

I am indebted to my friends Dr. Thomas Lie and Dr. Hankiat Ho for their generosity and kindness when I was trying to find my footing at the start of graduate school, and for their readiness to lend a listening ear or helping hand.

ACKNOWLEDMENTS

I would like to thank the other members of my committee, Dr. Robert Edwards, and Dr. Robert Nussbaum for the assistance they provided at all levels of the research project. Additional thanks go to Dr. Kurt Thorn and Alice Thwin of the Nikon imaging center at UCSF for their expertise and help in my microscopy studies. My gratitude also goes out to Lisa Magargal, Monique Piazza and the BMS administrative staff for their ready help with the administrative aspects of graduate school.

Last, but most definitely nowhere near the least, I would like to thank my family for the support they provided me through my entire life, and my parents in particular for putting up with some truly spectacular venting of frustration from time to time. I am eternally grateful that they kept pushing me to fulfill my greatest potential despite my grumblings and declarations of surrender.

In conclusion, I would like to thank the Agency for Science, Technology and Research board in Singapore for giving me this immense opportunity to pursue my undergraduate and graduate studies in the United States.

Genetic and cell biological dissection of alpha-synuclein trafficking defects in yeast and mammalian cells

Ching Fern S. Lee

α-Synuclein, a major player in Parkinson's disease pathogenesis, is thought to impair vesicle trafficking as a toxic gain of function through aggregation. Genetic screens for modifiers of α-synuclein toxicity have overwhelmingly identified a significant subset of genes involved in vesicle trafficking. While recent studies in yeast have shown that at toxic levels α-synuclein disrupts Rab homeostasis, causing an initial ER-to-Golgi block that precedes a generalized trafficking collapse, further studies in mammalian systems prove that several rabs downstream of ER-Golgi trafficking to rescue α-synuclein toxicity. Here, we show that constitutive expression of αSyn in yeast causes the accumulation of endocytic vesicles and impairs late-exocytic, early-endocytic and/or recycling trafficking and further, that this vesicle trafficking impairment can be attenuated by yeast casein kinase 1 and the small rab protein Ypt1p. Our work in mammalian cell culture models of Parkinson's disease demonstrate the ability of the human homologues of vacuolar protein sorting genes involved in endosomal transport to modulate the toxicity of α-synuclein. Furthermore, our findings suggest that α-synuclein-induced cytotoxicity is due to impairment in the endosomal trafficking pathway of the SH-SY5Y cells. Taken together, our results provide evidence of the potential contribution of endosome anomalies to the pathogenesis of Parkinson's disease.

CONTRIBUTIONS

Chapter 2 was submitted for publication to the journal *Human Molecular Genetics* entitled "Genetic Context-Dependent Modulation of α-synuclein Toxicity and Trafficking Defects by Phosphorylation of Serine 129" by Vicente Sancenon, Sue-Ann Lee, Christina Patrick, Janice Griffith, Amy Paulino, Angela Sia, Tiago F. Outeiro, Fulvio Reggiori, Eliezer Masliah, and Paul J. Muchowski. Figures 1 and 3H were contributed by Ching Fern S. Lee

The work and accompany figures in chapter 3 was submitted for publication to the *Journal of Neuroscience* entitled "Endosomal trafficking genes modulate α-synuclein toxicity in mammalian cells" by Sue-Ann Lee, Gaia Skibinski, Leonidas Stefanis, Guillermo Yudowski and Paul J. Muchowski. Figures 1-5, 7-8 and 9b-d were contributed by Ching Fern S. Lee

Aside from these items, the work presented in this thesis was conducted by its author, Ching Fern S. Lee, under the supervision of Dr. Paul J. Muchowski.

TABLE OF CONTENTS

CHAPTERS

LIST OF TABLES

Chapter 2

Chapter 3

LIST OF FIGURES

Chapter 2

LIST OF FIGURES

Chapter 3

CHAPTER 1 – GENERAL INTRODUCTION

GENERAL INTRODUCTION

Parkinson's disease (PD)

PD was first described by the English apocathery James Parkinson in his 1817 work “An essay on the shaking palsy”. A progressive neurodegenerative disorder, PD is second only to Alzheimer’s disease in causing neurodegeneration, and is estimated to affect 1% of the population over 65 years of age (de Rijk et al., 2000). Patients with PD are clinically diagnosed by symptoms such as muscle rigidity, and resting tremors. In advanced stages of the disease, PD is also associated with cognitive impairment. The clinical symptoms are pathologically correlated to the loss of neurons in the substantia nigra pars compacta, a brain region involved in the production of movement, as well as progressive loss of the neurotransmitter dopamine (Hornykiewicz, 1998). This observation led to the use of the dopamine precursor $_{L}$-dihydroxyphenylalanine (L-DOPA) as a therapy to alleviate symptoms associated with PD. However, L-DOPA does not stop progressive neurodegeneration in patients with PD (Tintner et al., 2002) and despite the various drug therapies involving dopamine agonists, surgical treatments and physical therapies, no cure yet exists for this disease (Olanow, 2004).

Although the etiology of PD remains unclear, age and exposure to neurotoxins are established risk factors (Vanitallie, 2008) while nicotine and caffeine are purportedly protective against the disease (Ross et al., 2001). Until recently, PD was considered a non-genetic disease as the vast majority of cases are idiopathic. It has since been shown that multiple gene loci and genes are associated with both autosomal dominant and recessive familial forms of the disease. In particular, missense mutations in one of these associated genes, SNCA, results in A53T, A30P or E46K substitutions in the α-synuclein

protein, each contributing to early-onset inherited PD (Polymeropoulos et al., 1997; Kruger et al., 1998; Zarranz et al., 2004). Multiplications of the wild-type SNCA gene as well as polymorphisms and variations in the length of the SNCA promoter region (Maraganore et al., 2006; Myhre et al., 2008; Sotiriou et al., 2009) also cause autosomal dominant PD, implying that increased concentrations of α-synuclein are sufficient to cause PD (Singleton et al., 2003). The SNCA gene product α-synuclein also plays a central role in the pathophysiology of idiopathic PD. Postmortem, diagnosis of PD is confirmed by the presence of Lewy bodies and Lewy neurites in the remaining surviving neurons. Lewy Bodies are intracellular inclusions of lipids and proteins, predominantly comprised of α-synuclein (Spillantini et al., 1997; Kuusisto et al., 2003).

The SNCA gene product α-synuclein (αSYN)

αSYN is a relatively small, 140 amino acid protein that is ubiquitously expressed in the brain and enriched in presynaptic nerve terminals (Jakes et al., 1994). In solution, it is a 'natively unfolded' protein with little secondary structure that takes on an amphipathic α-helical structure in the presence of phospholipids (Chandra et al., 2003). Over-expression of wild-type and mutant forms of αSYN in mice leads to aggregation of αSYN in brainstem and spinal cord neurons and motor phenotypes (Masliah et al., 2000; van der Putten et al., 2000; Giasson et al., 2002). On the other hand, αSYN knock-out mice do not exhibit impaired survival or brain function, nor is αSYN required for the basic neurotransmitter release machinery (Chandra et al., 2004).

Although the exact physiological function of αSYN remains undetermined, it has been implicated in the maintenance of synaptic homeostasis and plasticity. In addition, it can also reduce hydrolysis of lipid droplets (Cole et al., 2002), as well as regulate the size of pre-synaptic vesicular pools in cell culture (Murphy et al., 2000). Analysis of a mouse model where the αSYN gene was deleted suggests that αSYN is necessary for the regulation of pre-synaptic dopamine neurotransmission (Cabin et al., 2002). In transgenic mice, αSYN appears to act as a molecular chaperone, assisting in the folding and refolding of Synaptic proteins (Chandra et al., 2005). αSYN has been linked to learning, development and plasticity (di Rosa et al., 2003; Sidhu et al., 2004), and most likely plays a role in synaptic vesicle recycling (Ben Gedalya et al., 2009; Nemani et al., 2010).

Several disease mechanisms that are not necessarily mutually exclusive have been suggested: first, aggregation of αSYN into a toxic oligomeric/protofibrillar/fibrillar species perturbs the structure and/or function of downstream targets; second, packaging and secretion of dopamine is disrupted; third, the ubiquitin-proteasome system is impaired; fourth, molecular chaperone function is impaired; fifth, mitochondrial function is impaired and/or oxidative stress is incurred, which may be related to impairment in the packaging of dopamine; and sixth, intracellular trafficking pathways and synaptic transmission are impaired (Goldberg et al., 2000; Goedert, 2001; Lotharius et al., 2002). Fragmentation of the Golgi apparatus has been observed in PD brains (Fujita et al., 2006) and in cells overexpressing αSYN (Gosavi et al., 2002), which is thought to be a specific consequence of toxic pre-fibrillar αSYN aggregation. αSYN is also suggested to impair

ER-Golgi trafficking (Cooper et al., 2006). Additionally, redistribution of Synaptic SNARE proteins in αSYN transgenic mice and reduction in dopamine release has been shown to correlate with αSYN aggregation and locomotive defects (Garcia-Reitböck et al., 2010) while another study has demonstrated a loss of presynaptic proteins regulating endo- and exocytosis in αSYN transgenic mice and PD brains that is correlated with synaptic pathology (Scott et al., 2010).

In vitro studies suggest that αSYN protofibrils can bind and permeabilize acidic phospholipid vesicles (Volles et al., 2001; 2002). It has been proposed that this may lead to defective sequestration of dopamine into vesicles and subsequent generation of reactive oxygen species in the cytoplasm which contribute to neuronal dysfunction and cell death (Lotharius et al., 2002). Recently, αSYN has been found in human plasma and cerebral spinal fluid and has been shown to be secreted into the medium of cultured neuronal cells (El-Agnaf et al., 2003, 2006; Lee et al., 2005), suggesting that αSYN toxicity may be propagated through the extracellular matrix to neighboring cells.

Yeast and mammalian cell culture models of PD

If PD does indeed involve multiple disease mechanisms, it will be crucial to understand the genes and cellular pathways that are of primary significance for neuronal dysfunction and cell death from a temporal and spatial sense. The baker's yeast *Saccharomyces cerevisiae* is a powerful model organism to study the function and disease-causing attributes of αSYN in a PD context for two reasons. First, basic cellular mechanisms,

such as replication, recombination, cell division, protein folding, intracellular transport and metabolism are well conserved between yeast and mammals. Secondly, genetically engineered yeast cells over-expressing heterologous human αSYN that were generated by Outeiro et al. (2003) to study the mechanisms of αSYN toxicity recapitulate many features observed in PD, including the formation of inclusion bodies, disruption of vesicle trafficking, impairment of proteasomal function, and dose-dependent toxicity. Third, genetic manipulations can be rapidly performed in the organism. Various yeast genetic screens have shown that αSYN toxicity is exacerbated or alleviated in different yeast gene deletion strains. Among the genes that enhance or suppress αSYN toxicity when deleted, a significant number was clustered in the functionally related categories of lipid metabolism and vesicle trafficking, and a high percentage of those genes have human orthologs (Willingham et al., 2003). By conducting studies in yeast, toxicity mechanisms that are relevant to PD and potential disease-modulating proteins might be uncovered that could contribute to the development of therapies for PD.

It must be acknowledged that yeast as a model system for studies relating to neurodegeneration has obvious limitations, for example, some genes important for modulating neurodegeneration may not be present in the yeast genome (such as those that encode caspases involved in apoptosis or growth factors). Thus, the validity of using yeast as a model organism for studying αSYN dependent pathogenic mechanisms of PD will only be established by performing complementary approaches in more physiologically relevant models of neurodegeneration. Human cell lines also allow for

direct investigation of PD pathophysiology in a relatively short amount of time and labor. Although genetic manipulation is more limited than in yeast, the expression of specific genes can be readily suppressed or proteins of interest over-expressed in cell line culture systems, allowing for close study of their function. Furthermore, techniques for high-throughput screening can also be adapted for cell lines to develop novel therapeutic compounds.

As PD is characterized by the specific loss of dopaminergic neurons in the substantia nigra, it is unsurprising that the human neuroblastoma SH-SY5Y cell line, which has moderate levels of dopamine beta hydroxylase activity, is widely used as a neurotoxicity model for PD. When differentiated with retinoic acid, the SH-SY5Y cells acquire a neuronal phenotype and express high levels of the vesicular monoamine transporter 2 (Presgraves et al., 2004). Importantly, stable overexpression of wild-type αSYN in this cell line induces gradual degeneration of differentiated cells (Vekrellis et al., 2009) which capitulates the progressive, age-related onset of sporadic PD. Thus, this cell line is a useful tool to dissect cell autonomous pathways that might regulate toxicity induced by elevations of WT αSYN. Results from studies in this cell line can be subsequently validated in *in vivo* and more physiological relevant models of PD.

The importance of vesicle trafficking pathways in αSYN-induced toxicity has been demonstrated by identification of vesicle trafficking as a major category of genes that modulate αSYN toxicity by multiple genetic screens. Furthermore, overexpression of small Rab GTPase proteins (Cooper et al., 2006; Gitler et al., 2008) and hVps41, which

are involved in vesicle trafficking, have shown rescue αSYN toxicity. However, the site(s) of action impaired by αSYN toxicity and the mechanism by which these genetic modifiers alter αSYN toxicity remain poorly understood. We have sought to bridge this knowledge gap through a systematic analysis of genetic manipulation of several vesicle trafficking genetic modifiers on αSYN-induced toxicity and vesicle trafficking defects in the SH-SY5Y cell line.

CHAPTER 2 – GENETIC CONTEXT-DEPENDENT MODULATION OF α-SYNUCLEIN TOXICITY AND TRAFFICKING DEFECTS BY PHOSPHORYLATION OF SERINE 129

CHAPTER 2 – GENETIC CONTEXT-DEPENDENT MODULATION OF α-SYNUCLEIN TOXICITY AND TRAFFICKING DEFECTS BY PHOSPHORYLATION OF SERINE 129

ABSTRACT

The aggregation of α-Synuclein (αSyn) is a neuropathological hallmark of Parkinson's disease and other Synucleinopathies. In the aggregates, αSyn is extensively phosphorylated, predominantly at serine 129 (S129). Recent studies in yeast have shown that, at toxic levels, αSyn disrupts Rab homeostasis, causing an initial ER-to-Golgi block that precedes a generalized trafficking collapse. However, whether αSYN phosphorylation modulates trafficking defects has not been evaluated. Here, we show that constitutive expression of αSyn in yeast impairs late-exocytic, early-endocytic and/or recycling trafficking. Although members of the casein kinase I (CKI) family phosphorylate partially αSyn at S129, they attenuate αSYN toxicity and trafficking defects by a phosphorylation-independent mechanism. However, phosphorylation of S129 modulates αSyn toxicity and trafficking defects in a genetic background-dependent manner. Abnormal endosome morphology, increased levels of the endosome marker Rab5, and co-localization of mammalian CKI with αSYN aggregates are observed in brain sections from αSYN-overexpressing mice and human synucleinopathies. Our results provide evidence of the potential contribution of endosome anomalies and CKI dysfunction to the pathogenesis of synucleinopathies.

INTRODUCTION

Synucleinopathies comprise a subset of neurodegenerative disorders characterized by the accumulation of cytoplasmic inclusions, or Lewy bodies, that contain the protein α-

synuclein (αSyn) in selected populations of neurons [Parkinson's disease (PD) and dementia with Lewy bodies (DLB)] or in glia [multiple system atrophy (MSA)]. Although the etiology of these disorders is unknown, the discovery of mutations in the α Syn gene (*SNCA*) that cause PD implicates αSYN in the pathogenesis of synucleinopathies (Spillantini et al., 2000).

The precise cellular function of αSyn is unclear. αSyn is a presynaptic protein that stimulates the formation of synaptic vesicles and neuronal transmission *in vitro* and *in vivo* (Cabin et al., 2002; Liu et al., 2004; Chandra et al., 2005; Ben Gedalya et al., 2010). Importantly, the discovery that multiplications of the αSYN locus cause PD suggests that neurotoxicity is a quantitative trait of αSyn (Singleton et al., 2003). Therefore, overexpression of αSyn has been used to study the molecular mechanisms of disease pathogenesis in a variety of model systems. In addition to other phenotypes, overexpression of αSyn interferes with vesicular transport in cell-based and *in vitro* models, and in patients with PD (Gosavi et al., 2002; Fujita et al., 2006; Larsen et al., 2006; Lee et al., 2006; Thayanidhi et al., 2010). Yeast has proven useful as model to reconstitute αSyn dose-dependent cellular toxicity and trafficking defects. αSyn was shown to block ER-to-Golgi transport (Cooper et al., 2006) and other intracellular trafficking pathways (Gitler et al., 2008; Zabrocki et al., 2008) at toxic concentrations. These trafficking failures correlate with an accumulation of intracellular vesicles (Gitler et al., 2008; Soper et al., 2008). Interestingly, αSyn toxicity can be modulated by

manipulating the expression of genes involved in cellular trafficking (Willingham et al., 2003; Cooper et al, 2006; Flower et al., 2007; Kuwahara et al., 2008; Liang et al., 2008; van Ham et al., 2008).

Posttranslational modifications of αSyn *in vivo* may play an important role in the pathogenesis of PD and other synucleinopathies. The most abundant modification of α Syn in Lewy bodies is the phosphorylation of serine 129 (S129) (Fujiwara et al., 2002; Waxman et al., 2008) This residue is located within a casein kinase (CK) consensus recognition site and is phosphorylated by yeast and mammalian CKs and other kinases in cellular and animal models. However, the relevance of S129 phosphorylation for pathogenesis remains controversial. Studies in rats and flies argue for protective, innocuous and detrimental effects of phosphorylation on neurodegeneration (Chen et al., 2005; Gorbatyuk et al., 2008; Azeredo da Silveira et al., 2009; McFarland et al., 2009). Moreover, whether phosphorylation influences αSyn-induced intracellular trafficking defects has not been evaluated.

In this study, we show that late-exocytic, early-endocytic and/or recycling transport of PM proteins is altered by constitutive expression of αSyn in yeast. Yeast casein kinase 1 (Yck1) attenuates this defect by a phosphorylation-independent mechanism. However, blocking αSyn phosphorylation dramatically enhances αSyn toxicity and trafficking defects in a strain-specific manner, suggesting that the genetic context determines the

sensitivity to changes in the phosphorylation state of αSyn. We also report early endosome alterations and co-localization of mammalian CKIδ with αSyn-positive inclusions in mouse models and human synucleinopathy brains, providing evidence that endosome anomalies and CKIδ sequestration may contribute to the pathogenesis of synucleinopathies.

RESULTS

Overexpression of αSyn Causes Vesicles to Accumulate in Yeast

Wild-type (WT) αSyn-GFP ectopically expressed in yeast from the galactose-inducible promoter of the *GAL1* gene accumulates in intracellular inclusions (Outeiro et al., 2003). The earliest inclusions form at 3.5 h of induction in the cell periphery and subsequently spread towards the cell interior (Gitler et al., 2008). Immuno-electron microscopy (IEM) studies revealed that the inclusions observed by fluorescence microscopy are αSYN-positive clusters of vesicles (Gitler et al., 2008; Soper et al., 2008). To further investigate the composition of these clusters, we examined the ultrastructure and the subcellular localization of αSyn by IEM over time in yeast expressing αSyn-GFP by the *GAL1* promoter. Within the first 4 h of induction, αSyn-GFP immunoreactivity was almost exclusively observed at the plasma membrane (PM) (data not shown). At 6 h, we observed small clusters of vesicles in the vicinity of the PM (Fig. S1A and B). The vesicles were homogeneous in size (~20–40 nm in diameter), morphology and electron density, suggesting a common origin. At 12 h, the clusters were enlarged, and their

vesicular content became heterogeneous in morphology and size (up to ~100 nm in diameter), consistently with a widespread trafficking defect (Gitler et al., 2008) (Fig. S1C and D). Notably, αSyn-GFP immuno-reactivity was detected on the surface of the vesicles at 6 h and 12 h, in agreement with previous reports showing that the αSYN inclusions observed by fluorescence microscopy correspond to these clusters.

Constitutive αSyn Expression Disrupts Late-Exocytic, Early-Endocytic and/or Recycling Trafficking in Yeast

Although the Lindquist group initially showed that αSyn-inclusions co-localize with Ypt1, an endoplasmic reticulum (ER)-to-Golgi trafficking marker (Cooper et al., 2006), a follow on study by the same group showed co-localization with diverse trafficking markers, including Ypt31 (late Golgi), Sec4 (secretory vesicles-to-PM), Ypt6 (endosome-to-Golgi), Vps21 and Ypt52 [early endosome (EE)-to-late endosome (LE)], and Ypt7 (LE-to-vacuole), indicating that αSyn disrupts multiple trafficking route (Gitler et al., 2008). To further investigate the origin of the accumulated vesicles, we evaluated the effect of constitutively expressing untagged αSyn from the promoter of the glycerol-3-phosphate dehydrogenase (*GPD1*) in a 2 micron plasmid on the steady-state localization of a series of GFP-tagged protein markers of intracellular trafficking (Lewis et al., 2000; Reggiori et al., 2000; 2001) (Fig. 1A). GFP-Snc1, a transmembrane exocytic SNARE (soluble N-ethylmaleimide-sensitive factor attachment protein receptor), is targeted to the PM through the secretory pathway and subsequently recycled for re-use via EE and the

Golgi. Ste2-GFP, the transmembrane α-factor pheromone receptor, and GFP-Snc1-Sso1, an engineered variant of GFP-Snc1 containing a transmembrane domain of the SNARE Sso1, are targeted to the PM through the secretory pathway and, subsequently, after endocytosis, to the vacuolar lumen via EE and LE. The SNARE GFP-Pep12 is targeted to the membrane of the prevacuolar complex via the carboxypeptidase Y (CPY) bioSynthetic pathway. The transmembrane proteins GFP-Phm5 and Sna3-GFP are targeted to the vacuolar lumen via the CPY pathway by ubiquitin-dependent and independent mechanisms, respectively. GFP-Nyv1-Snc1, an engineered variant of the SNARE Nyv1 containing the transmembrane domain of Snc1, is targeted to the vacuole membrane via the alkaline phosphatase (ALP) pathway.

To quantitatively assess the effect of αSyn on trafficking, we counted the percentage of cells exhibiting a mislocalization phenotype, considered as any anomaly in the localization pattern of a trafficking marker that differs from the pattern displayed by the majority (>70%) of cells not expressing αSyn. Constitutive expression of untagged αSyn from the *GPD1* promoter selectively altered the targeting of GFP-Snc1 to the PM and of GFP-Snc1-Sso1 and Ste2-GFP to the vacuole lumen in more than 50% of the cells, but not of GFP-Pep12 and GFP-Nyv1-Snc1 to the vacuole membrane or GFP-Phm5 and Sna3-GFP to the vacuole lumen (Fig. 1B and C). The trafficking routes that are unique to the protein markers perturbed by αSyn include Golgi-to-PM, PM-to-endosome and endosome-to-Golgi. These observations suggest that, at the steady state expression levels

achieved by the *GPD1* promoter, αSyn impairs the delivery of proteins to the PM from the Golgi and/or their subsequent endocytic and recycling trafficking. In contrast, other markers that use the ER-to-Golgi pathway but bypass the PM (GFP-Pep12, GFP-Phm5, Sna3-GFP and GFP-Nyv1-Snc1) do not exhibit localization defects in αSyn expressing cells, suggesting that ER-to-Golgi trafficking is not impaired.

To confirm this hypothesis, we analyzed the subcellular distribution of αSyn and the exocytic SNARE Snc1 by co-IEM (Fig. 2). Consistent with the fluorescence microscopy studies, Snc1 immunoreactivity was detected in the αSyn-positive vesicular clusters, confirming anomalies in PM delivery, endocytic and/or recycling trafficking of Snc1. As αSYN has been reported to block the delivery of the dye FM 4-64 to the vacuole, but not its uptake (Outeiro et al., 2003), we propose that αSyn impairs post-endocytic and/or recycling trafficking that follows vesicle budding from the plasma membrane (Fig. 1A).

To gain further insights in the trafficking steps blocked by αSyn, we investigated the subcellular distribution of the trafficking marker Snc1-Sso1 and the dye FM 4-64 in two subsets of yeast trafficking mutants (Fig. S2A). First, in loss-off-function deletion mutants defective in intra-Golgi (*ypt31*Δ), endocytic (*end3*Δ, *ypt51*Δ), recycling (*ypt31*Δ), endosome-to-Golgi (*vps35*Δ), and endosome-to-vacuole (*vps23*Δ, *did3*Δ) transport, endosome and vacuole homotypic fusion (*ypt7*Δ) and actin remodeling (*sac6*Δ). Second, in temperature sensitive secretory mutants defective in ER-to-Golgi (*sec7-4*, *sec18-1*),

intra-Golgi (*sec7-4*), and Golgi-to-plasma membrane (*sec1-1*) transport at permissive (RT) and non-permissive (37ºC) temperature. Among all the mutants studied *did3*Δ and *vps23*Δ appear to mimic more closely the mislocalization pattern of Snc1-Sso1 caused by αSyn, suggesting a late endocytic defect (Fig. S2B and C). However, the mislocalization phenotype in αSyn expressing cells seems to rather be unique, suggesting that multiple trafficking steps are affected, in agreement with a previous study (Gitler et al., 2008).

Yck1 Attenuates αSyn-Induced Toxicity and Trafficking Defects through a Phosphorylation-Independent Mechanism

There is increasing evidence that αSyn disrupts endocytic trafficking. For example, αSyn overexpression perturbs the subcellular distribution of the endocytic tracker FM 4-64 (Outeiro et al., 2003) and diverse endocytic protein markers (Gitler et al., 2008). The endocytic pathway is more vulnerable to insults in αSyn-transgenic (tg) worms (Kuwahara et al., 2008). Therefore, we reasoned that genes regulating endocytosis might contribute to modulate αSyn-induced growth defects and vesicle accumulations. To test this hypothesis, we assessed whether Yck1 and Yck2, two functionally redundant PM-associated members of the CKI protein family that promote the endocytosis of PM proteins (Marcha et al., 2000; 2002), modulate αSyn toxicity. For these studies, we generated a yeast strain carrying two stably integrated copies of the human αSyn gene fused to GFP under the control of the *GAL1* inducible promoter (which allows to control for gene-specific effects in non-inducing conditions) in the BY4741 strain (Table I). As positive and negative controls, we deleted the genes *TLG2*, a known αSyn toxicity

modifier encoding a SNARE required for the targeting of Yck2 to the PM (Panek et al., 2000; Willingham et al., 2003), and *SPO14*, a non modifier gene encoding a yeast phospholipase D (Rose et al., 1995), respectively. In contrast to a previous study (Zabrocki et al., 2008), we found that deletion of *YCK1* and *YCK2* genes significantly increased the growth defect caused by αSyn (Fig. 3A and S3).

To confirm these genetic interactions, we reasoned that pharmacologic inhibition of CKI activity in yeast expressing αSyn should phenocopy the *yck1*Δ or *yck2*Δ alleles, and this effect should be more dramatic in yeast lacking either one of the two functionally redundant enzymes. Therefore, we tested the effect of the CKI-specific inhibitor D4476 on the viability of cells expressing αSyn. To make cells more sensitive to the compound, we knocked out the multidrug resistance gene *PDR1* in all the strains tested. Although *YCK1* or *YCK2* are not individually essential for cell growth, deletion of both genes results in growth arrest. As expected, the CKI-specific inhibitor D4476 decreased yeast growth in a concentration-dependent manner. Notably, this effect was more pronounced in cells expressing αSyn and was significantly increased in cells lacking one of the two redundant enzymes (Fig. S4), suggesting that CKI activity counteracts the detrimental effects of αSyn overload.

To determine whether the increase in growth inhibition caused by loss of CKI function correlates with increased trafficking defects, we studied the localization of mCherry

tagged Snc1-Sso1 in WT and *yck1*Δ cells carrying two o zero integrated copies of the galactose inducible αSyn-GFP gene. In cells not expressing αSyn, mCherry-Snc1-Sso1 is correctly delivered to the vacuolar lumen (Fig. 3E). In contrast, expression of αSyn-GFP prevented the proper targeting of Snc1-Sso1 in ~30% of WT cells (Fig. 3E and F). Note that the defect in these cells is less marked than in cells constitutively expressing untagged αSyn from a 2 micron plasmid, where ~75% of cells are affected (Fig. 1C). However, deletion of *YCK1* did not aggravate this phenotype (Fig. 3E and F), indicating that that the enhancement of growth defects by the *yck1*Δ mutation is not due to an enhancement of trafficking defects.

Next, we investigated the ability of *YCK1* to reverse αSyn-induced toxicity and trafficking defects (Fig. 3G and H). We observed that *YCK1* overexpression attenuates the growth defect caused by 2 copies of the αSyn-GFP gene in WT and *yck1*Δ cells. In addition, in contrast to the absence of trafficking defect enhancement upon deletion of *YCK1*, overexpression of *YCK1* significantly reduced the percentage of cells showing abnormal localization of GFP-Snc1-Sso1 in cells constitutively expressing αSyn (Fig. 3H). Interestingly, Ypt1, a Rab GTPase that also suppresses αSyn toxicity (Cooper et al., 2006), decreased mislocalization of GFP-Snc1-Sso1 to the same extent. These results suggest that Yck1 may alleviate αSyn toxicity by, at least in part, directly promoting PM endocytosis.

CHAPTER 2 – GENETIC CONTEXT-DEPENDENT MODULATION OF α-SYNUCLEIN TOXICITY AND TRAFFICKING DEFECTS BY PHOSPHORYLATION OF SERINE 129

αSyn contains a consensus CKI phosphorylation site on S129 that is phosphorylated by yeast and mammalian CKI *in vitro* and *in vivo* (Okochi et al., 2000; Zabrocki et al., 2008). To assess whether αSyn is phosphorylated at S129 in yeast, we monitored the levels of total and phosphorylated αSyn (pS129) over time in WT cells carrying 2 copies of the αSyn-GFP gene. Both αSyn and its phosphorylated form were detected after 1 h of inducing αSyn expression, indicating that αSyn is rapidly phosphorylated in yeast (Fig. 3B). To test whether CKI modulates directly or indirectly the phosphorylation of αSyn at S129 in our model, we compared the relative levels of pS129 in the WT, *yck1*Δ and *yck2* Δ strains after 1 h of induction. The *spo14*Δ strain was included as negative control. As previously shown , we observed a modest (~30%) decrease in the relative levels of pS129 in the *yck1*Δ and *yck2*Δ mutants compared to the WT strain (Fig. 3C and D), confirming that CKI contributes partially to the phosphorylation of S129.

To determine whether the attenuation of growth and trafficking defects by Yck1 are mediated by phosphorylation of αSyn, we measured the levels of pS129 in WT and *yck1* Δ cells transformed with a plasmid for the overexpression of *YCK1* or the corresponding empty vector at 5.5 and 11 h of induction (Fig. 3I). As control, we treated cells with a combination of the phosphatase inhibitors (PI) okadaic acid and activated Na_3VO_4. *YCK1* overexpression did not increase αSyn phosphorylation in either WT or *yck1*Δ cells, suggesting that the attenuation of toxicity and trafficking defects by *YCK1* is not mediated by phosphorylation.

CHAPTER 2 – GENETIC CONTEXT-DEPENDENT MODULATION OF α-SYNUCLEIN TOXICITY AND TRAFFICKING DEFECTS BY PHOSPHORYLATION OF SERINE 129

Phosphorylation Regulates the Toxicity and Trafficking Defects Caused by αSyn in a Context-Dependent Manner

The role of S129 phosphorylation on disease pathogenesis is unclear, as contradictory results have been published in different models (Chen et al., 2005; Gorbatyuk et al., 2008; Azeredo da Silveira et al., 2009; Chau et al., 2009; Kragh et al., 2009; McFarland et al., 2009). To investigate the effect of S129 phosphorylation on αSyn-induced toxicity and trafficking defects in yeast, we generated strains that stably express WT αSyn or the phosphorylation mutants S129A or S129E from one or two genomic loci in the BY4741 strain background (Table I). As expected, αSyn reduced cell growth in a dose-dependent manner (Fig. 4A). However, replacement of S129 by A or E did not alter αSyn toxicity or expression levels (Fig. 4A and B). These results suggest that phosphorylation does not modulate αSyn toxicity. However, the S129 phosphorylation status appears to govern α Syn neurotoxicity in at least a fly and rat model (Chen et al., 1992; Gorbatyuk et al., 2008), but not in two other models (Azeredo da Silveira et al., 2009; Mc Farland et al., 2009) Therefore, we reasoned that variations in the genetic background of the models may account for the differential sensitivity of cells to the αSyn phosphorylation status.

To test this hypothesis, we generated strains that stably express WT αSyn or the phosphorylation mutants S129A or S129E from one or two genomic loci in the W303-1A genetic background (Table I). This strain carries a mutation in the *YBP1* gene that

increases its sensitivity to oxidative stress (Veal et al., 2003), a known mechanism of α Syn toxicity (Witt et al., 2006). Whereas one copy of any of the three αSyn alleles had no impact on yeast growth, two copies were detrimental in an allele-specific manner (Fig. 4C). While the S129A mutation, that prevents phosphorylation, significantly increased the growth defect caused by WT αSyn, the S129E mutation, that mimics phosphorylation, had no effect, suggesting that preventing phosphorylation enhances α Syn toxicity in the W303-1A strain background. Interestingly, the S129A mutation caused a significant ~6-fold increase in the percentage of cells with αSyn inclusions in comparison to WT αSyn without altering expression levels (Fig. 4D-F), suggesting that blocking phosphorylation of S129 enhances trafficking defects caused by αSyn.

To confirm this hypothesis, we studied the trafficking of the dye FM 4-64 in the strains with 2 copies of the WT αSyn gene, or the S129A and S129E mutations in the W303-1A background. As previously reported (Outeiro et al., 2003), WT αSyn impaired the delivery of the dye to the vacuolar membrane (Fig. 4G and H). The S129A mutation enhanced this defect, indicating that the enhancement of toxicity correlates with increased trafficking defects. Importantly, these defects were typically observed in cells with αSyn inclusions (Fig. 4I), regardless of the αSyn variant expressed, confirming that the formation of inclusions is an indication of underlying trafficking defects and suggesting a molecular link between phosphorylation and trafficking.

CHAPTER 2 – GENETIC CONTEXT-DEPENDENT MODULATION OF α-SYNUCLEIN TOXICITY AND TRAFFICKING DEFECTS BY PHOSPHORYLATION OF SERINE 129

To verify whether the modulation of αSyn toxicity by Yck1 observed in the BY4741 derived strains is mediated by S129 phosphorylation or an independent mechanism, we deleted or overexpressed *YCK1* in strains expressing 2 copies of the WT αSyn gene, or the S129A and S129E mutations in the W303-1A background. Unexpectedly, either deletion or overexpression of *YCK1* did not alter the growth defect of these strains, whether expressing WT αSyn or the S129 mutations (Fig. 4J). These observations demonstrate that the genetic modification of a toxic phenotype is profoundly influenced by the genotype and may explain paradoxical observations reported in different models.

Evidence of Endosome Anomalies and CKIδ Mislocalization in αSyn Tg Mice and in Synucleinopathy Brains

To determine if defects in early-endocytic trafficking are a conserved pathological feature of Synucleinopathies, we studied the subcellular localization of the EE protein marker Rab5 in brain tissues from a tg mouse model of Synucleinopathy (Masliah et al., 2000) and human DLB/PD. In tg mice, overexpression of human αSyn results in the formation of αSyn-positive inclusion-like structures in the neocortex, hippocampus, and substantia nigra by two months of age (Masliah et al., 2000). In non tg mice, Rab5 labeled discrete punctuate endosomes in the cytosol of cortical neurons at six months of age whereas α Syn stained discrete puncta in the cell periphery. However, in tg animals, Rab5 labeled abnormally swollen endosomes in neurons that that contained αSyn-positive intracellular inclusions (Fig. 5). Interestingly, these outsized endosomes co-localized with small

granular aggregates of αSyn, but were excluded from large Lewy-body-like inclusions. Similarly, in cortical sections of human control subjects, Rab5 and αSyn exhibited a punctuate pattern that in some cases co-localized. However, in human DLB/PD cases, Rab5 stained abnormal endosomal compartments that co-localized with αSyn granular aggregates but not with Lewy bodies. While the nature of the enlarged Rab5-positive endosomes is unknown and they may not be equivalent to the accumulation of vesicles observed in yeast overexpressing αSyn, the presence of this abnormal endosomes suggest a dysfunction of the endocytic pathway in αSyn tg mice.

To examine the early-endocytic trafficking machinery in pathological states *in vivo*, we analyzed by western blot the levels of Rab5, and two other EE markers, Rab4 and EEA1, in the αSyn tg mice and in a tg mouse model of Alzheimer's disease (AD), a non-strict form of Synucleinopathy in which a processed fragment of αSyn deposits in extracellular amyloid plaques. In this model, expression of mutant human amyloid precursor protein (APP) leads to the formation of plaques in the frontal cortex by 4 months of age (Rockenstein et al., 2001). Interestingly, at 6 months of age, both models exhibited elevated levels of monomeric and high molecular weight (HMW) species of αSyn in detergent-insoluble brain fractions (Fig. 6A and B). This change correlated with an accumulation of low mobility forms of Rab5, but no alterations in the mobility or levels of Rab4 or EEA1.

To validate these observations, we analyzed Rab5, Rab4 and EEA1 levels in two subgroups of human amyloidopathies, including DLB/PD and AD. Consistent with the mouse studies, detergent-insoluble HMW species of αSyn accumulated in strict Synucleinopathies and AD cases compared to age-matched control subjects (Fig. 6C and D). In addition, levels of Rab5, but not Rab4 or EEA1, were markedly elevated in DLB/PD and AD relative to controls, suggesting upregulation or reduced turn-over of Rab5 in the two subgroups. As in the mice models, Rab5 exhibited a mobility shift in all the amyloidopathy cases studied, whereas the mobility of Rab4 or EEA1 was unchanged. Although the functional significance of the Rab5 mobility shift is unknown, the co-localization of αSyn granular aggregates with enlarged endosomes, and the correlation between accumulation of αSyn HMW species and Rab5 suggest a causative role for α Syn in early endosome dysfunction.

To investigate a possible involvement of mammalian CKI proteins in the pathogenesis of Synucleinopathies *in vivo*, we studied the subcellular localization of CKIδ, involved in vesicle transport (Milne et al., 2001; Yu et al., 2002), in brain sections from αSyn tg mice and human DLB/PD (Fig. 7). As expected, CKIδ localized predominantly to the cell periphery in cortical neurons from non-tg animals. In contrast, CKIδ co-localized with α Syn inclusions in tg animals. Importantly, this association was conserved in neuronal inclusions in human DLB/PD, consistent with the notion that CKIδ may be sequestered by αSyn inclusions in Synucleinopathies.

Elevated levels of CK1δ mRNA have been detected in AD brains (Yasojima et al., 2000), suggesting upregulation of CK1δ as a compensatory response in AD. To investigate whether CK1δ is upregulated in Synucleinopathies, we analyzed the levels of CK1δ by western blot in brains from αSyn and APP tg mice and human DLB/PD and AD cases (Fig. 6B and D). We did not detect any significant changes in the levels of CK1δ in mice models or human synucleinopathies, indicating that CK1δ is not upregulated in response to αSyn accumulation. Unexpectedly, CKIδ levels were also unchanged in AD cases, suggesting that the observed mRNA upregulation in AD does not lead to increased CK1δ Synthesis, or that the upregulation is tissue-specific and undetectable in whole brain homogenates.

DISCUSSION

A number of recent studies have shown that αSyn overexpression causes vesicle trafficking defects in a wide variety of model systems (Gosavi et al., 2002; Cooper et al., 2006; Fujita et al., 2006; Larsen et al., 2006; Lee et al., 2006; Gitler et al., 2008; Kuwahara et al., 2008; Soper et al., 2008) by perturbing SNARE function (Darios et al., 2010; Garcia-Reitbock et al., 2010; Thayanidhi et al., 2010). In yeast, an early effect of expressing αSyn by a strong galactose-inducible system is an ER-to-Golgi block that precedes a global trafficking failure (Cooper et al., 2006; Gitler et al., 2008). This trafficking collapse is accompanied by the formation of αSyn-positive vesicular clusters

that co-localize with protein markers of several trafficking routes, including ER-to-Golgi, intra-Golgi, Golgi-to-PM, EE-to-LE, and LE-to-vacuole (Gitler et al., 2008; Soper et al., 2008). The presence of endosome-to-Golgi markers in the clusters is controversial since Gitler and colleagues detected Ypt6, but Soper and colleagues failed to detect Vps17 or Vps29. Importantly, the Rab GTPase Ypt1 and the SNARE Ykt6, involved in ER-to-Golgi vesicle-mediated transport, suppresses αSyn-induced trafficking defects (Cooper et al., 2006; Gitler et al., 2008; Thayanidhi e tal., 2010)

In this study, we present evidence of the steady-state impairment of late-exocytic, early-endocytic and/or recycling trafficking by constitutive expression of αSyn in yeast from the *GPD1* promoter. In agreement with previous studies, we observed that trafficking defects coincide with an accumulation of αSyn-positive vesicles that originate in the vicinity of the cell surface and progressively expand towards the cell interior. The vesicles co-label with Snc1, an exocytic SNARE that is targeted to the PM and subsequently internalized and recycled for re-use via EE and the Golgi, implying that at least some of the vesicles originate in the Golgi or the PM. We propose that, in our system, αSyn blocks a trafficking step that follows vesicle budding from the Golgi or the PM and precedes fusion to target membranes. However, we cannot exclude the possibility that the observed vesicles constitute a cellular response to cope with the αSyn overload by compartmentalizing the toxic protein.

In our studies, αSyn did not impair the targeting of a number of protein trafficking markers traversing the ER and the Golgi towards the vacuole, indicating that ER-to-Golgi transport is unaffected in our model. The discrepancy between our findings and previous studies may be reconciled by differences in the expression levels, toxicity and duration of the insult attained by distinct expression systems (Mumberg et al., 1994; 1995). Whereas prior studies used a galactose-inducible promoter, our studies used a constitutive promoter to assess the effects of αSyn expression on protein trafficking. Interestingly, in the current study, we show that Ypt1 rescues the mislocalization of GFP-Snc1-Sso1 caused by constitutive αSyn expression. Although it is well established that Ypt1 functions in ER-to-Golgi trafficking, this protein also facilitates the recycling of internalized membrane material (Lafourcade et al., 2004). Therefore, we propose that Ypt1 rescues αSyn toxicity by promoting, at least in part, the recycling of PM proteins. Consistent with this interpretation, Ypt6, which is involved in endosome-to-Golgi and intra-Golgi retrograde transport (Luo et al., 2003), was also shown to partially suppress α Syn toxicity (Cooper et al., 2006; Gitler et al., 2008). Thus, although it is conceivable that the trafficking defects that we observed might be secondary to the sustained imposition of the primary ER-to-Golgi block, in our system, αSyn appears to directly impair late-exocytic, early-endocytic and/or recycling trafficking without affecting other pathways.

Our observations contribute to accumulating evidence that trafficking defects are a conserved mechanism of pathogenesis in human Synucleinopathies. In yeast, Rab

CHAPTER 2 – GENETIC CONTEXT-DEPENDENT MODULATION OF α-SYNUCLEIN TOXICITY AND TRAFFICKING DEFECTS BY PHOSPHORYLATION OF SERINE 129

GTPases governing multiple trafficking steps are sequestered by αSyn-induced vesicle clusters (Gitler et al., 2008). Similarly, in humans, members of the Rab family implicated in exocytosis (Rab3a), endocytosis (Rab5) and polarized traffic (Rab8a) interact aberrantly with αSyn in DLB and co-localize with αSyn glial inclusions in MSA (Dalfo et al., 2004; 2005). Conversely, Rab1 (involved in ER-to-Golgi transport), Rab3a and Rab8a are neuroprotective in cellular and animal models in which αSyn is overexpressed (Cooper et al., 2006; Gitler et al., 2008). In catecholaminergic cells αSyn impairs exocytosis, leading to an accumulation of docked vesicles (Larsen et al., 2006). Finally, clusters of dense core vesicles have been observed in the perimeter of Lewy bodies (Forno et al., 1976; Watanabe et al., 1977; Soper et al., 2008).

Our study provides evidence of anomalies in endosome morphology and the endocytic Rab5 in pathological states *in vivo*. In mouse models and human synucleinopathies, early endosomes are abnormally enlarged in cortical neurons and Rab5 co-localizes with αSyn granular inclusions and accumulates abnormally in detergent-insoluble fractions from brain lysates. In contrast, the levels of two other EE markers, Rab4 and EEA1, were unchanged. Although both Rab4 and Rab5 are involved in early endocytic trafficking, they differ in their functional specialization. Whereas Rab5 regulates the fusion between endocytic vesicles and early endosomes, as well as the homotypic fusion between early endosomes (Stenmark et al., 2001), Rab4 controls the function or formation of endosomes involved in endocytic recycling (van der Sluijs et al., 1992). Likewise,

although EEA1 is a Rab5 effector (Simonsen et al., 1998), accumulation of Rab5 may not necessarily affect EEA1 levels. Therefore, αSyn appears to selectively alter Rab5 expression and function without altering the levels of downstream effectors. In agreement with our observations, inhibition of Rab5 GTPase activity results in the formation of unusually large early endocytic structures (Stenmark et al., 1994), a phenotype mimicked by the overexpression of αSyn. These alterations suggest that endocytic trafficking defects might also occur and contribute to neuronal dysfunction in Synucleinopathies. In striking similarity to our yeast studies, an RNAi screen in the nematode *C. elegans* showed that endocytosis-defective mutants potently exacerbate αSyn neurotoxicity (Flower et al., 2007). Worms that over-expressed αSyn displayed decreased neurotransmitter release, similar to endocytosis-defective mutants. These authors also reported that the knock down of a CK1 gene enhances αSyn toxicity, and showed that αSyn phosphorylated at S129 accumulated in mutants defective in endocytosis (Kuwahara et al., 2008).

In agreement with this model, we found that deletion of *YCK1* or *YCK2*, two redundant kinases of the CKI family that promote the endocytosis and delivery of PM proteins to the vacuole, led to an increase in αSyn toxicity. Interestingly, *yck1*Δ cells accumulate cargo normally destined for the vacuole in an endocytic compartment, but do not affect trafficking through the CPY and ALP pathways to the vacuole (Marcha et al., 2002). These results are further supported by our previous studies in which the yeast SNARE

CHAPTER 2 – GENETIC CONTEXT-DEPENDENT MODULATION OF α-SYNUCLEIN TOXICITY AND TRAFFICKING DEFECTS BY PHOSPHORYLATION OF SERINE 129

Tlg2 was identified as a loss-of-function enhancer of αSyn toxicity (Willingham et al., 2003). Tlg2 participates in endosome-to-Golgi recycling and is required for targeting Yck2 to the PM (Panek et al., 2000), suggesting that exacerbation of αSyn toxicity in *tlg2*Δ cells might be due, at least in part, to decreased CKI activity at the PM. Although we did not detect any significant increase in trafficking defects upon deletion of *YCK1*, we observed a reduction in αSyn-induced growth and trafficking defects upon overexpression of *YCK1*. Although Yck1 contributes modestly to the phosphorylation of αSyn at S129, our results indicate that the attenuation of the toxicity and trafficking defects is not mediated by increased phosphorylation of αSyn. Thus, it is conceivable that CKI activity protects against αSyn toxicity by directly promoting PM endocytosis. This hypothesis is consistent with the observation that knocking down the *C. elegans YCK1* ortholog *csnk-1* by RNAi causes Synaptic deficits selectively in αSyn transgenic worm (Kuwahara et al., 2008).

The function of S129 phosphorylation in physiological and pathological conditions is unclear. While only a small fraction of αSyn is phosphorylated in the healthy brain, αSyn is hyperphosphorylated at S129 in pathological lesions (Fujiwara et al., 2002; Hirai et al., 2004; Waxman et al., 2008). However, the relevance of S129 phosphorylation to disease pathogenesis is unknown since conflicting observations have been reported. Mimicking phosphorylation has been shown to be neuroprotective (Gorbatyuk et al., 2008) or innocuous (Azeredo da Silveira et al., 2009; MacFarland et al., 2009) in rats, but

detrimental in *Drosophila* (Chen et al., 2005) and SH-SY5Y cells (Chau et al., 2009; Kragh et al., 2009). We showed that, in yeast, the effect of S129 phosphorylation on α Syn toxicity is strain-specific. Blocking S129 phosphorylation is innocuous in BY4741-derived strains, but markedly increased the toxicity and trafficking defects caused by α Syn in W303-1A-derived strains, supporting a protective role for phosphorylation in a background-specific manner. Interestingly, W303-1A carries a mutation in the *YBP1* gene that abolishes the oxidative stress response and increases the sensitivity to oxidative stress. This genetic variability could be responsible for the differential sensitivity between the two strain backgrounds to S129A αSyn. Consistent with this hypothesis, αSyn causes oxidative stress and ROS accumulation and increase the vulnerability of yeast to hydrogen peroxide . Conversely, antioxidants and genes involved in the stress response suppress αSyn toxicity in yeast (Griffioen et al., 2006; Liang et al., 2008).

Taken together, our studies indicate that αSyn toxicity is linked to trafficking defects and that this phenotype is modulated by phosphorylation-dependent and independent pathways. For example, the attenuation of toxicity and trafficking defects by *YCK1* appears to be uncoupled from S129 phosphorylation. However, the relative contribution of each pathway to αSyn toxicity appears to be dependent on the global genetic landscape of the cell.

A previous study by Zabrocki and colleagues showed that Yck1, Yck2, Yck3 and CKII

phosphorylate αSyn at S129 (Zabrocki et al., 2008). However, while deletion of *YCK1* and *YCK2* modestly alleviated an αSyn-induced growth defect and stabilized αSyn at the PM, deletion of *YCK3* and the four subunits of CKII (*CKA1*, *CKA2*, *CKB1* and *CKB2*) exacerbated the growth defect and resulted in αSyn accumulation in intracellular compartments. The latter observation is consistent with the genetic context-dependent enhancement of αSyn toxicity and inclusion formation by the S129A allele we report in this study. Therefore, despite some discrepancies regarding the effects of casein kinases on αSyn toxicity, the general conclusion arising from both studies is that impairment of endocytic trafficking can at least partially account for increased αSyn toxicity.

There is substantial evidence that mammalian CKs phosphorylate αSyn at S129 in cultured cells and *in vivo* (Okochi et al., 2000; Ishii et al., 2007; Waxman et al., 2008). In neurons, a number of mammalian CKI isoforms associate with Synaptic vesicles, and the phosphorylation of CKI substrates is thought to regulate Synaptic vesicle trafficking and neurotransmission. Mammalian CK substrates include proteins implicated in Synaptic vesicle formation (AP-3 adaptor complex) (Faundez et al., 2000), docking and fusion (p65) (Bennett et al., 1993), and exocytosis (Synaptotagmin I) (Davletov et al., 1993), or in the storage of neurotransmitters (VMAT2) (Krantz et al., 1997). Interestingly, some CKI mRNA isoforms (α, δ and ε, but especially δ) are dramatically upregulated in the hippocampus and associated with tau-containing neurofibrillary tangles in AD and other dementias (Yasojima et al., 2000). Here, we describe for the first time the co-localization

of CKIδ with Lewy bodies in DLB/PD, suggesting sequestration and loss of CKIδ activity in Synucleinopathies. However, we did not detect any increase in the levels of CK1δ protein in mice models or human DLB/PD cases, revealing that upregulation of CK1δ is not a compensatory mechanism in synucleinopathies.

Based on our observations and previous studies, we have generated a model to describe the cascade of pathogenic events that lead to neuronal dysfunction and death in synucleinopathies (Fig. 8). As αSyn is normally a synaptic-vesicle associated protein, we hypothesize that, under physiological conditions, CKIδ regulates neurotransmission by phosphorylating synaptic proteins, including αSyn. Under pathological conditions, the progressive accumulation of αSyn may lead to sequestration of Rab GTPases and deficits in synaptic trafficking and neurotransmission. CKIδ-dependent phosphorylation of synaptic substrates may play a protective role by attenuating vesicular trafficking defects and restoring synaptic transmission. However, when all binding sites in synaptic vesicles are saturated, excess αSyn may associate with other compartments, including endosomes, leading to sustained defects in synaptic vesicle homeostasis and neurotransmission. In addition, excess αSyn deposited in Lewy bodies may irreversibly sequester CKIδ and other vesicle-associated proteins, resulting in loss of CKIδ activity and reduced protection against these defects. In summary, our study points that endosome defects and CKIδ dysfunction may be relevant for the pathogenesis of synucleinopathies.

CHAPTER 2 – GENETIC CONTEXT-DEPENDENT MODULATION OF α-SYNUCLEIN TOXICITY AND TRAFFICKING DEFECTS BY PHOSPHORYLATION OF SERINE 129

TABLES

Table I. Strains used in this study

Strain	MT[1]	Genotype	Source
BY4741	*MAT***a**	*his3Δ1 leu2Δ0 met15Δ0 ura3Δ0*	
FRY346	*MAT***a**	BY4741 *TPI1pr-8xMYC-SNC1::URA3*	This study
Y5563	*MAT*α	*can1Δ::MFA1pr-HIS3 lyp1Δ his3Δ1 leu2Δ0 met15Δ0 ura3Δ0 LYS2+*	
VSY1	*MAT***a**	BY4741 *ade2*Δ0::*SNCA*(WT)-*GFP NatR*	This study
VSY2	*MAT*α	Y5563 *trp1*Δ0::*SNCA*(WT)-*GFP URA3+*	This study
VSY4	*MAT*α	VSY2 *ade2*Δ0::*SNCA*(WT)-*GFP NatR*	This study
VSY57	*MAT***a**	VSY4 *yck1*Δ0::*KanR*	This study
VSY58	*MAT***a**	VSY4 *yck2*Δ0::*KanR*	This study
VSY59	*MAT***a**	VSY4 *tlg2*Δ0::*KanR*	This study
VSY60	*MAT***a**	VSY4 *spo14*Δ0::*KanR*	This study
*yck1*Δ	*MAT***a**	BY4741 *yck1*Δ0::*KanR*	
*yck2*Δ	*MAT***a**	BY4741 *yck2*Δ0::*KanR*	
*spo14*Δ	*MAT***a**	BY4741 *spo14*Δ0::*KanR*	
*tlg2*Δ	*MAT***a**	BY4741 *tlg2*Δ0::*KanR*	
*pdr1*Δ	*MAT***a**	BY4741 *pdr1*Δ0::*KanR*	
*did3*Δ	*MAT***a**	BY4741 *did3*Δ0::*KanR*	
*end3*Δ	*MAT***a**	BY4741 *end3*Δ0::*KanR*	
*rcy1*Δ	*MAT***a**	BY4741 *rcy1*Δ0::*KanR*	
*sac6*Δ	*MAT***a**	BY4741 *sac6*Δ0::*KanR*	
*vps23*Δ	*MAT***a**	BY4741 *vps23*Δ0::*KanR*	
*vps35*Δ	*MAT***a**	BY4741 *vps35*Δ0::*KanR*	
*ypt7*Δ	*MAT***a**	BY4741 *ypt7*Δ0::*KanR*	
*ypt31*Δ	*MAT***a**	BY4741 *ypt31*Δ0::*KanR*	
*ypt51*Δ	*MAT***a**	BY4741 *ypt51*Δ0::*KanR*	
RSY255	*MAT*α	*ura3-52 leu2-3,-112*	
RY782	*MAT*α	*his4-619 ura3-52 sec1-1*	
RY112	*MAT***a**	*his4-619 ura3-52 leu2-3,-112 trp1-289 sec 7-4*	
RY271	*MAT*α	*his4-619 ura3-5 sec18-1*	
VSY64	*MAT*α	VSY4 *pdr1*Δ0::*KanR*	This study
VSY65	*MAT***a**	VSY57 *yck1*Δ0::*kanR*Δ0::*LEU2*	This study
VSY66	*MAT***a**	VSY65 *pdr1*Δ0::*KanR*	This study
W303-1A	*MAT***a**	*can1-100 his3-11 15 leu2-3 112 trp1-1 ura3-1 ade2-1*	
VSY67	*MAT***a**	W303-1A *ura3-1*::*pRS306 URA3+*	This study
VSY68	*MAT***a**	W303-1A *ura3-1*::*GAL1pr-SNCA*(WT)-*GFP URA3+*	This study
VSY69	*MAT***a**	W303-1A *ura3-1*::*GAL1pr-SNCA*(S129A)-*GFP URA3+*	This study
VSY70	*MAT***a**	W303-1A *ura3-1*::*GAL1pr-SNCA*(S129E)-*GFP URA3+*	This study
VSY71	*MAT***a**	VSY67 *trp1-1*::*pRS304 TRP1+*	This study
VSY72	*MAT***a**	VSY68 *trp1-1*::*GAL1pr-SNCA*(WT)-*GFP TRP1+*	This study
VSY73	*MAT***a**	VSY69 *trp1-1*::*GAL1pr-SNCA*(S129A)-*GFP TRP1+*	This study
VSY74	*MAT***a**	VSY70 *trp1-1*::*GAL1pr-SNCA*(S129E)-*GFP TRP1+*	This study
VSY75	*MAT***a**	VSY71 *yck1*Δ0::*KanR*	This study
VSY76	*MAT***a**	VSY72 *yck1*Δ0::*KanR*	This study
VSY77	*MAT***a**	VSY73 *yck1*Δ0::*KanR*	This study
VSY78	*MAT***a**	VSY74 *yck1*Δ0::*KanR*	This study
VSY79	*MAT*α	Y5563 *trp1*Δ0::*pRS405 LEU2+*	This study
VSY80	*MAT*α	Y5563 *trp1*Δ0::*SNCA*(WT)-*GFP LEU2+*	This study
VSY81	*MAT*α	Y5563 *trp1*Δ0::*SNCA*(S129A)-*GFP LEU2+*	This study
VSY82	*MAT*α	Y5563 *trp1*Δ0::*SNCA*(S129E)-*GFP LEU2+*	This study
VSY83	*MAT*α	VSY79 *pdr1*Δ0::*pRS465 URA3+*	This study
VSY84	*MAT*α	VSY80 *pdr1*Δ0:: *SNCA*(WT)-*GFP URA3+*	This study
VSY85	*MAT*α	VSY81 *pdr1*Δ0:: *SNCA*(S129A)-*GFP URA3+*	This study
VSY86	*MAT*α	VSY82 *pdr1*Δ0:: *SNCA*(S129E)-*GFP URA3+*	This study

[1]Mating type

CHAPTER 2 – GENETIC CONTEXT-DEPENDENT MODULATION OF α-SYNUCLEIN TOXICITY AND TRAFFICKING DEFECTS BY PHOSPHORYLATION OF SERINE 129

Table II. Characteristics of human cases analyzed in this study

Group	Age (years)	Gender M/F[1]	Blessed score (range)	Braak stage (range)	Plaques per mm^2	Tangles per 0.1 mm^2	Lewy bodies	Brain weight (grams)
Non demented (n=4)	83+/-2	2/2	0-1	0-1	0.25	0	0	1150+/-40
AD (n=6)	81+/-2	3/3	13-33	5-6	25+/-3	5+/-1	0	1070+/-35
DLB/PD (n=8)	83+/-1	5/3	6-33	2-4	28+/-3	2+/-1	3+/-1	1110+/-60

[1]Males/Females

CHAPTER 2 – GENETIC CONTEXT-DEPENDENT MODULATION OF α-SYNUCLEIN TOXICITY AND TRAFFICKING DEFECTS BY PHOSPHORYLATION OF SERINE 129

FIGURES

Figure 1

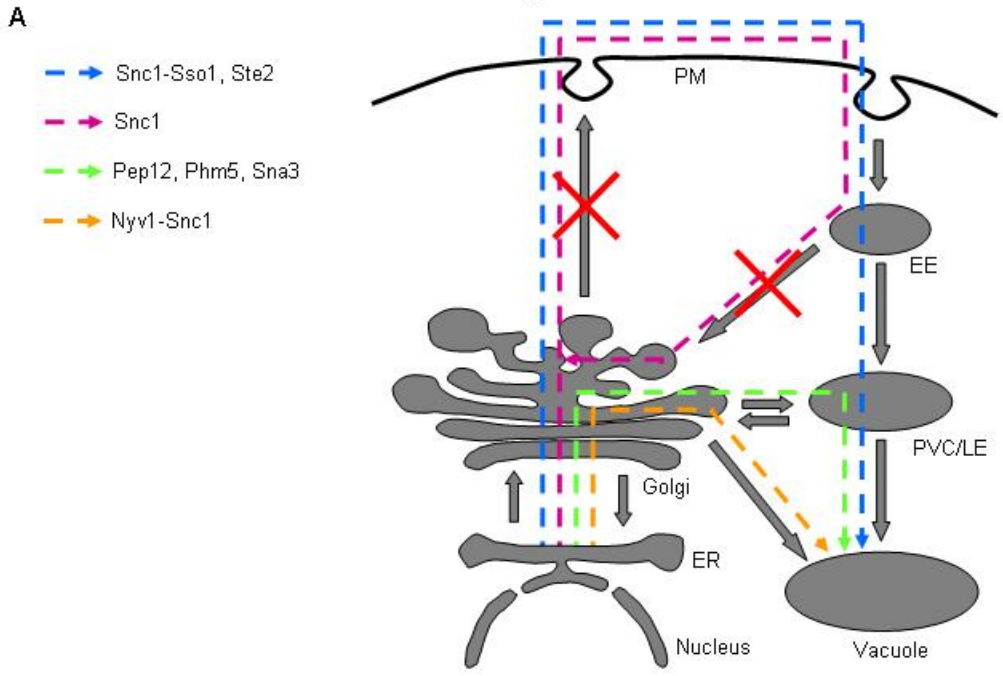

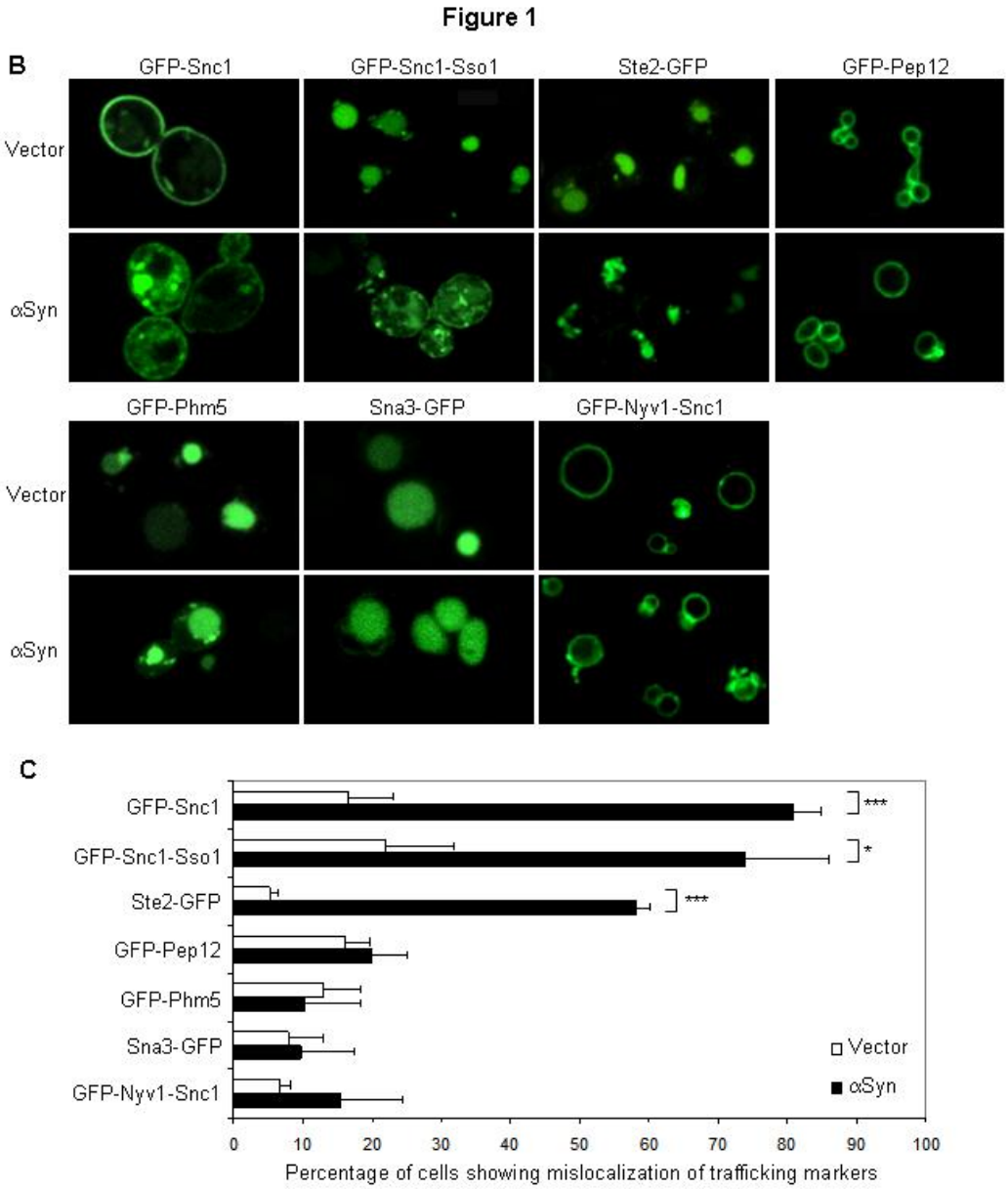

Figure 1. αSyn overexpression causes the mislocalization of late-exocytic and early-endocytic protein markers. (A) Schematic representation of the routes tracked by the indicated protein markers in yeast. Red crosses indicate putative trafficking steps blocked by constitutive αSyn expression. EE: early endosome; ER: endoplasmic reticulum; PM:

plasma membrane; PVC/LE: prevacuolar complex/late endosome. (B) Effect of αSyn on the localization of the indicated protein trafficking markers. The BY4741 strain co-transformed with plasmids for the expression of the indicated protein markers and untagged WT αSyn under the control of a *GPD1* constitutive promoter or the corresponding empty vector was photographed in log phase. (C) Quantification of the percentage of cells from (B) exhibiting mislocalization of the indicated trafficking markers. Error bars represent standard deviations of three experiments. **P*< 0.05; ***P*<0.01; ****P*<0.001; student's t test.

Figure 2

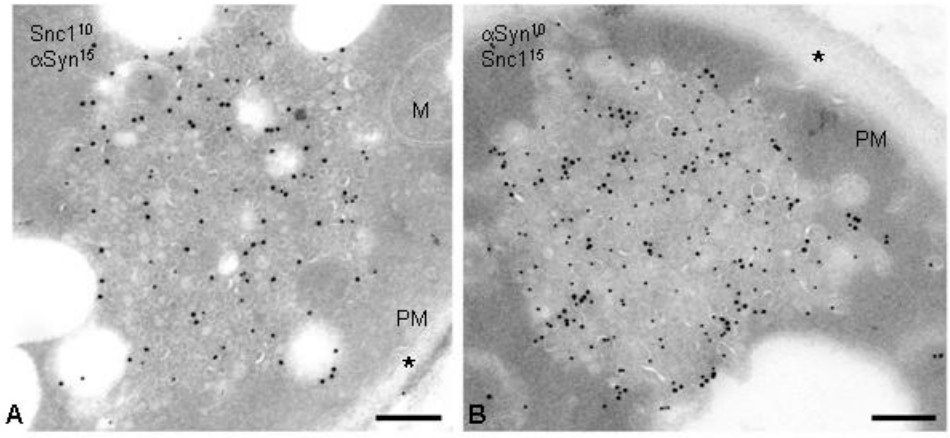

Figure 2. αSyn-induced vesicular clusters contain the exocytic SNARE Snc1. The strain FRY346 carrying an integrated *8xMYC-SNC1* fusion and transformed with a plasmid for the expression of αSyn-GFP under the control of a constitutive *GPD1* promoter was grown to log phase, and cells were processed for IEM. In the left panel (A), cryosections were first incubated with anti-myc antibodies and then with anti GFP antibodies (αSyn^{15}, 15-nm gold particles; $Snc1^{10}$, 10-nm gold particles) whereas in the right panel (B) the sequence of the antibodies was inverted (αSyn^{10}, 10-nm gold; $Snc1^{15}$, 15-nm gold particles). PM, plasma membrane; M, mitochondria; *, cell wall. Bar, 200 nm.

CHAPTER 2 – GENETIC CONTEXT-DEPENDENT MODULATION OF α-SYNUCLEIN TOXICITY AND TRAFFICKING DEFECTS BY PHOSPHORYLATION OF SERINE 129

Figure 3

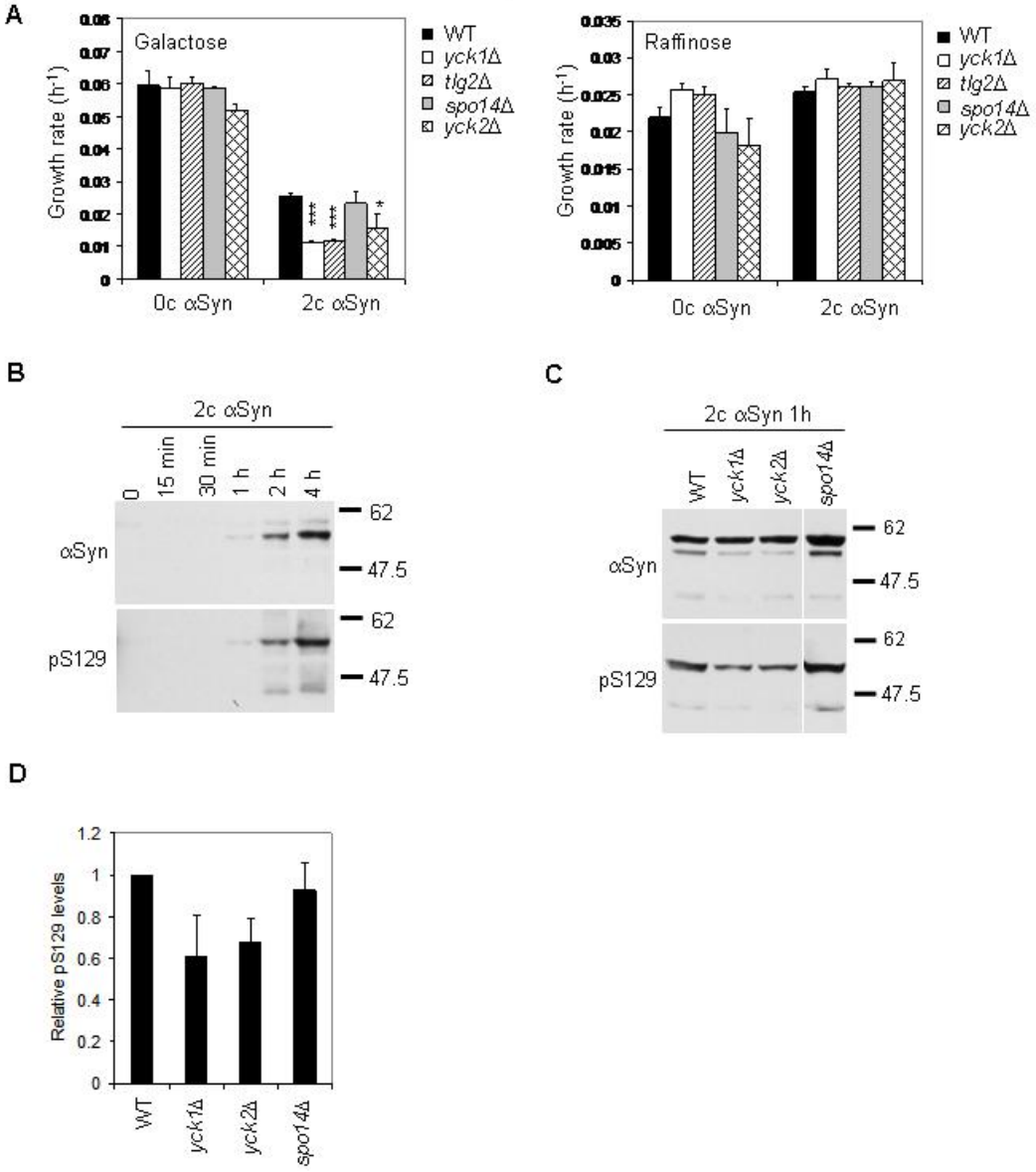

Figure 3

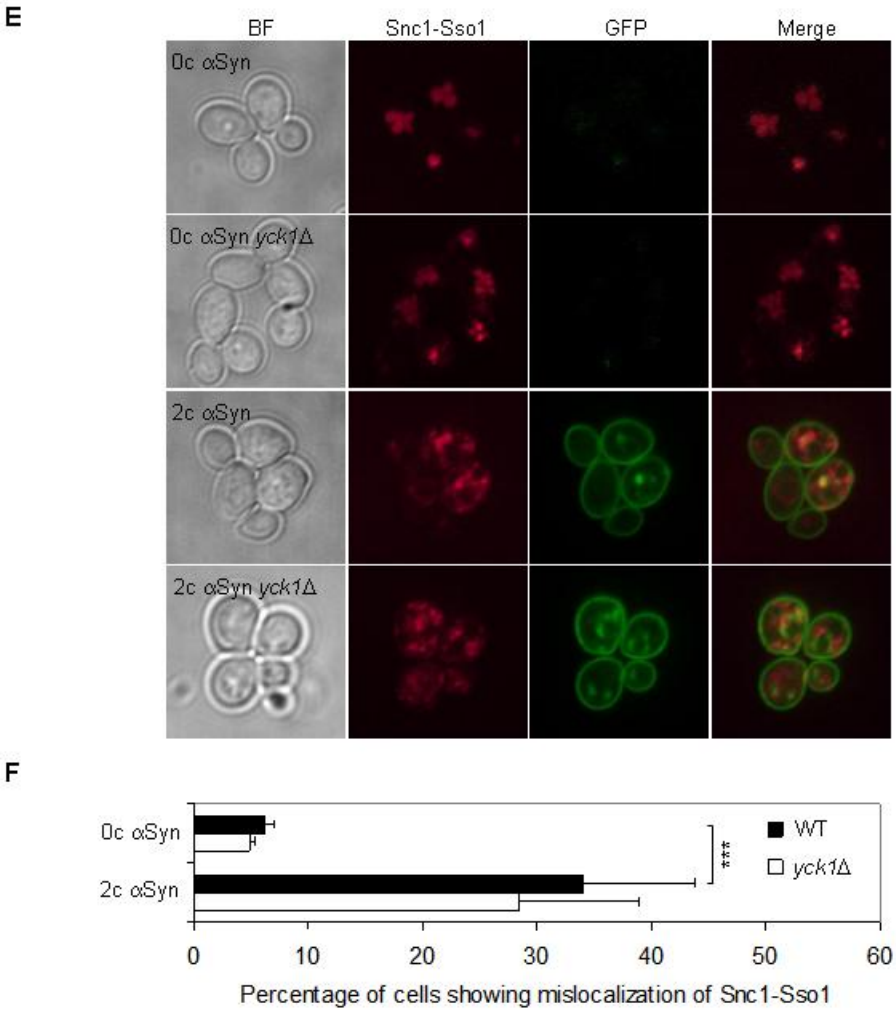
E
BF
Snc1-Sso1
GFP
Merge
0c αSyn
0c αSyn yck1Δ
2c αSyn
2c αSyn yck1Δ
F
0c αSyn
2c αSyn
WT
yck1Δ
***
0
10
20
30
40
50
60
Percentage of cells showing mislocalization of Snc1-Sso1

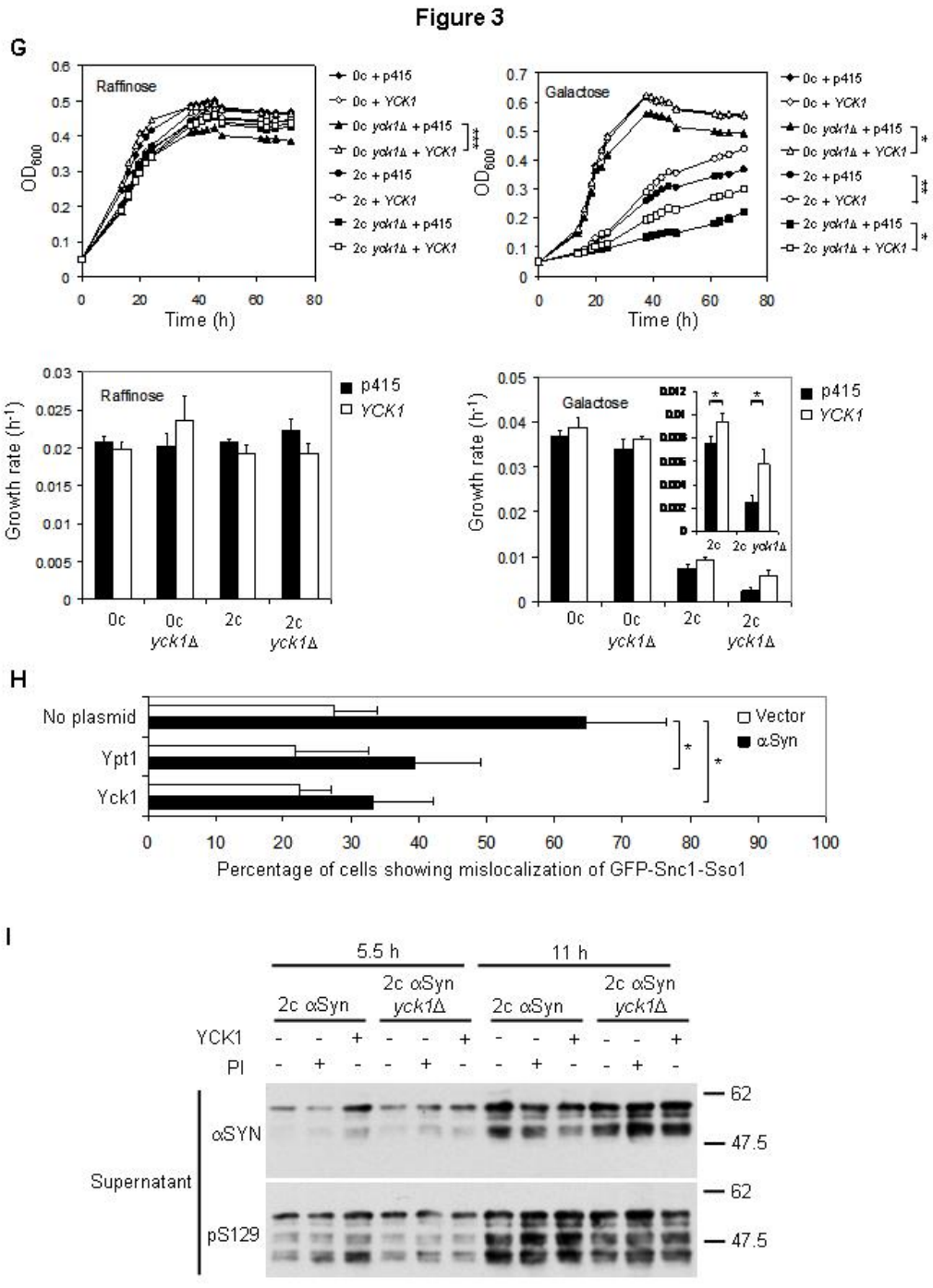

Figure 3. Yck1 attenuates αSyn-induced toxicity and trafficking defects through a

S129 phosphorylation-independent mechanism. (A) Deletion of CKI genes (*yck1*Δ, *yck2*Δ) enhances the growth defect caused by αSyn overexpression in the BY4741 genetic background. Growth rates of WT cells or the indicated mutant strains containing either two copies (2c) or no copies (0c) of the αSyn gene in the BY4741 genetic background in conditions that do (galactose) or do not (raffinose) induce the expression of αSyn. The *tlg2*Δ and *spo14*Δ mutants are included as positive and negative controls, respectively. Growth rates were determined as the slope of the growth curves shown in Fig. S3 during logarithmic phase. (B) Kinetics of αSyn induction and phosphorylation in WT cells containing 2 copies of the αSyn gene in the BY4741 genetic background. Cells were grown to logarithmic phase (OD_{600} ~0.8) in raffinose-containing media and expression of αSyn was induced with galactose. Aliquots were collected at the indicated times and levels of phosphorylated (pS129) and total αSyn were analyzed by western blot. The soluble fraction is shown. The earliest αSyn was detected after 1 h of induction. (C) Deletion of CKI genes reduces moderately αSyn phosphorylation. The indicated strains were induced for 1 h and analyzed by western blot as described in (B). (D) Quantification of the S129 phosphorylation levels were estimated as the ratio of the band densities of phosphorylated relative to total αSyn from (C). (E) Deletion of *YCK1* does not enhance the defects in the trafficking of the marker Snc1-Sso1 caused by αSyn. WT or *yck1*Δ cells containing 2 copies (2c) or no copies (0c) of the αSyn-GFP gene in the BY4741 genetic background were transformed with a plasmid for the expression of trafficking marker mCherry-Snc1-Sso1, induced overnight in galactose-containing media

and imaged in logarithmic phase. (F) Quantification of the percentage of cells from (E) showing mislocalization of Snc1-Sso1. (G) Overexpression of *YCK1* attenuates αSyn-induced growth defects. Growth curves (upper panels) and growth rates (lower panels) of WT or *yck1*Δ cells containing 2 copies (2c) or no copies (0c) of the αSyn-GFP gene in the BY4741 genetic background and transformed with a plasmid for the over-expression of *YCK1* or the corresponding empty plasmid (p415). Growth rates were determined as the slope of the growth curves during logarithmic phase. (H) Yck1 and Ypt1 partially restore targeting of GFP-Snc1-Sso1 to the vacuolar lumen. BY4741 cells expressing GFP-Snc1-Sso1 were transformed with either untagged WT αSyn under the control of a constitutive *GPD1* promoter or the corresponding empty vector and the indicated plasmids for the over-expression of *YPT1* or *YCK1*. After transfer to a galactose-containing medium, cells were photographed in logarithmic phase. The percentage of cells exhibiting mislocalization of GFP-Snc1-Sso1 is shown. (I) Overexpression of *YCK1* does not increase αSyn phosphorylation at S129. WT or *yck1*Δ cells containing 2 copies (2c) or no copies (0c) of the αSyn-GFP gene in the BY4741 genetic background and transformed with a plasmid for the over-expression of *YCK1* or the corresponding empty plasmid were grown to logarithmic phase in raffinose-containing medium and induced with galactose. Aliquots were collected at the indicated times for western blot analysis. The indicated cultures were treated with the phosphatase inhibitors (PI) okadaic acid and activated Na_3VO_4 for 15 min before being collected. Error bars represent standard deviations from three experiments in panels (A), (F), (G) and (H) and two experiments in

panel (D). **P*< 0.05; ***P*<0.01; ****P*<0.001; (A), (F), (G, lower panels), and (H), student's t test; (G, upper panels), ANOVA for repetitive measurements.

CHAPTER 2 – GENETIC CONTEXT-DEPENDENT MODULATION OF α-SYNUCLEIN TOXICITY AND TRAFFICKING DEFECTS BY PHOSPHORYLATION OF SERINE 129

Figure 4

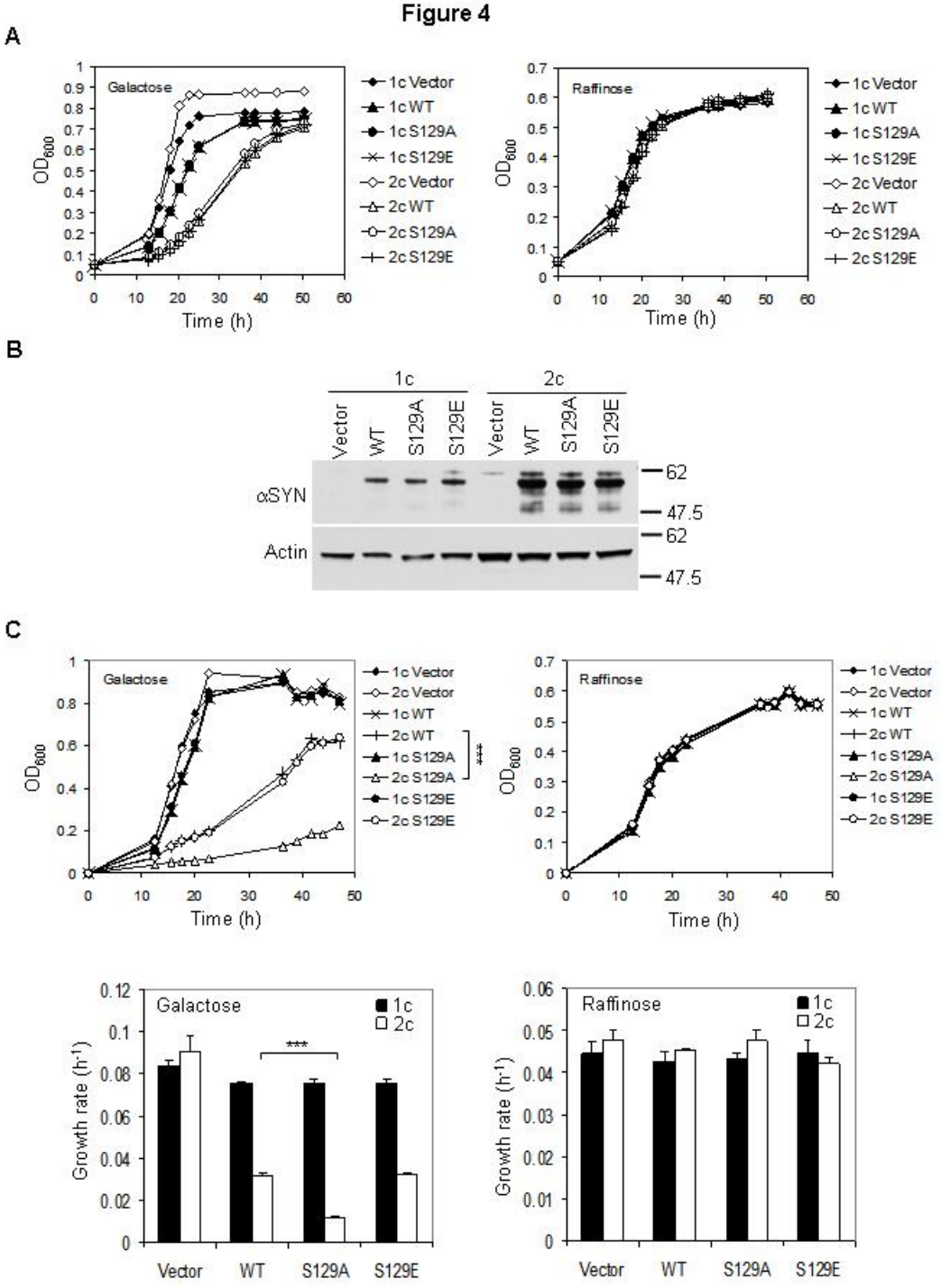

Figure 4

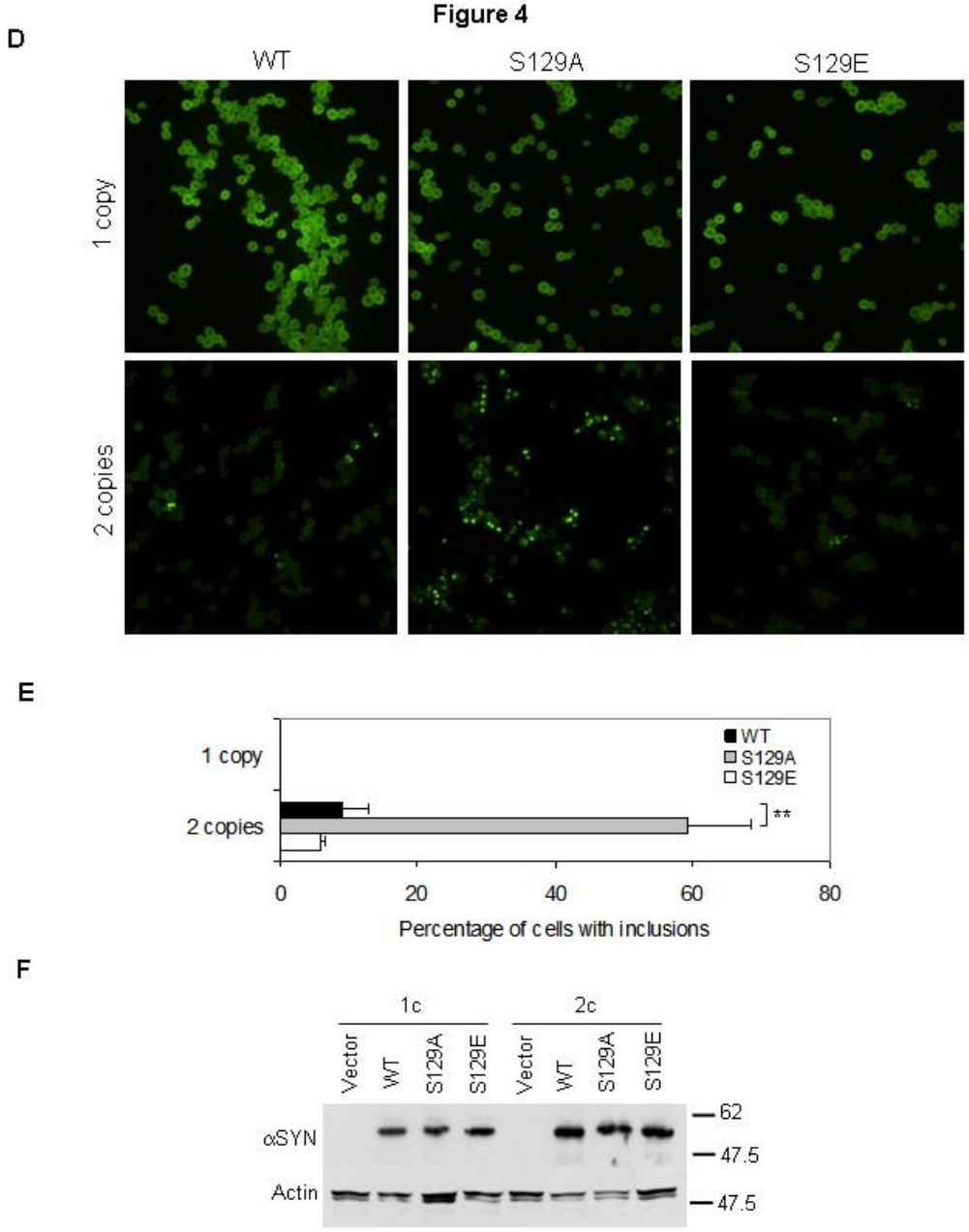
D
WT
S129A
S129E
1 copy
2 copies
E
1 copy
2 copies
WT
S129A
S129E
**
0
20
40
60
80
Percentage of cells with inclusions
F
1c
2c
Vector
WT
S129A
S129E
Vector
WT
S129A
S129E
αSYN
Actin
62
47.5
47.5

Figure 4

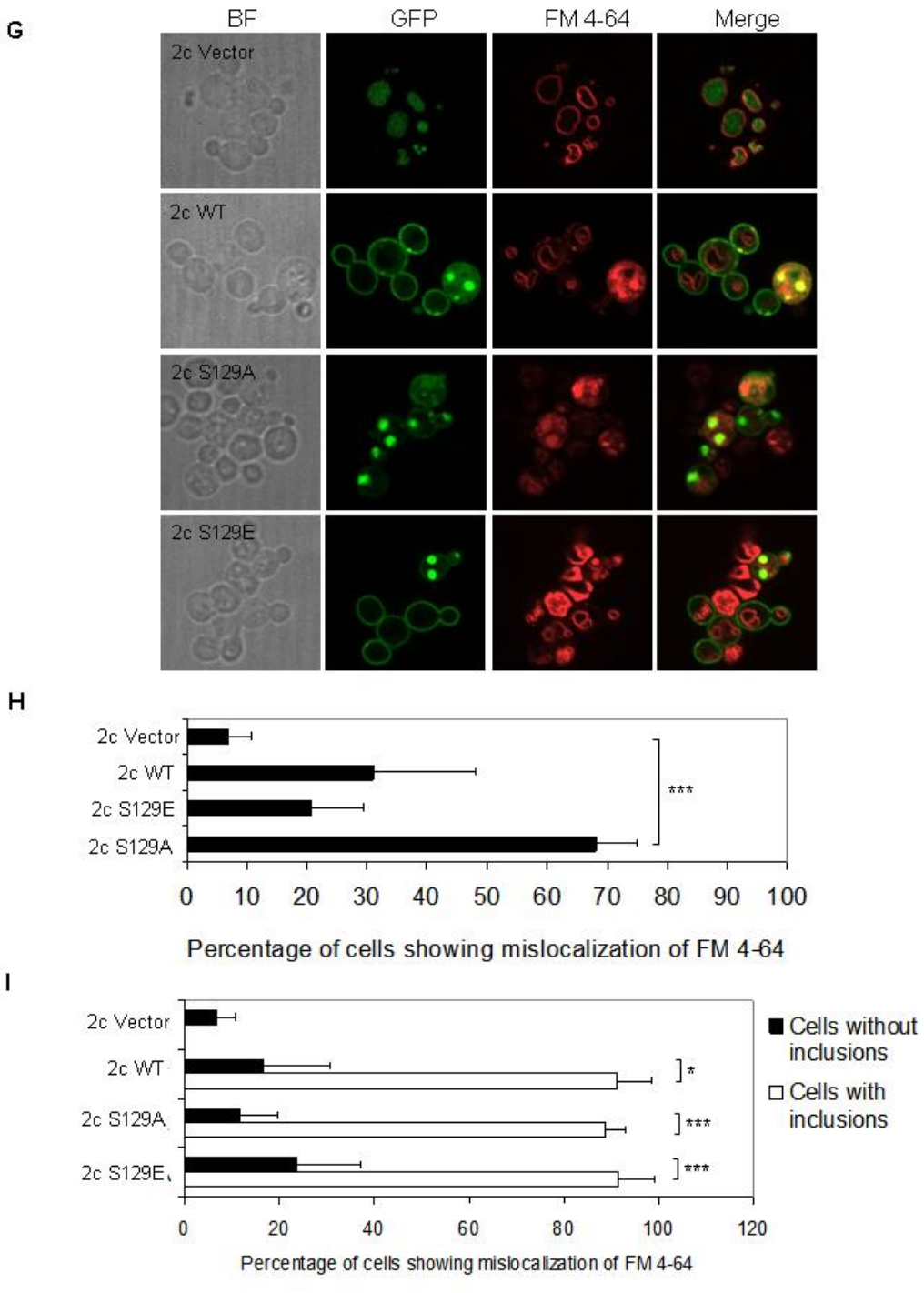
G
BF
GFP
FM 4-64
Merge
2c Vector
2c WT
2c S129A
2c S129E
H
2c Vector
2c WT
2c S129E
2c S129A
***
0
10
20
30
40
50
60
70
80
90
100
Percentage of cells showing mislocalization of FM 4-64
I
2c Vector
2c WT
2c S129A
2c S129E
*
***
***
Cells without inclusions
Cells with inclusions
0
20
40
60
80
100
120
Percentage of cells showing mislocalization of FM 4-64

Figure 4

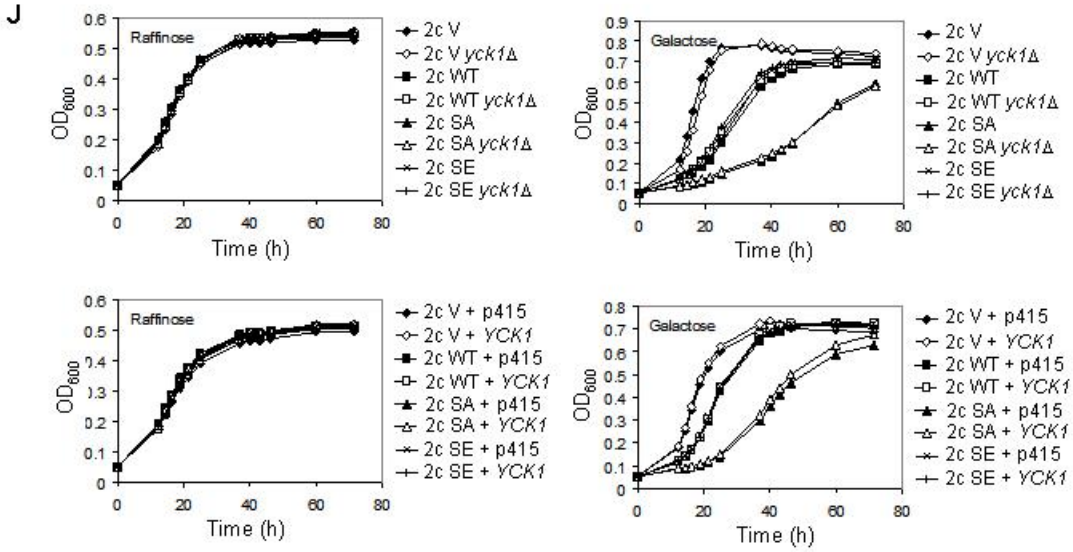

Figure 4. Preventing phosphorylation of S129 increases αSyn-induced toxicity and trafficking defects in a genetic context-dependent manner. (A) Growth curves of strains containing one (1c) or two (2c) copies of either the wild type (WT) αSyn gene or the phosphorylation mutants (S129A, S129E) or the corresponding empty vector in the BY4741 genetic background in conditions that do (galactose) or do not (raffinose) induce the expression of αSyn. (B) S129 mutations do not alter the levels of αSyn in the BY4741 background. Western blot of strains from (A) grown for 8 h in galactose-containing medium. (C) Growth curves (upper panels) or growth rates (lower panels) of strains containing one (1c) or two (2c) copies of either the wild type (WT) αSyn gene or the phosphorylation mutants (S129A, S129E) or the corresponding empty vector in the W303-1A genetic background in conditions that do (galactose) or do not (raffinose)

induce the expression of αSyn. Growth rates were determined as the slope of the growth curves during logarithmic phase. (D) Localization of αSyn in the strains from (C) photographed in logarithmic phase. (E) Quantification of the percentage of cells from (D) exhibiting αSyn inclusions. (F) S129 mutations do not alter the levels of αSyn in the W303-1A background. Western blot of strains from (C) grown for 8 h in galactose-containing medium. (G) Preventing S129 phosphorylation enhances mislocalization of FM 4-64 caused by αSyn in the W303-1A background. Strains from (C) were co-stained with the dye FM 4-64 and imaged in logarithmic phase. (H) Quantification of the percentage of total cells from (G) showing mislocalization of the dye FM 4-64. (I) Quantification of the percentage of cells with and without inclusion from (G) showing mislocalization of FM 4-64. Typically, cells with inclusions display anomalies in the localization pattern of FM 4-64. (J) Deletion or overexpression of *YCK1* in the W303-1A background does not modify αSyn-induced growth defects. Growth curves of strains from (A) in which *YCK1* was either deleted (*yck1*Δ, upper panels) or overexpressed (*YCK1*, lower panels) in conditions that do (galactose) or do not (raffinose) induce the expression of αSyn. SA, S129A; SE, S129E. In panels (C), (E), (H), and (I), error bars represent standard deviations from three experiments. **P*< 0.05; ***P*<0.01; ****P*<0.001; (C, lower panels), (E), (H), and (I), student's t test; (C, upper panels), ANOVA for repetitive measurements.

Figure 5

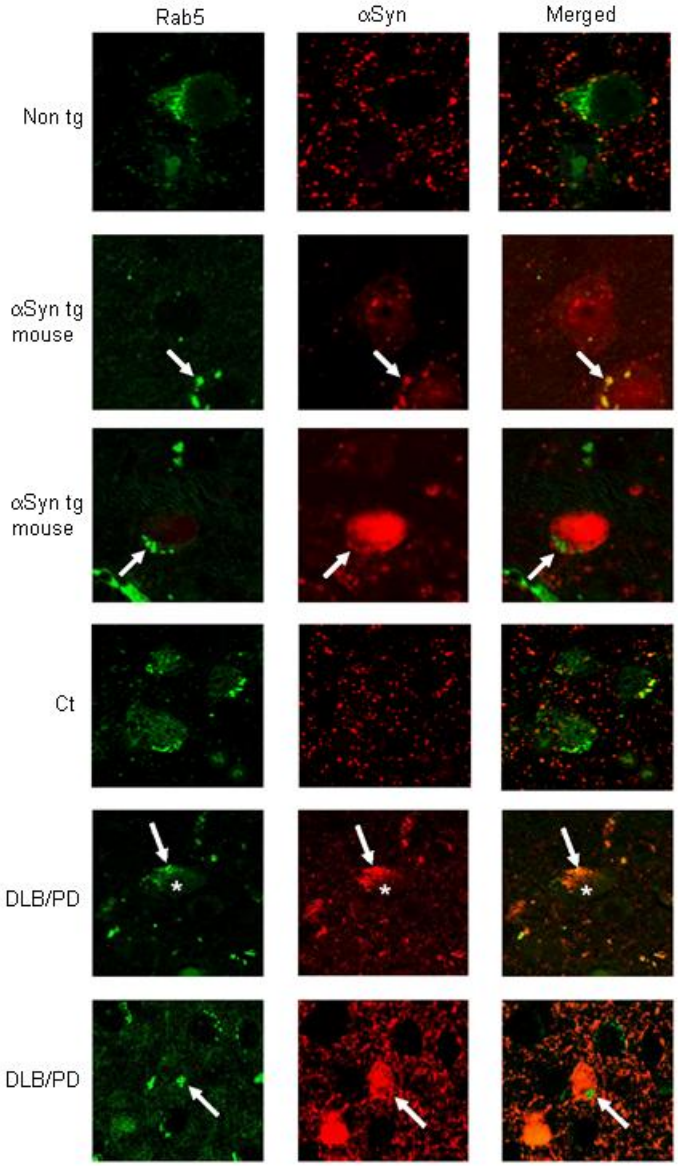

Figure 5. Abnormal endosome morphology in αSyn Tg Mice and in synucleinopathy brains. Abnormally enlarged Rab5-positive endosomes co-localize with granular inclusions of αSyn and accumulate in the vicinity of αSyn inclusions in αSyn tg mice

and human DLB/PD. Cortical sections from αSyn tg mice or DLB/PD cases were double-labeled with antibodies against αSyn and Rab5 and detected with Tyramide Red or fluorescein isothiocyanate (FITC)-conjugated secondary antibodies, respectively. Images of non tg animals and control (Ct) subjects are included for reference. Arrows indicate the Rab5-positive compartments.

Figure 6

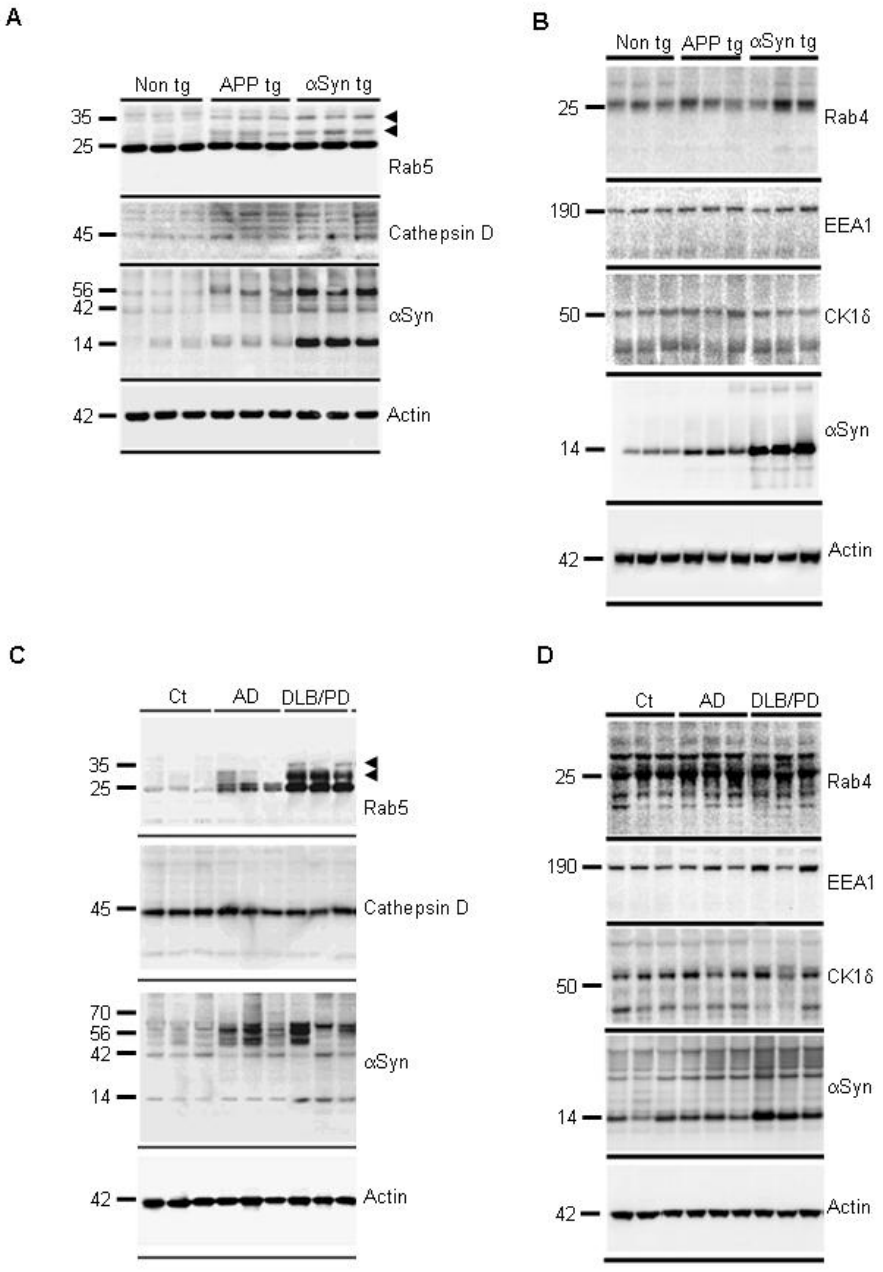

Figure 6. Anomalies in the mobility and levels of the early endosome marker Rab5, but not Rab4, EEA1 or CK1δ, in mice models and human synucleinopathies. Brain

particulate fractions from αSyn tg, APP tg, or non-tg mice (A and B) or from human DLB/PD or AD patients or control (Ct) subjects (C and D) were analyzed by western blot with the indicated antibodies. Arrowheads indicate Rab5 low mobility forms.

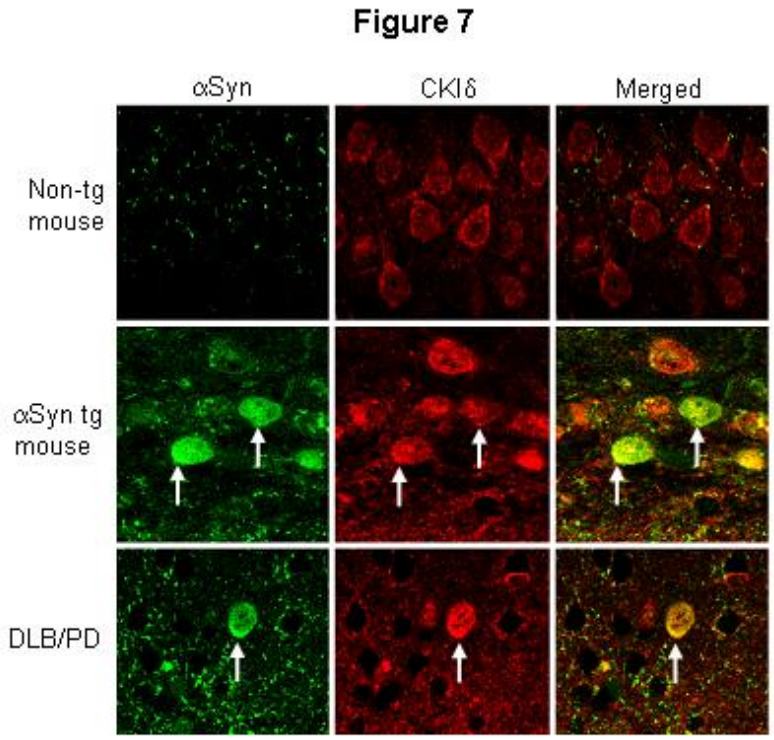

Figure 7. CKIδ co-localizes with αSyn inclusions in αSyn tg mice and human DLB/PD. Cortical sections from non-tg mice, αSyn tg mice, or human DLB/PD cases were double-labeled with antibodies against αSyn and CKIδ and detected with FITC and Tyramid Red-conjugated secondary antibodies, respectively. Arrows indicate the αSyn-positive inclusions.

Figure 8

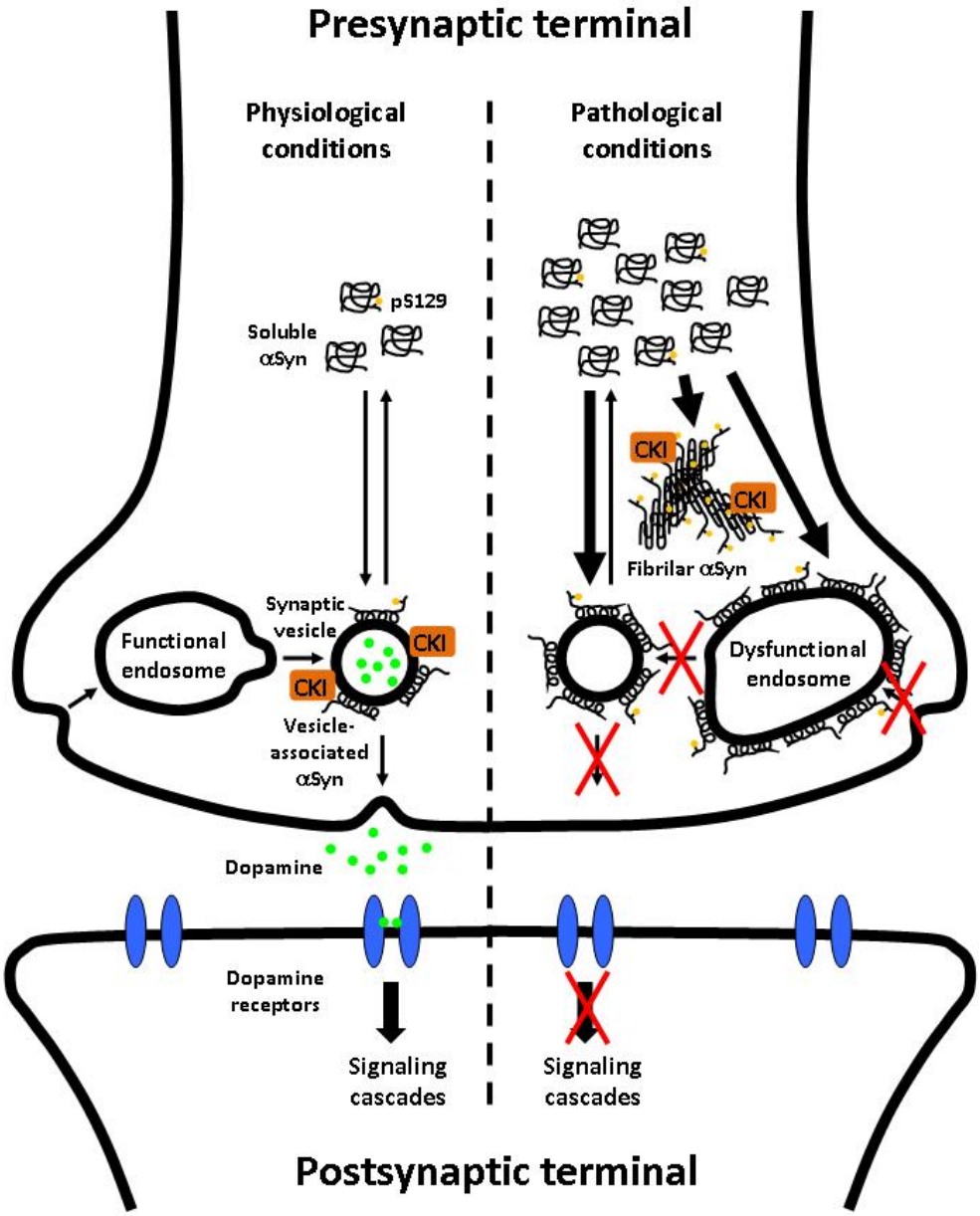

Figure 8. A model depicting how αSyn accumulation may cause neurotransmission defects in PD. We hypothesize that, under normal conditions, CKI regulates αSyn function and possibly association with Synaptic vesicles and neurotransmitter release by

phosphorylating synaptic proteins, including αSyn at S129. Under pathological conditions in which αSyn accumulates and synaptic trafficking and neurotransmission are compromised, CKI may play a protective role in attenuating vesicular trafficking defects and restoring synaptic transmission. However, when all binding sites in synaptic vesicles are saturated, excess αSyn may associate with other compartments, such as endosomes, leading to abnormally enlarged endosomes and defects in synaptic vesicle homeostasis and neurotransmission. In addition, excess αSyn may form insoluble fibrilar deposits that sequester CKI, depleting CKI activity and enhancing synaptic defects. Red crosses indicate possible trafficking steps blocked by αSyn.

Figure S1

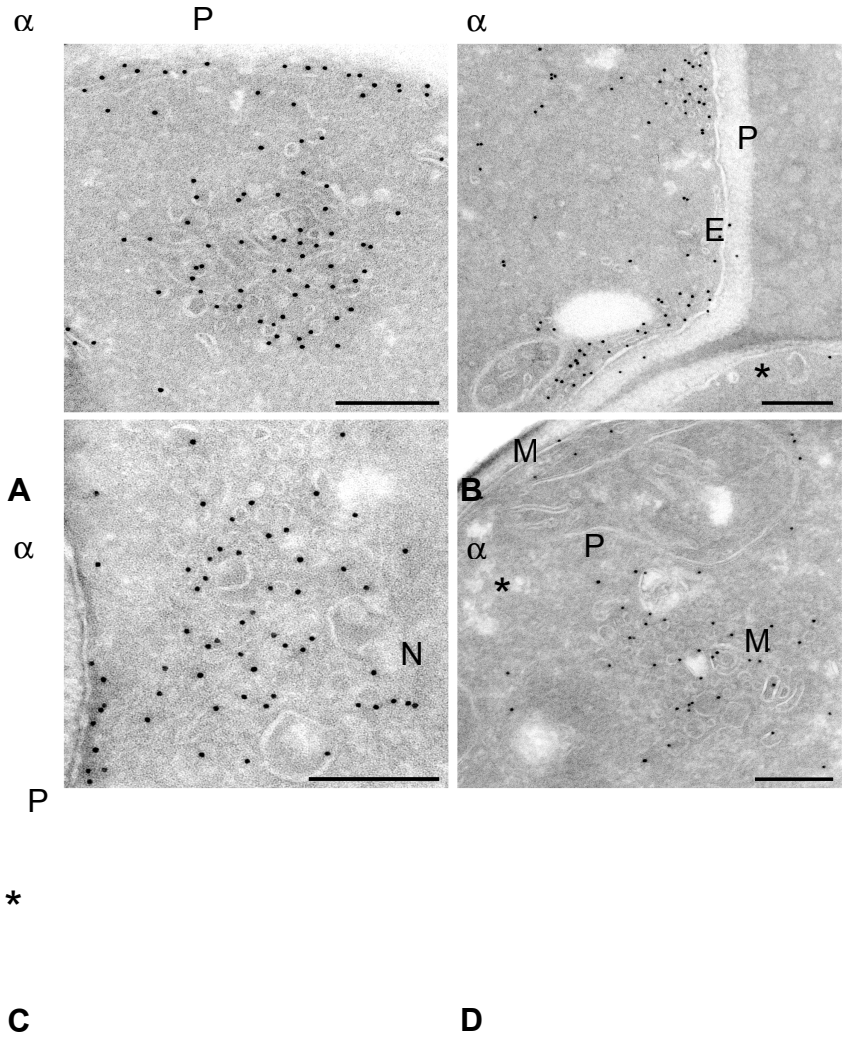

Figure S1. Expression of αSyn in yeast cells leads to the formation of clusters of vesicles. αSyn-GFP expression was induced in the yeast strain BY4741 for either 6h (A and B) or 12h (C and D) and cells were fixed and processed for IEM. At both time points, αSyn (αSyn[10], 10-nm gold particles) is detected on the PM but also on the surface of vesicles that accumulate in cytoplasmic clusters. PM, plasma membrane; ER, endoplasmic reticulum; N, nucleus; M, mitochondria; *, cell wall. Bar, 200 nm.

CHAPTER 2 – GENETIC CONTEXT-DEPENDENT MODULATION OF α-SYNUCLEIN TOXICITY AND TRAFFICKING DEFECTS BY PHOSPHORYLATION OF SERINE 129

ABBREVIATIONS

AD, Alzheimer's disease; CK, casein kinase; CPY, carboxypeptidase Y; DLB, dementia with Lewy bodies; EE, early endosomes; ER, endoplasmic reticulum; GFP, green fluorescent protein; GPD, glyceraldehyde-3-phosphate dehydrogenase; IEM, immuno-electron microscopy; LE, late endosomes; PD, Parkinson's disease; PM, plasma membrane; S129, serine 129; αSyn, α-Synuclein; SNARE, soluble N-ethylmaleimide-sensitive factor attachment protein receptor; WT, wild type.

CHAPTER 3 - ENDOSOMAL TRAFFICKING GENES MODULATE a-SYNUCLEIN TOXICITY IN MAMMALIAN CELLS

CHAPTER 3 – ENDOSOMAL TRAFFICKING GENES MODULATE α-SYNUCLEIN TOXICITY IN MAMMALIAN CELLS

ABSTRACT

α-Synuclein (αSYN), a major player in Parkinson's disease pathogenesis, is thought to impair vesicle trafficking as a toxic gain of function through aggregation. Genetic screens for modifiers of αSYN toxicity have overwhelmingly identified a significant subset of genes involved in vesicle trafficking. Through shRNA-mediated gene knock down and overexpression studies, we show that genetic manipulation of Stx7, Vps24, Vps28, Vps34, Vps45 and Vps52, genes involved in endosomal transport, is sufficient to modulate the toxicity of αSYN in a SH-SY5Y cell line and rat primary cortical neurons. Furthermore, we demonstrate that αSYN toxicity correlates with impairments in exocytosis, increase in constitutive receptor recycling of the transferrin receptor and enlargement of the Golgi apparatus. These abnormalities in the vesicle trafficking pathways can be altered by genetic modifiers of αSYN toxicity. Our findings are indicative of a key role for early endosomal trafficking in αSYN pathogenesis.

INTRODUCTION

Parkinson's disease (PD), a common movement disorder generally affecting individuals above the age of 60, is caused by degeneration of dopaminergic neurons in the *substantia nigra pars compacta* region of the brain (reviewed by Moore et al., 2005). Intracytoplasmic inclusions termed Lewy bodies, a hallmark of PD, are found in the affected neurons (Lücking and Brice, 2000), and are primarily comprised of the protein α SYN (Baba et al., 1998). A highly conserved protein of 140 amino acid residues that is ubiquitously expressed in the brain and found abundantly in presynaptic terminals

(George and Clayton, 1998), αSYN has been implicated in the pathogenesis of both sporadic and familial forms of PD (Polymeropoulos et al., 1997; Kruger et al., 1998; Chiba-Falek et al., 2006; Mizuta et al., 2006). While the physiological function of αSYN remains poorly understood, overexpression of the protein in cultured cells has been shown to inhibit phospholipase D (Jenco et al., 1998), induce the oxidative stress and the unfolded protein response (Cookson and van der Brug, 2008), cause proteasome dysfunction (Lindersson et al., 2004; Betarbet et al., 2005), impair vesicle trafficking (Cooper et al., 2006; Gitler et al., 2008) and inhibit neurotransmitter release (Abeliovich et al., 2000; Nemani et al., 2010).

Impairment of any of these key cellular processes could understandably cause neuronal toxicity. In order to develop effective therapeutic treatments for PD however, it is essential to distinguish between direct pathogenic effects of the αSYN protein and indirect consequences of abnormal αSYN interactions. Multiple genetic screens have been conducted in *Saccharomyces cerevisiae* (Willingham et al., 2003; Cooper et al., 2006; Flower et al., 2007) and *Caenorhabditis elegans* (Hamamichi et al., 2008; van Ham et al., 2008) to identify genes that protect cells from αSYN toxicity. In these screens, genes involved in vesicle trafficking and lipid metabolism were over-represented as modifiers of αSYN toxicity. However, the physiological relevance of these studies needs to be ascertained as these organisms do not natively express a synuclein homolog.

In this study, we used a WT αSYN –Tet-off inducible SH-SY5Y cell culture system that

has been shown to exhibit αSYN toxicity when αSYN expression is induced in differentiated cells (Vekrellis et al., 2009) to determine whether vesicle trafficking genes can modulate αSYN toxicity. We show that down-regulation of human orthologs of yeast vacuolar protein sorting (Vps) genes increase αSYN toxicity. Furthermore, overexpression of these human orthologs is protective against αSYN toxicity in the SH-SY5Y cell culture model, as well as in primary neuronal cultures. Here we show that human orthologs of VPS genes are both necessary and sufficient to modulate αSYN toxicity in SH-SY5Y cells. Thus, manipulation of the expression of Vps genes might be a neuroprotective strategy to treat PD and other synucleinopathies.

RESULTS

Validation of yeast genetic modifiers of αSYN toxicity in SH-SY5Y cells

Our prior genetic screens in yeast identified genes involved in vesicle trafficking as both potent enhancers and suppressors of αSYN-induced toxicity (Willingham et al., 2003). As a first step, we sought to confirm that vesicle trafficking genes also modulated αSYN-induced toxicity in mammalian cells. For that purpose, we decided to study 11 yeast genetic modifiers involved in vesicle trafficking based on the functional homology of their human orthologs (table 1). We designed shRNA against the human orthologs of the yeast genetic modifiers to study the effect of regulating their expression levels in a SH-SY5Y cell line stably transfected with wild type-αSYN under the control of a Tet-off promoter (Vekrellis et al., 2009). In this cell line, we found that induction of αSYN induces toxicity, resulting in the retraction of neuronal processes and membrane blebbing

(fig. 1), approximately 7 days after induction and differentiation as measured by the amount of LDH released into culture media by dead cells (Fig.2a). We confirmed our result using an alternate assay for cell death based on the fluorescence of the dye calcein-AM in the LIVE/DEAD assay (Fig. 2b).

We observed between 30 and 50 % knockdown of gene expression through transfection of the shRNA constructs (fig. 3a), with a transfection efficiency of approximately 40%. (fig. 3a). 10 of the 11 genetic modifiers tested in this study are orthologs of yeast loss of function enhancers of αSYN toxicity. Syntaxin 7 (Stx7), a SNARE involved in homotypic late endosome fusion and late endosome to lysosome fusion, is the ortholog of the yeast vacuolar SNARE, Vam3, a loss of function suppressor of αSYN toxicity. Knockdown of Stx7 showed 30% suppression of αSYN-induced toxicity compared to the scrambled shRNA control (Fig. 3b), corroborating results of our yeast studies. . Despite knockdown of up to 40% at the mRNA level, the three loss of function enhancer human orthologs of Tlg2, a Golgi SNARE, Syntaxin1a, Syntaxin 12 and Syntaxin 16 did not alter αSYN-induced toxicity. 53% & 46% knockdown of Cog6 and Rabgef1 respectively induced toxicity independent of αSYN (data not shown). Strikingly, knocking down expression levels of the human orthologs of yeast vacuolar sorting (Vps) genes, Vps24, Vps28, Vps34, Vps45 and Vps52 all significantly increased αSYN-induced toxicity by 25-60% (Fig. 3c), validating our observations in yeast that Vps genes are potent loss of function enhancers of αSYN-induced toxicity.

Expression of Vps24, Vps28 and Stx7 reduces αSYN toxicity in differentiated SH-SY5Y cells

We next overexpressed Stx7, Vps24, Vps28, Vps34 and Vps45 in the αSYN overexpressing SH-SY5Y cell line. To confirm proper expression and localization patterns for these proteins, we subcloned the full length cDNAs into a vector encoding a C-terminal mcherry tag. The majority of the mcherry-tagged proteins showed a punctate localization, consistent with their predicted localization pattern in cells (Fig. 4). We found that overexpression of Vps34-mcherry and Vps45-mcherry did not affect αSYN-induced toxicity in the SH-SY5Y cells. Overexpression of Vps24-mcherry and Vps28-mcherry, which function in endosomal cargo sorting as members of the endosomal sorting complex required for transport (ESCRT) complexes downstream of Vps34 did have a small but significant reduction of αSYN-induced toxicity. Surprisingly, overexpression of Stx7-mcherry also decreased αSYN-induced toxicity by approximately 20%, which was compaRable to the approximate 20% decrease of αSYN-induced toxicity observed by the overexpression of Vps24-mcherry and Vps28-mcherry. (Fig. 5a, b).

Expression of Vps34 and Stx7 rescues αSYN toxicity in rat primary cortical neurons

We next tested the ability of Stx7 and Vps34 to rescue αSYN-induced toxicity in rat primary neurons transfected with WT human αSYN. Cumulative risk of death curves indicate that primary neurons expressing αSYN have a significantly greater risk of death than control cells (*$p < 0.0001$, log-rank test). Overexpression of Vps34 and Stx7 resulted in almost complete abolishment of αSYN-induced toxicity (Fig. 6). Together

with our experiments in differentiated SH-SY5Y cells, these results suggest that overexpression of Vps24, Vps28, Vps34 and Stx7, genes involved primarily in early endosomal trafficking, modulate αSYN-induced toxicity.

αSYN-induced Golgi abnormalities do not correlate with modulation of toxicity by genetic modifiers in differentiated SH-SY5Y cells

Neuronal Golgi fragmentation has been reported in several neurodegenerative diseases (Fujita et al., 2002; Gonatas et al., 2006), including PD (Gosavi et. al., 2002; Fujita et. al., 2006) and it has been suggested that Golgi fragmentation is specifically due to αSYN aggregation. We stained differentiated SH-SY5Y cells with and without overexpression of αSYN with the GM130 antibody to assay the morphology of the Golgi over several days. We observed no differences in Golgi morphology between the αSYN expressing and non-expressing cells in the days leading to αSYN-induced toxicity. However, we found significantly enlarged, albeit unfragmented, Golgi in αSYN-overexpressing cells close to onset of αSYN-induced toxicity (Fig. 7a, b). We next determined if modulation of αSYN-induced toxicity by vesicle trafficking genes is correlated to the magnitude of Golgi enlargement in SH-SY5Y cells. Although knockdown of Vps24, Vps28 and Vps34 exacerbates αSYN toxicity, they decreased Golgi size in αSYN expressing cells relative to the scrambled control. Knockdown of Vps45 and Vps52 had no effect on Golgi enlargment, despite their exacerbation of αSYN toxicity. We also observed a lack of effect on Golgi enlargment due to the suppression of toxicity by Stx7 knockdown. (Fig.

7c). These results suggest that that genetic modification of αSYN toxicity in SH-SY5Y cells does not correlate with enlargement of Golgi, suggesting that this phenotype is unlikely to play a primary role in toxicity.

αSYN-induced exocytosis impairment does not correlate with modulation of toxicity by genetic modifiers in differentiated SH-SY5Y cells

Our studies in yeast suggest that a post-endocytic and/or early exocytic step in yeast is impaired by the overexpression of αSYN (Sancenon et al.t, manuscript in review). In addition, studies in *C. elegans* also implicate the endocytic pathway in αSYN-induced toxicity (Kuwahara et al., 2008). To examine if αSYN-expression interferes with exocytosis, we studied the retention of the lipophilic dye FM1-43 in SH-SY5Y cells with or without overexpression of αSYN. KCl depolarization evokes exocytosis, which is followed by compensatory endocytosis that traps FM1-43 in the retrieved vesicles. Subsequent redepolarization by KCl results in fusion of FM1-43 labeled vesicles with the plasma membrane and the release of dye into the extracellular medium. This results in decreased fluorescence within the cell, which is a measure of exocytosis. We found that the fluorescence intensity of FM1-43 in αSYN-overexpressing cells was significantly stronger compared to non αSYN-overexpressing cells after the second KCl depolarization event, indicating increased retention of FM1-43 in the αSYN-overexpressing cells (Fig. 8a, b). This suggests impairment in exocytosis in αSYN overexpressing cells.

CHAPTER 3 – ENDOSOMAL TRAFFICKING GENES MODULATE α-SYNUCLEIN TOXICITY IN MAMMALIAN CELLS

Stimulated exocytosis of synaptic vesicles is temporally coupled to endocytosis of vesicular membrane and inhibition of Rab5 has been shown to reduce endo-exocytic rates at the synapse, possibly due to inhibition of membrane exchange between synaptic vesicles and the early endosome. (Wucherpfennig et al., 2003). Active recruitment of Vps34 to the early endosome by Rab5 results in a local enrichment of phosphoinositol-3-phospate (PI3P, which is critical for endosomal trafficking. We wanted to determine whether exacerbation of αSYN-induced toxicity due to the knock down of Vps34 was correlated with changes in FM1-43 retention in differentiated SH-SY5Y cells. We co-transfected cells with scrambled shRNA or shRNA against Vps34 and examined retention of FM1-43 in successfully transfected cells. Despite significantly exacerbating αSYN toxicity, knock down of Vps34 gene expression had no effect on the increased retention of FM1-43 in αSYN-overexpressing cells (Fig. 8c)

αSYN-induced increase in constitutive receptor recycling is nullified by Vps34 knockdown in SH-SY5Y differentiated cells.

Vesicles labeled by FM1-43 constitute a 'fast recycling' pool of vesicles (Sara et al., 2002) that likely involves the early endosome (Maxfield et al., 2004). A separate pool of vesicles termed the 'slow storage pool' regulated by Rab11 (Filipeanu et al., 2006) is involved in the recycling of constitutive receptors, e.g. the transferrin receptor. To determine whether this slow recycling endocytosis pathway is impaired by αSYN overexpression, we performed total internal reflection fluorescence to image differentiated SH-SY5Y cells transfected with GFP-tagged transferrin receptor (TfR).

Fusion of TfR containing vesicles with the plasma membrane is termed an 'insertion event' and the number of insertion events of TfR in the cell plasma membrane is representative of TfR recycling activity. Regardless of aSYN overexpression, insertion events in the differentiated SH-SY5Y cells were exclusively 'transient' events, characterized by rapid dispersion of TfR after insertion into the plasma membrane (Fig. 9a) (Yudowski et al., 2006). We found that cells overexpressing αSYN displayed significantly more insertion events and thus an increase in TfR recycling (Fig. 9b), further suggesting αSYN-induced perturbations in the exo-endocytic pathway. We also tested the effect of Vps34 and Stx7 knockdown on the increase in TfR recycling induced by αSYN-overexpression. The decrease in Vps34 gene expression in αSYN-overexpressing cells markedly reduced TfR recycling activity to normal levels found in cells without αSYN-overexpression. However, knock down of Stx7 or overexpression of Stx7 and Vps34 did not alter the increased TfR recycling activity in αSYN overexpressing cells (Fig. 9c).

DISCUSSION

The pioneering yeast genetic screen for modifiers of αSYN toxicity by Willingham et al. (2003) identified multiple genes involved in vesicle trafficking. Since then, other genetic screens in model organisms of PD (Cooper et al., 2006; Hamamichi et al., 2008; Liang et al., 2008) have also identified vesicle trafficking genes as a major gene category in modulating αSYN toxicity. Our findings described represent a systematic study on the effect of modulating vesicle trafficking genes on αSYN toxicity and pathogenesis in an inducible WT-αSYN SH-SY5Y cell line. We show that manipulating the gene expression

level of endosomal trafficking genes by shRNA exacerbates αSYN-induced toxicity in differentiated SH-SY5Y cells, while knockdown of Stx7 ameliorates αSYN-induced toxicity. We also demonstrate that overexpression of Vps24, Vps28 and Stx7 reduces α SYN-induced toxicity in the SH-SY5Y cell line while expression of Stx7 and Vps34 is sufficient to rescue αSYN-induced toxicity in primary cortical neurons.

Recent studies have implicated impairments in mammalian orthologs of yeast Vps genes in neurodegeneration. A missense mutation in Vps54, a co-complex protein of Vps52, which results in depletion of the Golgi associated retrograde protein (GARP) complex is reportedly responsible for motor neuron degeneration in a murine model of amyotrophic lateral sclerosis (Schmitt-John et al., 2005). Deletion of Vps34 in sensory neurons has been reported to induce rapid neurodegeneration through endosomal defects (Zhou et al., 2010). Furthermore, overexpression of Vps41 has been shown to be neuroprotective in various invertebrate and cellular models of PD (Ruan et al., 2009). In agreement with these findings, we found that decreased expression of Vps genes involved in endosomal trafficking, Vps24, Vps28, Vps34, Vps45 and Vps52, enhance αSYN-induced toxicity in a neuronal cell line. Conversely, overexpression of Vps24, Vps28 and Stx7 were sufficient to reduce αSYN toxicity. While overexpression of Vps34 and Vps45 had no effect on αSYN toxicity in the SH-SY5Y cells, overexpression of Vps34 almost completely ameliorates αSYN-induced toxicity in primary cortical neurons. The lack of rescue by Vps34 overexpression in the SH-SY5Y cells might be due to several reasons. One possibility is that Vps34 regulates endosomal trafficking in a complex with p150 and

Beclin 1 (reviewed by Lindmo et al., 2006), thus suppression of αSYN toxicity might require overexpression of multiple members of Vps34 complex. Another possibility is that the Vps34 overexpression does reduce αSYN toxicity in the SH-SY5Y cells but low transfection efficiency masked the decrease in toxicity in transfected cells when overall toxicity was measured. This would account for the lack of observed rescue of αSYN toxicity in the SH-SY5Y cells compared to the rescue seen in neurons where individual transfected neurons were tracked for survival. Alternatively, lower expression levels of the Vps34 cDNA construct in the SH-SY5Y cells compared to neurons might account for the lack of αSYN toxicity rescue in the cell line.

Results from mechanistic experiments in yeast suggested αSYN induced impairment in a post-endocytic and/or early exocytic pathway (Sancenon et al., manuscript in review). We observed a similar defect in differentiated SH-SY5Y cells where αSYN overexpression induced an abnormal retention of FM1-43, reflecting a defect in KCl stimulated exocytosis. A similar retention of FM1-43 induced by αSYN has recently been reported in neurons from αSYN transgenic mice by Scott et al. (2010) and in a PC12 cell line expressing αSYN by Garcia-Reitböck et al. (2010). We also observed an increase in constitutive receptor recycling of the transferrin receptor in αSYN overexpressing cells. Given the role of several of the genetic modifiers in endosomal trafficking, we hypothesize that the exacerbation of αSYN toxicity upon knockdown of the genetic modifiers might be due to a worsening of the αSYN-induced endo-exocytosis defects. We

cannot rule out the possibility that exacerbation of αSYN-induced toxicity by decreased levels of Vps genes is due to disruptions in the lysosomal system, given the role of the ESCRT complex and associated proteins, Vps24, Vps28 and Vps34, in lysosomal degradation of proteins (reviewed by Hurley and Emr, 2006). However, we did not observe a change in αSYN protein levels in cells treated with shRNA against the Vps genes (data not shown), suggesting that an impairment in αSYN degradation is not responsible for the exacerbation of αSYN-induced toxicity.

Strikingly, we found that knock down of Vps34 gene expression mimicked the effects of αSYN on vesicle trafficking in wild-type cells, inducing enlargement of the Golgi, abnormal retention of FM1-43, an increase in transferrin receptor recycling (Fig. 7d, 8d, 9d), and impairment in neurotransmitter release in neurons (R. Edwards, personal communication). Furthermore, the conditional knock out of Vps34 in mice is thought to induce rapid neurodegeneration through defects in endosomal trafficking rather than autophagy (Zhou et al., 2010). It is conceivable that toxicity cause by αSYN accumulation may be due to an impairment of trafficking at the early endosome, which is regulated in part by Vps34. Depletion of Vps34 in αSYN overexpressing cells would presumably exacerbate the early endosome trafficking impairment, leading to the observed increase in αSYN toxicity.

Vps34, the only class III PI3K in mammalian cells, converts PI to phosphatidyinositol-3-phosphate, a phospholipid that establishes the identity of the early endosome and

therefore is critical for trafficking at the early endosome (Gillooly et al., 2003). Vps34 is recruited to early endosomes by the small GTPase Rab5 (Yan and Becker, 2007). It has been shown that Rab5 accumulates in enlarged endosomes that colocalizes with αSYN in both αSYN transgenic mice and PD patient brains (Sancenon et al., manuscript in review). Furthermore, direct interaction between Rab5 and αSYN has been reported (Dalfó et al., 2004), suggesting that pathogenesis of αSYN involves early endosome trafficking. Given that the bulk of exocytosed vesicles are derived from endosomes, impairment of Rab5 function and therefore early endosome trafficking affects rates of endocytosis and exocytosis (Stenmark et al., 1994), which could explain the abnormal retention FM1-43 in the αSYN-overexpressing SH-SY5Y cells.

We speculate that cells compensate for the exocytosis block due to early endosome impairment by upregulating alternate pathways for exocytosis to maintain proper balance of membranes and proteins at the plasma membrane. One pathway is the route that the transferrin receptor takes through recycling endosomes, which is regulated by a different set of Rabs, namely Rab4 and 11 (Deneka and van de Sluijs, 2002) and not affected by specific Vps34 inhibition **(**Johnson et al., 2006). This would account for the observed increase in transferrin receptor recycling in both the αSYN-overexpressing SH-SY5Y cells and non αSYN-overexpressing cells with Vps34 gene knockdown. As recycling endosomes are closely associated with the trans-Golgi network (Ang et al., 2004), the enlarged Golgi seen in cells under those conditions might be related to the increase in recycling endosomal activity and further indicative of increased secretion.

In addition to maintaining normal operational status quo of the secretory pathway and plasma membrane, upregulation of transferrin receptor recycling may be a cellular coping mechanism to eliminate unwanted molecules and even toxic αSYN species. Indeed, Emmanouilidou et al. (2010) recently reported exosome-dependent αSYN secretion into the extracellular medium of SH-SY5Y cells. Exosomes, small intraluminal vesicles formed within multivesicular bodies that fuse with the plasma membrane, purportedly clear unwanted proteins from the cell and establish cell-independent signaling (van Niel et al., 2006). Notably, the role of exosomes and secretion of the amyloid precursor protein and prion proteins has already been implicated in the pathogenesis of other neurodegenerative diseases such as Alzheimer's disease and Creutzfeldt-Jakob disease respectively (reviewed by Vella et al., 2008). Exosome formation is regulated by the recycling endosome Rab 11 (Savina et al., 2002), and an increase in a Rab11-associated protein Rab4 has been observed in αSYN transgenic mouse brains (unpublished data), further linking αSYN pathogenesis to an upregulation of the constitutive receptor recycling pathway. We observed that knock down of Vps34 in αSYN-overexpressing SH-SY5Y cells exacerbates αSYN toxicity that is correlated with persistent retention of FM1-43, and strikingly, ablation of the enlarged Golgi phenotype and a sharp decrease in transferrin receptor recycling. This suggests that the double insult of αSYN accumulation and Vps34 knock down overwhelms the cells' endosomal trafficking capabilities such that upregulation of alternate secretory pathways is impeded. If upregulation of constitutive receptor recycling is a pathogenic compensatory mechanism for αSYN-induced

endosomal defects, overexpression of a protein that promotes trafficking to the recycling endosome could rescue αSYN toxicity. Indeed, Gitler et al. (2008) have demonstrated that αSYN toxicity in neurons is ameliorated by overexpression of Rab8, a regulator of transferrin receptor trafficking and putative mediator of membrane recycling that partially colocalizes with the recycling endosome marker Rab11 on small vesicles (Hattula et al., 2006).

Similar to other highly polarized cells, the health and proper function of neurons undoubtedly depends on proper delivery of proteins to the axonal or somadendritic membrane surface to ensure received signals are spatially separated from transmitted signals. Polarity of neurons is regulated at the level of endosomes (reviewed by Schmidt and Haucke, 2007). An impairment in endosome trafficking would therefore conceivably lead to mislocalization of important presynaptic terminal proteins, affecting neurotransmitter release among other consequences. Not only has the redistribution of SNAREs been reported in the striatum of PD patients, as well as a mouse model of PD with a corresponding reduction in exocytosis and dopamine release (Garcia-Reitböck et al. 2010; Scott et al., 2010), impairment in neurotransmitter release is clearly linked to neurodegeneration (Dong et al., 2003; Zhang et al., 2009; Nemani et al., 2010; Shen, 2010).

In conclusion, our findings demonstrate that genetic manipulation of vesicle trafficking genes can modulate αSYN-induced toxicity in mammalian cells, and that trafficking at

the early endosome may be critical to αSYN pathogenesis. The mechanism of action is likely to involve regulation of the exo-endocytic pathways, thereby exacerbating or counteracting the toxic effects of αSYN on the trafficking machinery of the cell, or perhaps even modulating the propagation of neurodegeneration from cell to cell due to extracellular secretion of αSYN. Further studies on the interaction of vesicle trafficking genes with αSYN will be important to elucidate the mechanism of vesicle-trafficking related αSYN pathogenesis and may give rise to novel therapeutic targets for PD.

TABLE

Yeast gene	Loss of function effect in yeast	Mammalian homologue	Mammalian gene function
Vam3	suppressor	Stx7	Late endosome fusion
Cog6	enhancer	Cog6	Retrograde Golgi trafficking
Vps9	enhancer	Rabgef1	Homotypic endosomal fusion
Tlg2	enhancer	Stx1a	PreSynaptic vesicle trafficking
Tlg2	enhancer	Stx12	Early and recycling endosomal trafficking
Tlg2	enhancer	Stx16	Trans-Golgi network trafficking
Vps24	enhancer	Vps24	Trans-Golgi network and endosomal trafficking
Vps28	enhancer	Vps28	Trans-Golgi network and endosomal trafficking
Vps34	enhancer	Vps34	Endosomal trafficking
Vps45	enhancer	Vps45	Trans-Golgi network trafficking
Vps52	enhancer	Vps52	Retrograde Golgi trafficking

Table 1. Loss of function yeast genetic modifiers of αSYN toxicity and corresponding mammalian orthologs.

FIGURES

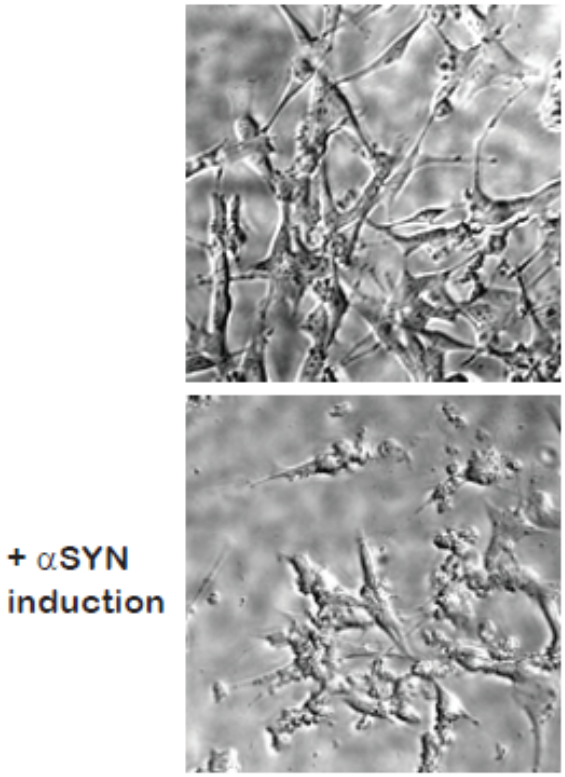

Figure 1. WT aSYN expression causes retraction of neuritic processes, membrane blebbing, and eventually death. Representative bright field photomicrographs of SH-SY5Y cells with or without αSYN induction at day 7 of differentiation are shown.

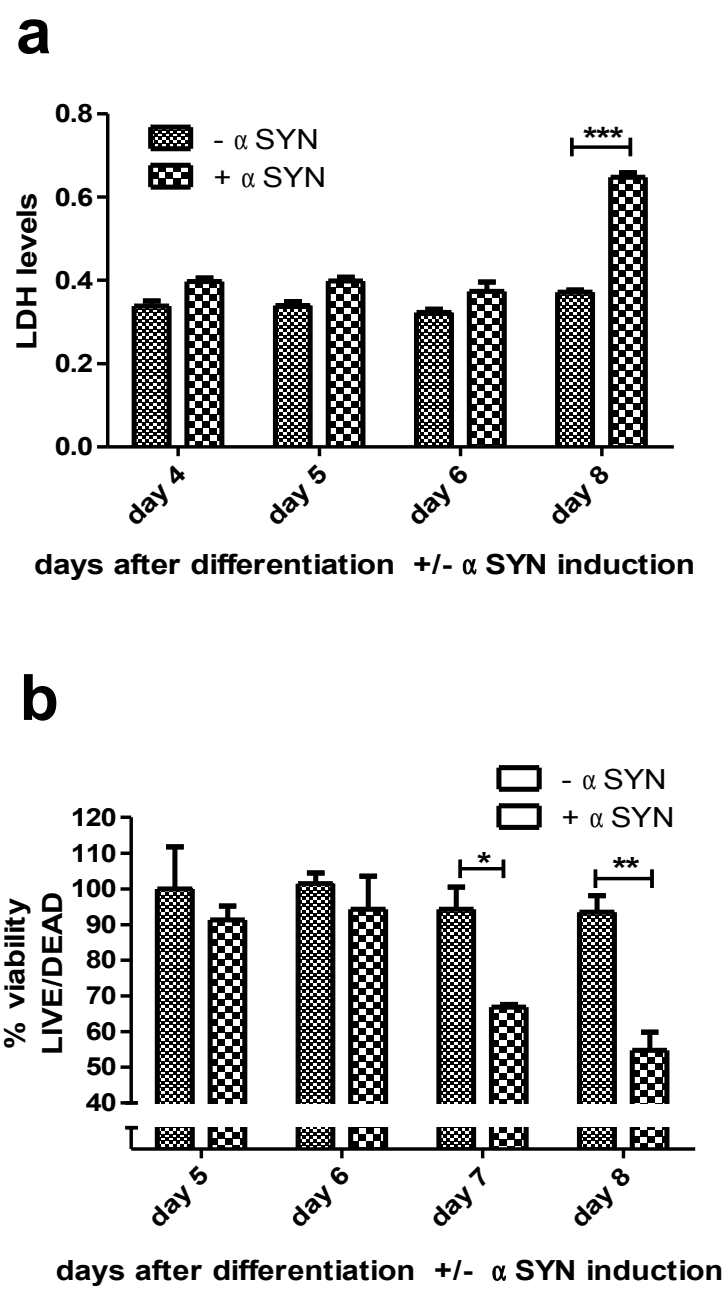

Figure 2. Overexpression of αSYN induces toxicity in differentiated SH-SY5Y cells after 6 days. (a) Culture medium was collected from differentiated SH-SY5Y cells with or without overexpression of αSYN over a time course of 8 days and the levels of LDH in the medium was assayed as a function of cell death (b) Differentiated SH-SY5Y cells

with or without overexpression of αSYN were stained with LIVE/DEAD reagents as a measure of cell viability over a time course of 8 days. *P<0.05, **P<0.01, ***P<0.001; 2 way anova with Bonferroni posthoc analysis. Mean ± SEM, n = 3 experiments.

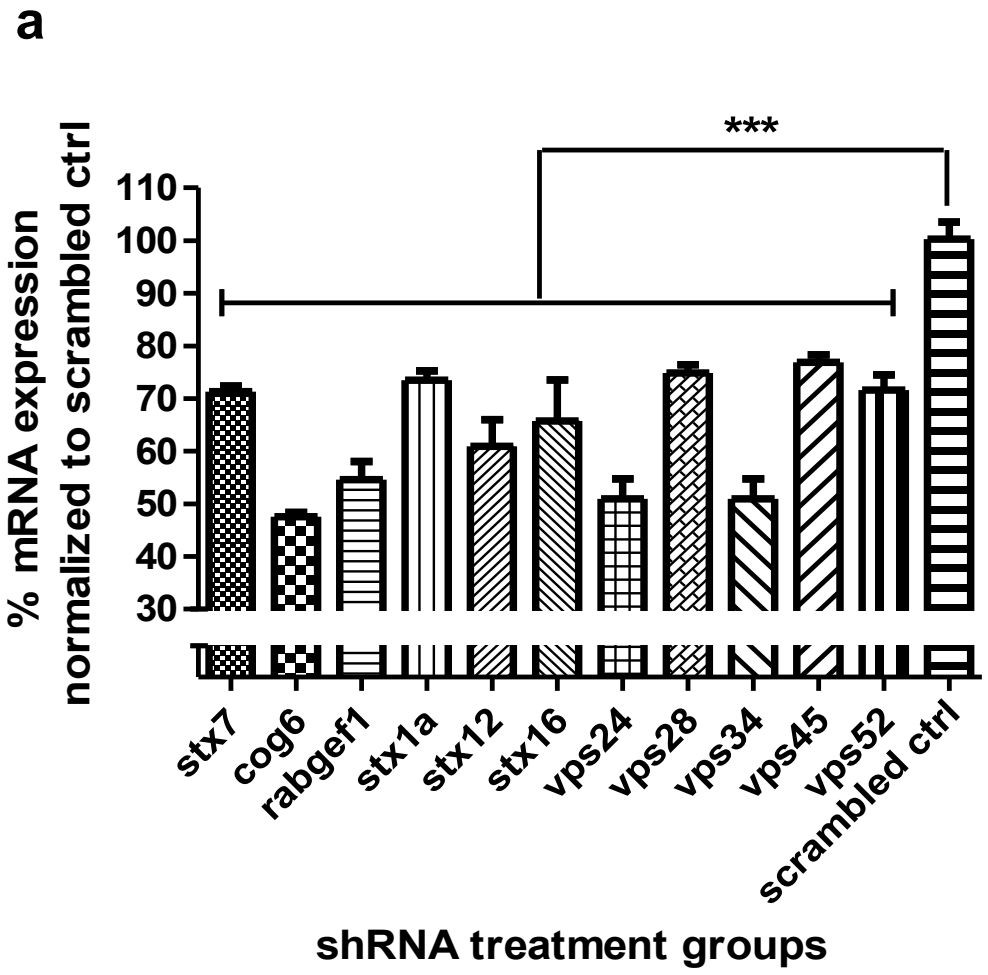
a
***
% mRNA expression
normalized to scrambled ctrl
110
100
90
80
70
60
50
40
30
stx7
cog6
rabgef1
stx1a
stx12
stx16
vps24
vps28
vps34
vps45
vps52
scrambled ctrl
shRNA treatment groups

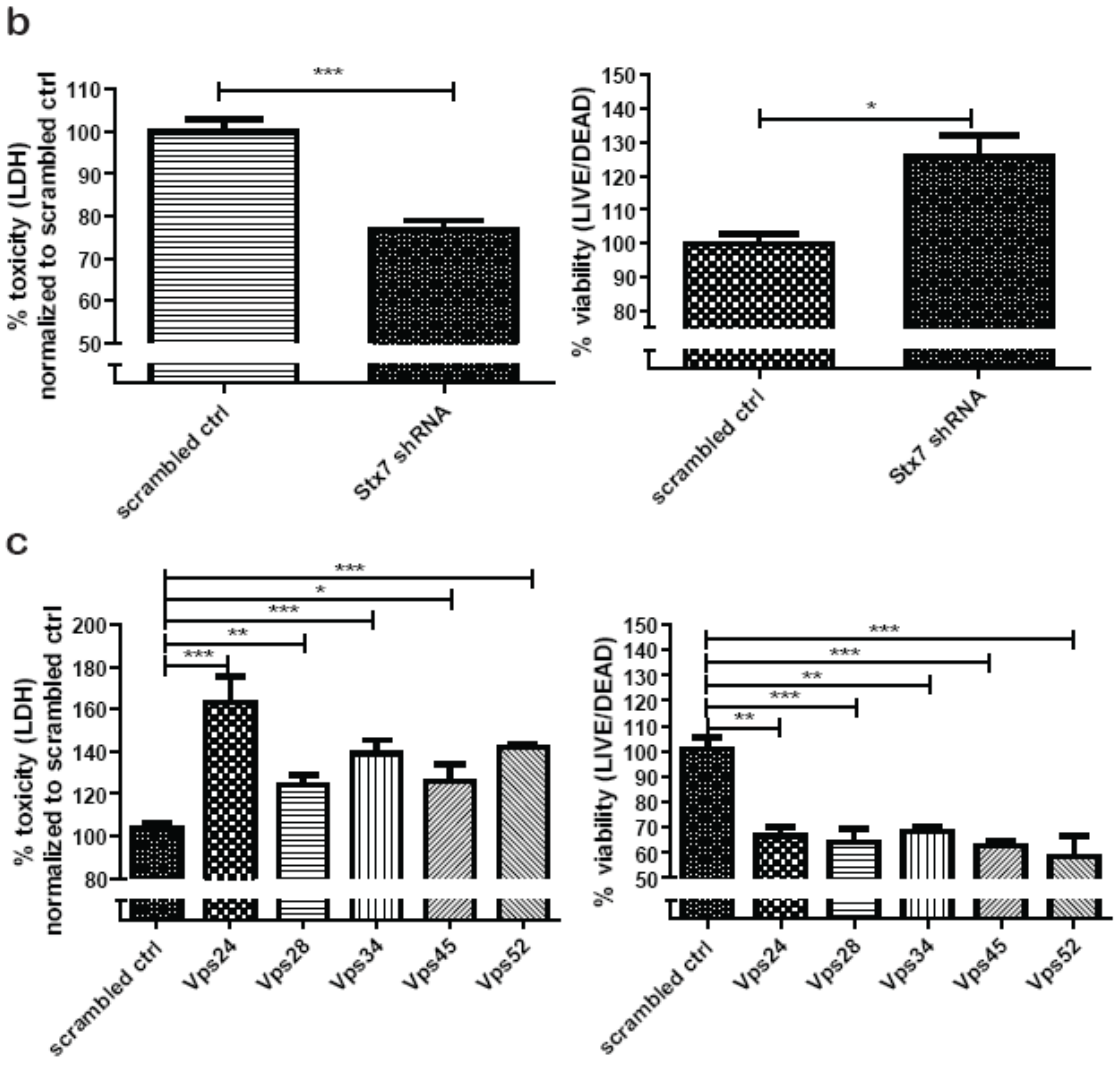

Figure 3. Knock down of gene expression of human orthologs of yeast genetic modifiers modulates αSYN-induced toxicity in differentiated SH-SY5Y cells. Culture medium was collected from cells 7 days after differentiation and toxicity was assayed by the levels of LDH present. (a) Transfection of shRNA against vesicle trafficking genes results in 30-50% decrease in gene expression compared to scrambled shRNA control, which was set to 100%. *** P<0.001, one way ANOVA. (b) Knock down of Stx7 gene

expression decreased αSYN-induced toxicity in differentiated cells compared to cells transfected with scrambled shRNA control in the LDH and LIVE/DEAD assays. (c) Knock down of gene expression of human Vps genes showed significant increases in α SYN-induced toxicity compared to cells transfected with scrambled shRNA control in the LDH and LIVE/DEAD assays. **P<0.01, ***P <0.001, Student's t-test. Mean ± SEM, n = 3 experiments.

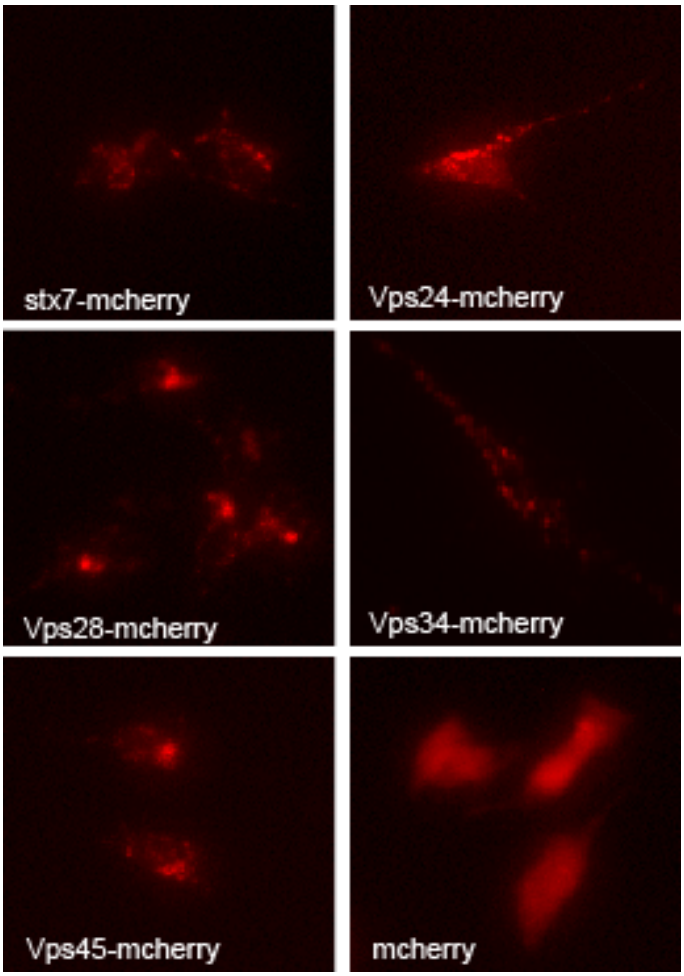

Figure 4. Expression of genetic modifier fusions to mcherry in SH-SY5Y cells.

Punctate localization of mcherry tagged Stx7, Vps24, Vps28, Vps34, Vps45 and mcherry in SH-SY5Y cells consistent with their predicated localization pattern.

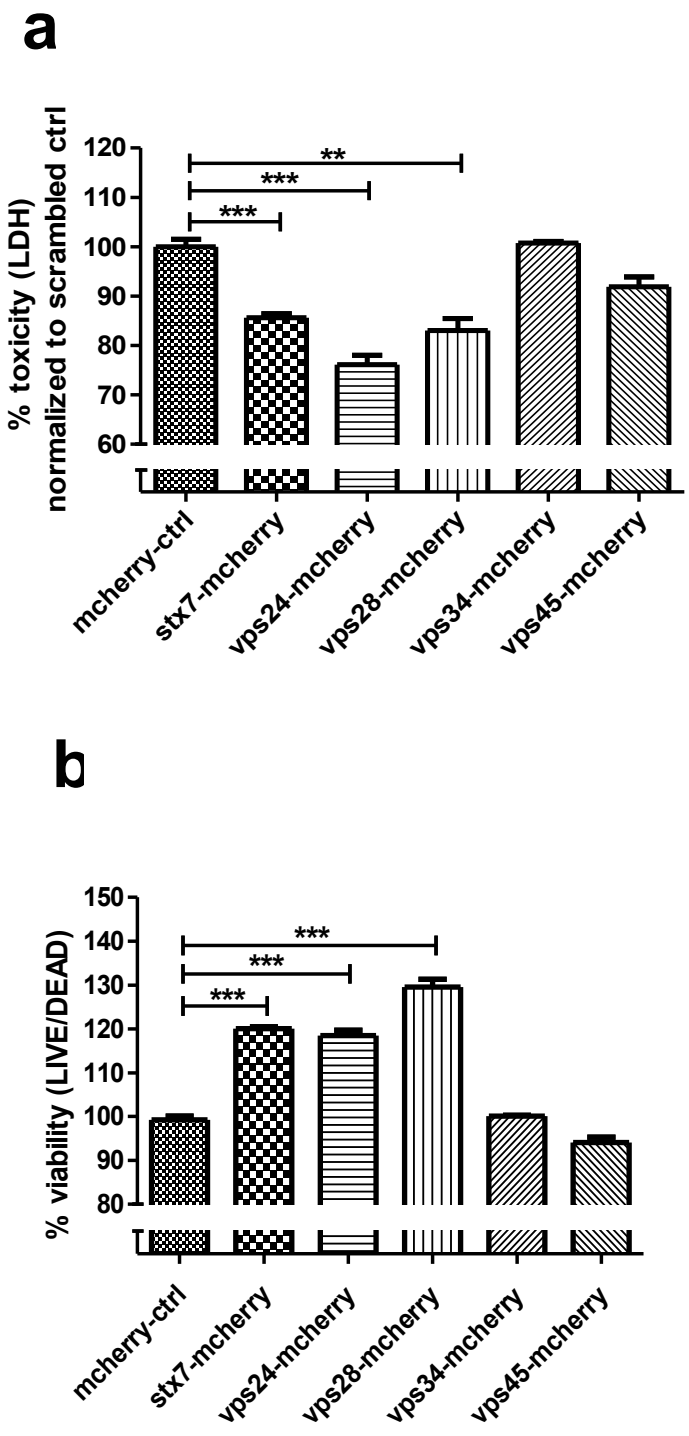

Figure 5. Expression of Vps genes is sufficient to rescue αSYN toxicity in SH-SY5Y cells. SH-SY5Y cells transfected with mcherry-tagged Stx7, Vps24, Vps28, Vps34,

Vps45 and the mcherry vector and differentiated for 7 days were assayed for αSYN-induced toxicity by the (a) LDH assay and (b) LIVE/DEAD assay. **P<0.01, ***P<0.001, Student's t-test. Mean n ± SEM, n = 3 experiments.

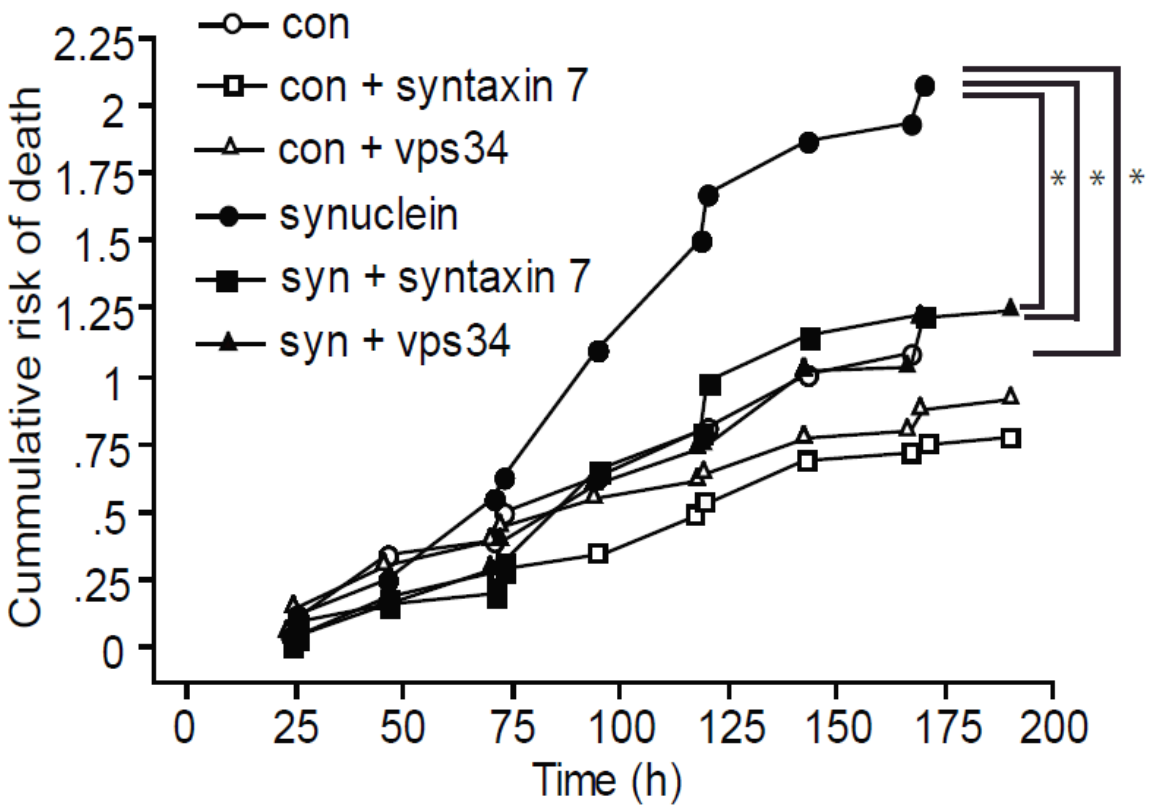

Figure 6. Overexpression of Stx7 and Vps34 rescues αSYN toxicity in rat cortical neurons. Rat cortical neurons were transfected five days after plating with Venus (a variant of yellow fluorescent protein), αSYN (SYN) or vector control (con), and either with or without modifiers Vps34 or Stx7. Cumulative risk of death curves indicate that primary neurons expressing αSYN have a significantly greater risk of death than control cells (*$p < 0.0001$, log-rank test). Overexpression of Vps34 and Stx7 significantly reduced αSYN-induced toxicity (*$p < 0.0001$). Neurons were combined from 3

independent experiments and p values were calculated with the log rank test, n = 115-200 neurons per group.

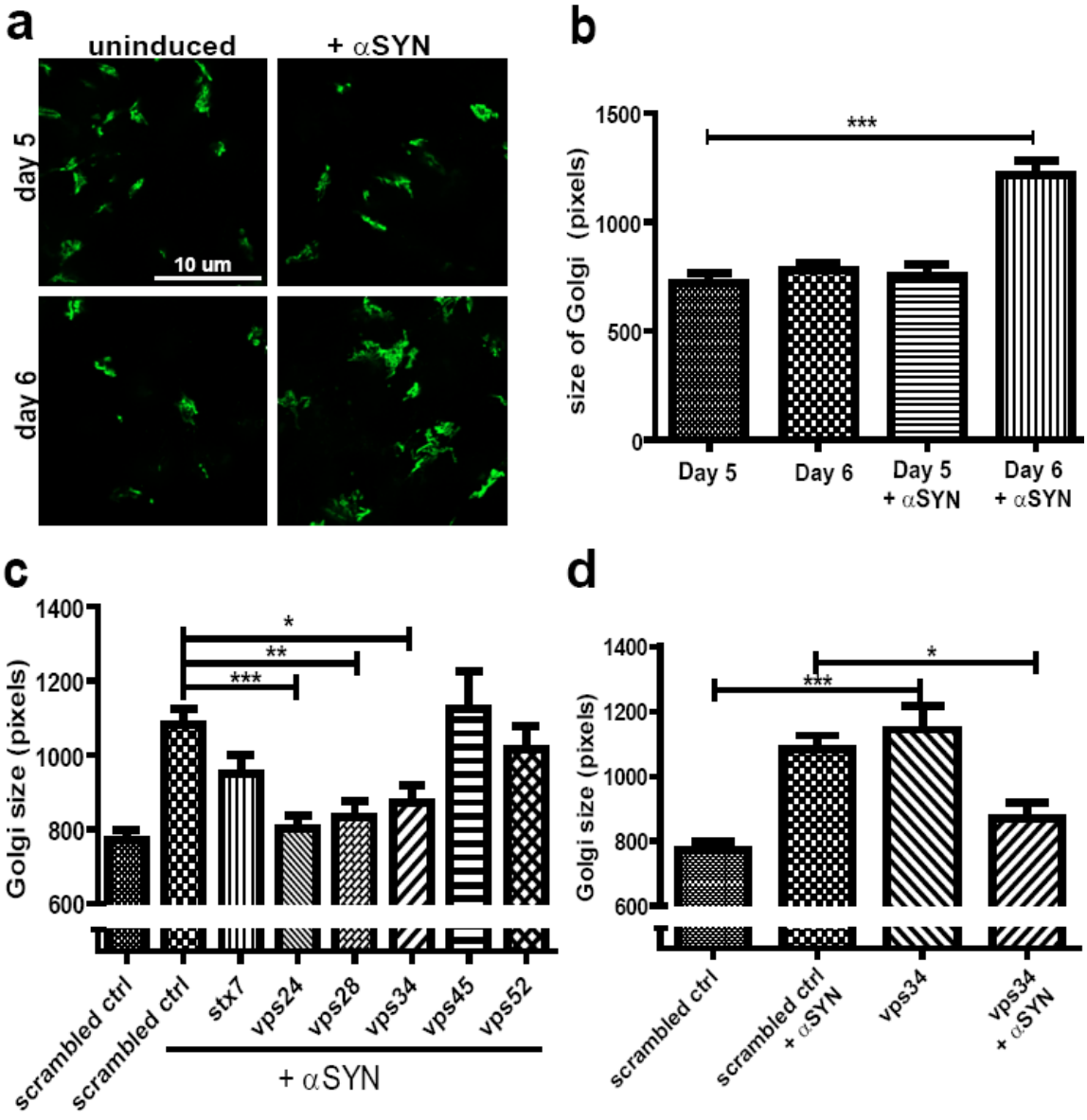

Figure 7. αSYN-induced Golgi abnormalities do not correlate with modulation of toxicity by genetic modifiers. (a) Confocal microscopy of SH-SY5Y cells 5 or 6 days post differentiation with or without overexpression of αSYN stained with αGM130. (b) Quantification of Golgi surface area. ***P<0.001, one way ANOVA. Mean ± SEM, n= 3 experiments, > 50 cells per experiment. (c) Quantification of the effect of knocking down expression of vesicle trafficking genes on αSYN-induced Golgi phenotype in SH-SY5Y

cells 6 days post differentiation. (d) Quantification of Golgi size in day 6 post-differentiation SH-SY5Y cells without without αSYN-overexpression transfected with scrambled shRNA or Vps34 shRNA. *P <0.05, **P<0.01, ***P<0.001, Student's t-test. Mean ± SEM, n = 3 experiments. 1 pixel represents 61 nm.

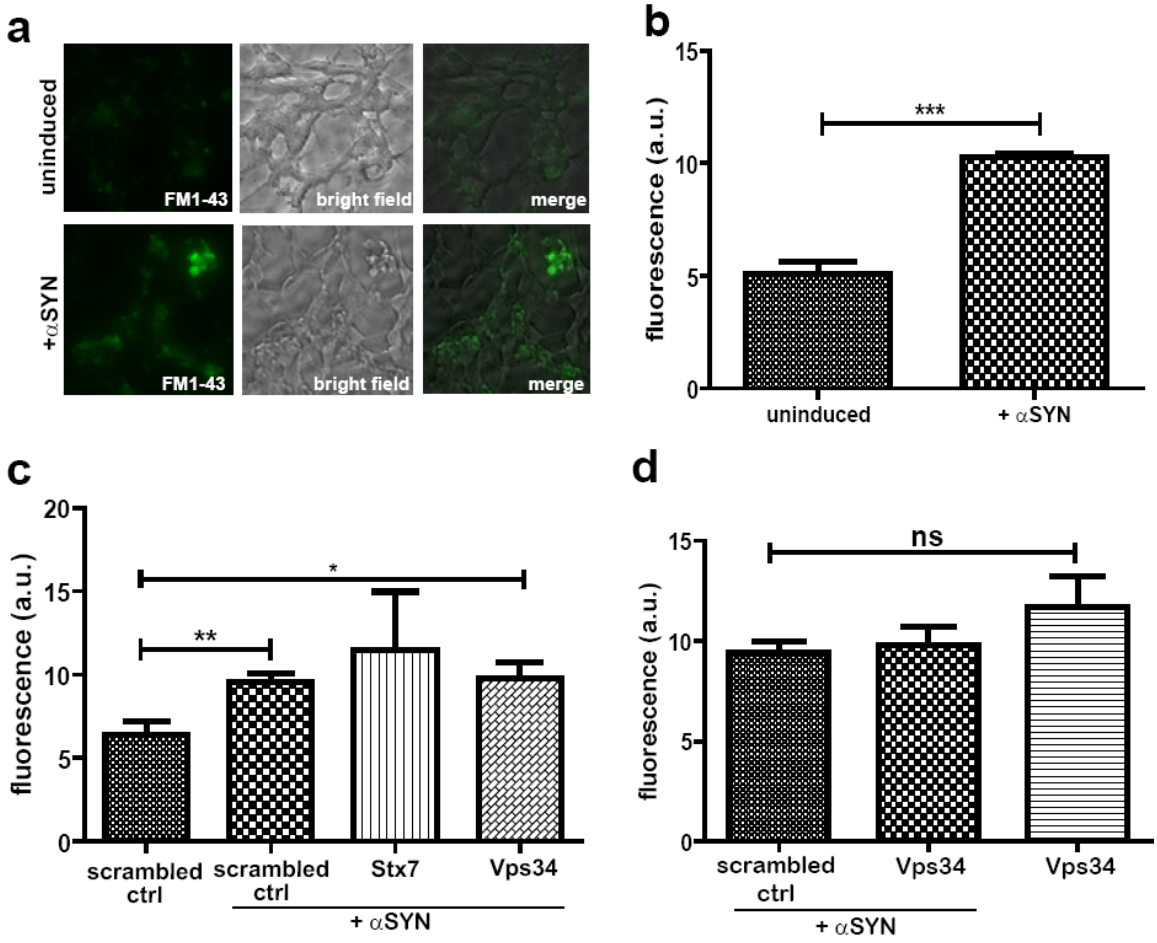

Figure 8. αSYN-induced exocytosis impairment does not correlate with modulation of toxicity by genetic modifiers. (a) Retention of FM1-43 in differentiated SH-SY5Y cells with or without αSYN overexpression following KCl depolarization. (b) Quantification of FM1-43 fluorescence intensity. (c) Retention of FM1-43 in SH-SY5Y cells transfected with shRNA against Stx7 and Vps34 with or without αSYN overexpression 6 days post differentiation. *P<0.05 **P<0.01 ***P<0.001, Student's t-test. Mean ± SEM, n = 3 experiments, 4 fields per experiment. (d) Quantification of FM1-43 fluorescence intensity in day 6 post-differentiation SH-SY5Y cells with or without αSYN-overexpression transfected with scrambled or Vps34 shRNA.

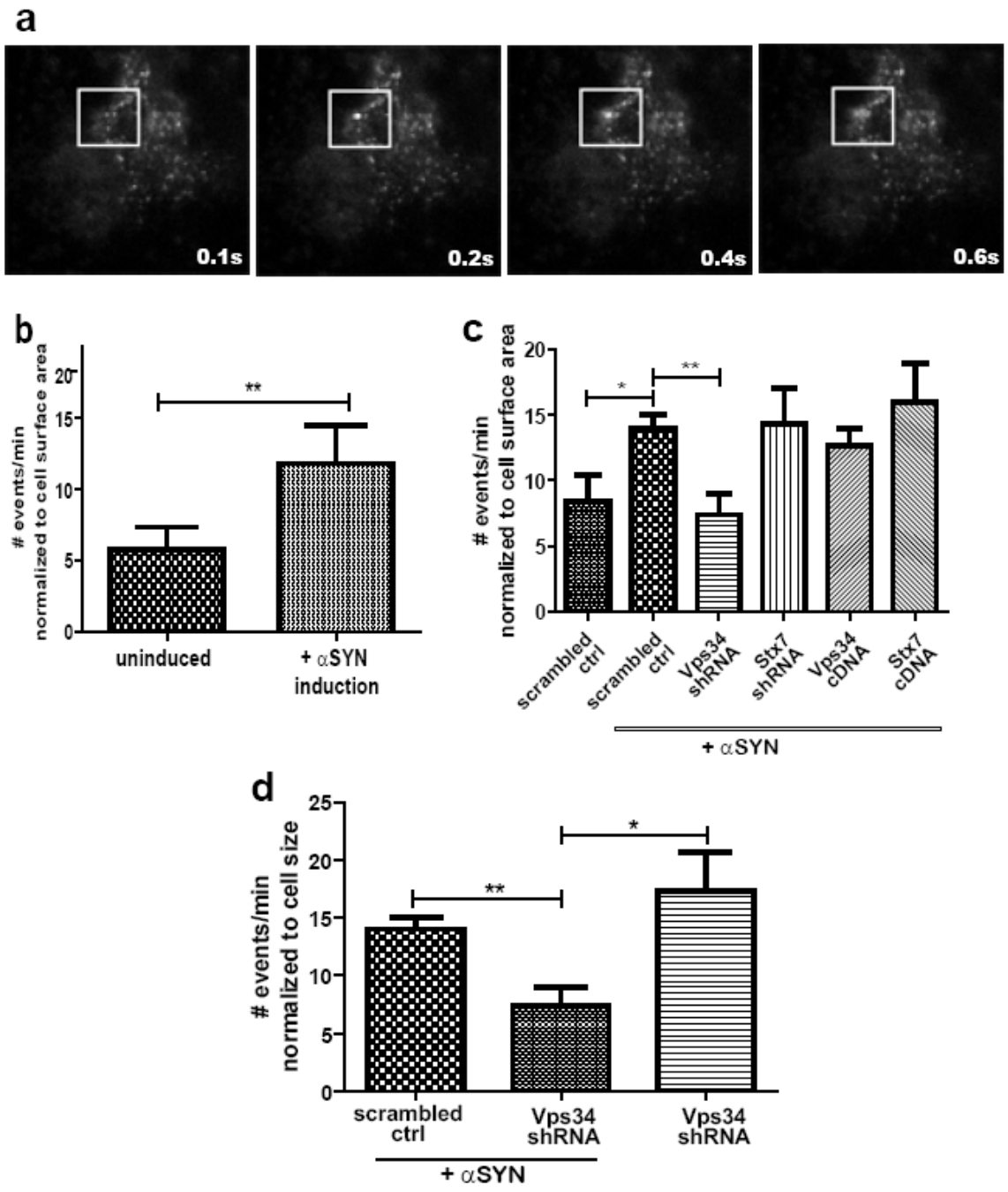

Figure 9. Overexpression of αSYN induces increased transferrin receptor (TfR) recycling in differentiated SH-SY5Y cells. (a) Rapid TIR-FM image series of differentiated SH-SY5Y cell exprsesing TfR. Boxed area show representative TfR

exocytic insertion event in the plasma membrane. (b) Quantification of TfR exocytic insertion events per minute normalized to cell surface area. **P<0.01, Student's t-test. Mean ± SEM, n > 12 cells per condition. (c) Quantification of TfR exocytic insertion events per minute normalized to cell surface area in αSYN-induced cells transfected with shRNA against or overexpression constructs for Stx7 and Vps34 6 days after differentiation. *P<0.05 **P<0.01, Student's t-test. Mean ± SEM, average n = 8 cells per condition. (d) Quantification of TfR exocytic insertion events per minute normalized to cell surface area in cells transfected with shRNA against Vps34 in cells with or without αSYN induction. *P<0.05, **P<0.01, Student's t-test. Mean ± SEM, average n = 8 cells per condition.

CHAPTER 4 – CONCLUSIONS AND FUTURE DIRECTIONS

CHAPTER 4 – CONCLUSIONS AND FUTURE DIRECTIONS

Our initial genetic and cell biological analyses in yeast suggest that αSYN disrupts the endosomal trafficking of transmembrane proteins destined for intravacuolar degradation. Based on the observation that loss-of-function alleles (*Vps24Δ, Vps28Δ, Vps60Δ)* of genes encoding distinct subunits of endosomal sorting (ESCRT) complexes required for transport exacerbate αSYN-induced growth defects in yeast, we hypothesized that αSYN pathogenesis in neuronal cells is driven, at least in part, by a similar endosomal trafficking defect. Indeed, we found evidence of endo-exocytic trafficking abnormalities in differentiated neuroblastoma cells that could be the direct result of, or possibly arose as a compensatory mechanism for, toxic αSYN accumulation. In validation of our yeast studies, we also showed that human orthologs of the ESCRT genes and others also involved in the endosomal protein trafficking pathways (Vps34, Vps45, Vps52, Stx7) are able to modulate αSYN-induced toxicity through complementary shRNA knock down and overexpression experiments.

Although the degeneration of dopaminergic neurons in PD appear to be specific to their biology, there may be a more basic biological explanation underlying PD and αSYN pathogenesis. The proper trafficking of proteins and membranes is especially critical in highly polarized cells like neurons, which have morphologically segregated compartments of the axon and dendrites for specialized functions. A general trafficking impairment that disrupts the fine-tuned balance of neurons would thus have devastating consequences. Dopaminergic neurons, which are the primary target cells in PD would be especially sensitive to disruptions in vesicle trafficking as dopamine is a neurotransmitter

prone to producing reactive oxygen species in the cytoplasm of the cell unless sequestered into vesicles.

The accumulation of vesicles, similar to our observations in yeast, have long been observed in neurons before Lewy body formation in early stages of the disease (Hayashida et al., 1993), and in close proximity to Lewy bodies in later stages of the disease (Watanabe et al., 1977). Furthermore, the consequences of a malfunctioning protein trafficking system have been characterized in various neurological diseases. Mutations in the charged multivesicular body protein 2B (CHMP2B), a subunit of the human ESCRT-III complex together with Vps24, are linked to autosomal dominant forms of frontotemporal dementia (Skibinski et al., 2005). Further, Almeida et al. (2006) documented defects in multiivesicular body sorting in a neuronal model of β-amyloidopathy. Similarly, deletion of the lipid kinase Vps34, which produces the PI3P responsible for targeting ESCRT-I complex to endosomes (Katzmann et al., 2003), gives rise to rapid neurodegeneration in mice (Zhou et al., 2010). Mice lacking in Vac14, a regulator of PI(3,5)P2 synthesis also experience drastic loss of midbrain and peripheral sensory neurons (Zhang et al., 2007). In addition, mutations in SNARE proteins have been implicated in neurological disorders, such as schizophrenia and the CEDNIK syndrome (Saito et al., 2001; Sprecher et al., 2005).

A basic understanding of the pathogenic mechanism of αSYN may lead to the identification of novel drug targets and even drugs. Our studies illustrate the novel findings that trafficking at the early endosome is critical to αSYN toxicity, and that we

can modulate αSYN toxicity by altering levels of genetic modifiers regulating endosomal trafficking. Validation of these results *in* vivo would have tremendous implications for the treatment of PD and would provide potential pharmacologic targets for early therapeutic intervention of PD.

METHODS

METHODS

Chemicals and antibodies

The reagents were from Sigma unless specified. The mouse monoclonal GM130 antibody was from BD Biosciences. The mcherry antibody was from Clontech. The p42/44 map kinase antibody was from Cell Signaling Technology. The mouse monoclonal alpha-SYNuclein antibody was from BD Biosciences. AlexaFluor® 488-, 555-, and 647-conjugated goat anti-mouse secondary antibodies, and HRP-conjugated secondary anti-mouse and anti-rabbit antibodies were from Jackson Immunoresearch.

Plasmids

Plasmids p426GPDαSYN(WT)GFP, p426GALαSYN(WT)GFP, pGS416 (*GFP-SNC1*), pGSSO416 (*GFP-SNC1-SSO1*), pGNS416 (*GFP-NYV1-SSO1*), pPEP416 (*GFP-PEP12*), pPHM5 (*GFP-PHM5*) and pSNA3416 (*SNA3-GFP*) have been described .

Plasmid pSTE2416 was created by replacing the *SNA3* gene from plasmid pSNA3416 with the *STE2* gene as a *Hind*III-*Age*I digested product of PCR amplification.

Plasmid p8xmycSNC1416 (8x*MYC-SNC1*) was created by replacing the *GFP* gene from plasmid pGS416 by the 8x*MYC* sequence as a *Hind*III-*Eco*RI digested product of PCR amplification. Plasmid p8xmycSNC1406 was then created by subcloning the *TPI1pr-8xMYC-SNC1* fusion from plasmid p8xmycSNC1416 into the *Xho*I and *Bam*HI sites of the pRS406 integrating vector . p8xmycSNC1406 was linearized with *Eco*RV for integration.

METHODS

Plasmid pmCheSSO416 (*mCherry-SNC1-SSO1*) was created by replacing the GFP tag from plasmid pGSSO416 with the mCherry gene from plasmid pmCheV5ATG8406 as an *XhoI-EcoRI* fragment. Plasmid pmCheSSO415 was created by then created by subcloning the *TPI1pr-mCherry-SNC1-SSO1* fusion from plasmid pmCheSSO416 into the *Xho*I and *Sac*I sites of the plasmid p415TEF .

Plasmid p423GPDαSYN(WT)GFP was created by subcloning the *SNCA*(WT)-*GFP* fusion from plasmid p426GALαSYN(WT)GFP into the *Spe*I and *Xho*I sites of plasmid p423GPD .

Plasmid p423GPDαSYN(WT) was created by subcloning *SNCA*(WT) from plasmid p426GPDαSYN(WT)GFP into the *Sac*I and *Xho*I sites of p423GPD .

Plasmids p426GALαSYN(S129A)GFP and p426GALαSYN(S129E)GFP were created by recombining PCR-amplified *SNCA*(S129A) and *SNCA*(S129A) (kindly provided by Dr. Robert Edwards, UCSF) into *Bam*HI-linearized p426GALαSYN(WT)GFP. Plasmids pRS304αSYN(WT)GFP, pRS304αSYN(S129A)GFP, pRS304αSYN(S129E)GFP, pRS306αSYN(WT)GFP, pRS306αSYN(S129A)GFP, pRS306αSYN(S129E)GFP, were then created by subcloning the *GAL1pr-SNCA*(WT, S129A and S129E)-*GFP* fusions from the p426GAL-derived plasmids into the *Sac*I and *Kpn*I sites of the integrating vectors pRS304 and pRS306 . Plasmids pRS304(MCS-) and pRS306(MCS-), lacking the multiple cloning site, were created by digesting pRS304 and pRS306 with *Sac*I and *Kpn*I,

blunting the ends with DNA Polymerase I, Large (Klenow) Fragment (New England Biolabs) and re-circularizing the plasmids. pRS304 and pRS306-derived plasmids were linearized with *Eco*RV for integration into the W303-1A strain.

Plasmids pRS405TRP1αSYN(WT)GFP, pRS405TRP1αSYN(S129A)GFP, pRS405TRP1 αSYN(S129E)GFP were generated by sequential insertion of the *GAL1pr-SNCA*(WT, S129A and S129E)-*GFP* fusions from the p426GAL-derived plasmids into the *Sac*I and *Kpn*I sites of the integrating vector pRS405 followed by insertion of the first and the last 300bp of the *TRP1* ORF in inverted order (3'5') separated by a *Xma*I site into the *Sac*I site of plasmid pRS405 for gamma integration into the *TRP1* locus. Plasmid pRS405TRP13'5' was generated by removing the *GAL1pr-SNCA*(WT, S129A and S129E)-*GFP* insert within the *Spe*I and *Xho*I sites, blunting the ends with DNA Polymerase I, Large (Klenow) Fragment (New England Biolabs) and re-circularizing the plasmids.

Plasmids pRS406PDR1αSYN(WT)GFP, pRS406PDR1αSYN(S129A)GFP, and pRS406PDR1αSYN(S129E)GFP were generated by sequential insertion of the *GAL1pr-SNCA*(WT, S129A and S129E)-*GFP* fusions from the p426GAL-derived plasmids into the *Sac*I and *Kpn*I sites of the integrating vector pRS406 followed by insertion of the first and the last 300bp of the *PDR1* ORF in inverted order (3'5') separated by a *Mfe*I site into the *Sac*I site of plasmid pRS406 for gamma integration into the *PDR1* locus. Plasmid pRS406PDR13'5' was generated by removing the *GAL1pr-SNCA*(WT, S129A and S129E)-*GFP* insert within the *Age*I and *Xho*I sites, blunting the ends with DNA

Polymerase I, Large (Klenow) Fragment (New England Biolabs) and re-circularizing the plasmids.

pRS405 and pRS406-derived plasmids were linearized with *Xma*I and *Mfe*I, respectively, for integration into the Y5563 strain.

Plasmids p425GALYPT1 and p425GALYCK1 were created by subcloning *YPT1* and *YCK1* from the Yeast ORF collection (Open Biosystems) into p425GAL (Addgene) using Gateway Technology (Invitrogen).

Plasmid p415YCK1 was created by cloning *YCK1* with its endogenous promoter into plasmid p415TEF as a *Sac*I-*BamH*I digested product of PCR-amplification from yeast genomic DNA.

Yeast strains and manipulation

The strains used in this study are summarized in Chapter 2, table 1.

To generate strain VSY1, the *GAL1pr-SNCA*(WT)-*GFP* fusion was PCR-amplified from plasmid p426GALαSYN(WT)GFP and the *MX4-NatR* cassette was PCR-amplified from plasmid p4339 (kindly provided by Dr. Charles Boone, University of Toronto). Primer sequences were designed to enable the merging of both fragments in a third PCR reaction and the site-directed integration of the resulting *GAL1pr-SNCA*(WT)-*GFP-NatR* fusion at the *ADE2* locus by homologous recombination in the BY4741 strain .

METHODS

To generate strain VSY2, the *GAL1pr-SNCA*(WT)-*GFP* fusion was PCR-amplified from plasmid p426GALαSYN(WT)GFP and the *URA3-MX6* cassette was PCR-amplified from plasmid p4348 (kindly provided by Dr. Charles Boone, University of Toronto). Primer sequences were designed to enable the merging of both fragments in a third PCR-reaction and the site-directed integration of the resulting *GAL1pr-SNCA*(WT)-*GFP-URA3* fusion at the *TRP1* locus by homologous recombination in the Y5563 strain .

To generate strain VSY4, strains VSY1 and VSY2 were crossed. Diploid cells were selected on SD–Ura + G418 (Invitrogen)/ClonNAT (Werner BioAgents) plates and sporulated. Spores were germinated and haploid cells of both mating types were selected in SD – Arg/Lys/Ura + canavanine (Sigma-Aldrich)/thialysine (Sigma-Aldrich)/G418/clonNAT plates. *MAT*□ cells were selected by their inability to grow on SD–His plates and the mating type was subsequently confirmed by mating test.

Strains VSY53-61 were obtained from a cross between strain VSY4 and the corresponding deletion strains.

Strains *pdr1*Δ, *yck1*Δ, *yck2*Δ, *tlg2*Δand *spo14*Δ were retrieved from the Yeast *MAT***a** Genome Deletion Collection (Open Biosystems).

Strain VSY64 was generated by disruption of the *PDR1* gene from strain VSY4 with the *kanMX4* cassette obtained by PCR-amplification of genomic DNA from the strain *pdr1Δ*.

METHODS

Strain VSY65 was generated by disruption of the *kanMX4* cassette from strain VSY57 with the *LEU2* cassette obtained by PCR-amplification from plasmid pRS415.

Strain VSY66 was generated by disruption of the *PDR1* gene from strain VSY65 with the *kanMX4* cassette obtained by PCR-amplification of genomic DNA from the strain *pdr1Δ.*

Strain FRY346 was generated by integration of *Eco*RV-linearized p8xmycSNC1406 plasmid in the BY4741 strain.

Strains VSY67 to VSY74 were generated by consecutive integration of *Eco*RV-linearized pRS306-derived and pRS304-derived plasmids in the W303-1A strain.

Strains VSY75-78 were generated by disruption of the *YCK1* gene from strains VSY71-78 with the *kanMX4* cassette obtained by PCR-amplification of genomic DNA from the strain *yck1Δ.*

Strains VSY79-86 were generated by consecutive integration of *Xma*I linearized pRS405-derived plasmids followed by integration of *Mfe*I-linearized pRS406-derived plasmids in the Y5563 strain.

Strains BY4741 and FRY346 were transformed with the indicated plasmids using the one-step protocol and cultured in SYNthetic complete medium without the corresponding nutrients for auxotrophic selection and with the indicated carbon sources.

METHODS

The integrated strains were transformed using the standard protocol and cultured in rich (YEP) medium with the indicated carbon sources.

Yeast growth curves

The indicated strains were inoculated in triplicate in 100 µl of raffinose-containing medium in 96-well plates and grown for 48 h to stationary phase. Cultures were then diluted 100-fold in raffinose and galactose-containing media and incubated at 30ºC. The OD_{600} was recorded at the indicated times. Growth rates were determined as the slope of the growth curves during logarithmic phase.

Pharmacologic inhibition of CKI activity

For the CKI inhibitor studies, strains *pdr1*Δ (0c αSYN in *pdr1*Δ), VSY64 (2c αSYN in *pdr1*Δ), and VSY65 (2c αSYN in *pdr1*Δ *yck1*Δ) were grown in raffinose-containing medium to stationary phase, diluted to $OD_{600} = 0.1$ in raffinose and galactose-containing media and dispensed in 100 µl aliquots to 96-well plates. Aliquots were treated in triplicate with the indicated concentrations of D4476 (Calbiochem, CA) or vehicle DMSO alone.

Phosphorylation assays

For the time-course experiment, strain VSY4 (2c αSYN in WT) was grown to logarithmic phase (OD_{600}~ 0.8) in raffinose-containing medium and αSYN expression was induced by adding 0.2% galactose. Eight ml aliquots were collected at the indicated times. For protein extraction, cells were collected by centrifugation, washed with water, and resuspended in 200 µl of extraction buffer [200 mM Tris pH 8.0, 150 mM

ammonium sulfate, 10% glycerol, 1 mM EDTA, 1 μM microcystin LR, 200 μM activated Na_3VO_4, and 1x complete protease inhibitor cocktail (Roche)] and 100 μl of acid-washed glass beads (425–600 μm) (Sigma-Aldrich). Cells were lysed by vortexing two times for 5 min at 4ºC. Supernatants were separated from cell debris and beads by centrifugation at 5,000 rpm for 5 min and then cleared by centrifugation at 13,000 rpm for 30 min. The soluble fractions (supernatant) were separated by SDS-PAGE and proteins analyzed by immuno-blot with mouse anti-αSYN (1:20,000) (BD Transduction Laboratories) and anti-S129 phospho-specific antibodies (1:20,000) (JH22.11A5, Elan Pharmaceuticals).

For comparison of αSYN phosphorylation levels in different deletion backgrounds, strains VSY4, VSY57, VSY58 and VSY60 were grown to logarithmic phase (OD_{600}~ 0.8) in raffinose-containing medium and αSYN expression was induced by adding 0.2% galactose for 1 h. Samples were treated as described before and soluble fractions were analyzed by western blot. Band densities were quantified with ImageQuant 5.2 (Molecular Dynamics).

To assess αSYN phosphorylation in *YCK1* overexpressing cells, the indicated strains were grown for 12 h to logarithmic phase in raffinose-containing medium and induced with 2% galactose. Ten ml aliquots were collected at 5.5 h and 11 h. When indicated, cultures were treated with 500 nM microcystin and 200 μM cell-permeable Na_3VO_4 for 15 min prior to cell harvesting. Samples were analyzed as described before.

METHODS

Analysis of αSYN levels in yeast

Strains VSY67-74 and VSY79-86 were grown to logarithmic phase in raffinose-containing medium and induced with 2% galactose for 8 h. Samples were processed and analyzed by western immuno-blot as described before.

Analysis of αSYN, Rab5, Rab4, EEA1 and CK1δ cellular levels

Brain homogenates were solubilized in lysis buffer (1% Triton X-100, 10% glycerol, 50 mM HEPES, pH 7.4, 140 mM NaCl, 1 mM EDTA, 1 mM Na_3VO_4, 20 mM β-glycerophosphate, and proteinase inhibitor cocktails), and separated into cytosolic and particulate fractions by centrifugation. Twenty mg of the particulate fractions were resolved by SDS-PAGE and blotted onto membranes before be decorated with rabbit polyclonal anti-αSYN (Chemicon), mouse monoclonal anti-Rab5 (BD Transduction Laboratories), mouse anti-human EEA1 (BD Transduction Laboratories), mouse anti-human Rab4 (BD Transduction Laboratories), goat anti-CK1δ (C-18) (Santa Cruz Biotechnology), and mouse monoclonal anti-actin (Chemicon).

Mouse models

For this study, 12 heterozygous transgenic (tg) 6 month old mice expressing human αSYN under the regulatory control of the platelet-derived growth factor-β (PDGFβ) promoter (Line D) and 12 littermate non transgenic (non-tg) age-matched controls were used. These animals were selected because they display abnormal accumulation of detergent-insoluble αSYN, develop cytoplasmic αSYN-immunoreactive inclusion-like structures in the brain, and display neurodegenerative and motor deficits that mimic

certain aspects of DLB/PD. Comparisons of the patterns of αSYN and Rab5 distribution were performed with 6 tg 6 months old mice that mimic AD-like pathology by expressing the human mutant amyloid precursor protein (APP) (line 41) under the thy1 promoter .

Human cases and neuropathological evaluation

This study examined a total of 18 subjects (Table II), including 8 cases of dementia with Lewy bodies (DLB/PD), 6 cases of Alzheimer's disease (AD) and 4 non-demented controls. Autopsy material was obtained from patients studied neurologically and psychometrically at the Alzheimer Disease Research Center/University of California, San Diego (ADRC/UCSD). For each case, paraffin sections from 10% buffered formalin-fixed neocortical, limbic system and sub-cortical material stained with haematoxylin and eosin (H&E) and thioflavin-S were used for routine neuropathological analysis that included Braak stage. The diagnosis of DLB/PD was based on the clinical presentation of dementia followed by parkinsonism and the pathological findings of Lewy bodies (LBs) in the locus coeruleus, substantia nigra (SN), or nucleus basalis of Meynert, as well as in cortical and subcortical regions. LBs were detected using H&E anti ubiquitin and anti α SYN antibodies as recommended by the Consortium on DLB criteria for a pathologic diagnosis of DLB/PD. In addition to the presence of LBs, the great majority of these cases display sufficient plaques and tangles to be classified as Braak stages III-IV. Specifically, DLB/PD cases had abundant plaques in the neocortex and limbic system but fewer tangles compared to AD cases.

METHODS

Fluorescence microscopy of yeast

For the S129 mutagenesis study, strains VSY67-74 were grown to stationary phase at 30°C in raffinose-containing medium and diluted 100-fold in galactose-containing medium. Cells were induced for 16 h, mounted and sealed as described.

For the trafficking studies, strain BY4741 cotransformed with plasmids p423GPDαSYN(WT) or p423GPF and pGS416 (*GFP-SNC1*), pGSSO416 (*GFP-SNC1-SSO1*), pGNS416 (*GFP-NYV1-SSO1*), pPEP416 (*GFP-PEP12*), pPHM5 (*GFP-PHM5*), pSNA3416 (*SNA3-GFP*) or pSTE2416 (*GFP-STE2*), was grown for 12 h to logarithmic phase at 30°C in glucose-containing medium and mounted as described. Strains BY4741, *yck1*Δ, VSY4 and VSY57 transformed with plasmid pmCheSSO416 (*mCherry-SNC1-SSO1*) were grown for 12 h to logarithmic phase at 30°C in galactose-containing medium and mounted as described.

For FM 4-64 labeling, the indicated strains were grown for 12 h in medium containing glucose [deletion and temperature-sensitive mutant strains transformed with plasmid pGSSO416 (*GFP-SNC1-SSO1*)] or galactose (strains VSY71-74) at 30°C (deletion strains and VSY71-74) or room temperature (temperature sensitive strains). A total of 0.16 culture ODs were centrifuged and resuspended in 40 µl of medium containing 40 µM FM 4-64 to a final OD_{600} of 4.0. Cells were pulsed with the dye for 15 min, washed with 1 ml of H_2O, resuspended in 0.5 ml of unlabeled medium and incubated for 1 h to let the dye internalize. The deletion and VSY71-74 strains and were labeled at 30°C whereas the temperature sensitive strains were pre-incubated at 37°C or room temperature for 30

min prior to the FM 4-64 pulse and kept at the same temperature throughout all the steps for imaging.

For the rescue studies, strain BY4741 cotransformed with plasmids p423GPDα SYN(WT) or p423GPF alone, and pGSSO416 (*GFP-SNC1-SSO1*), was transformed with plasmids p425GALYPT1, p425GALYCK1 or left untransformed (No plasmid). Cells were grown in glucose-containing medium at 30°C to stationary phase and diluted down 20-fold in galactose-containing medium. Cultures were induced for 16 h and prepared for imaging as described.

For the mutagenesis, trafficking, rescue and FM 4-64 studies, cells were imaged with a Nikon Plan Apo VC 100x (N.A. 1.4) objective on a spinning disk confocal microscope (Nikon) and images were acquired with a Cascade II digital camera (Photometrics) using Micro-Manager 1.3 (University of California, San Francisco).

Immunoelectron microscopy of yeast

For single labeling, strain BY4741 transformed with the plasmid p426GALαSYN(WT)GFP was grown at 30°C in glucose-containing medium to early logarithmic phase, washed with water, resuspended in galactose-containing medium, and incubated for 6 h or 12 h. For double labeling, the strain FRY346 transformed with plasmid p423GPDαSYN(WT)GFP was grown for 12 h at 30°C in glucose-containing medium to logarithmic phase. In both cases, cells were fixed with 2% glutaraldehyde-0.2% para-formaldehyde and prepared for the Tokuyasu cryosectioning procedure

according to a protocol optimized for *S. cerevisiae*. Ultrathin sections were incubated first with antibodies recognizing the tags and subsequently with protein A-gold conjugates . After standard staining with uranyl and embedding in methylcellulose, sections were visualized in a JEOL 1010 electron microscope (JEOL) and images were recorded on Kodak 4489 sheet films.

For single labeling, a polyclonal anti-GFP antiserum was used (Abcam). For double labeling, a monoclonal anti-myc antibody (Santa Cruz Biotechnology) and the same anti-GFP antiserum were used. Untransformed cells were treated in the same way and used as background controls.

Immunofluorescence of mammalian cells

For the co-localization studies, sections from the temporal cortex of DLB/PD and control cases and from αSYN tg and non-tg mice were used. Free-floating 40 mm thick vibratome sections were washed with Tris buffered saline (TBS, pH 7.4), pre-treated in 3% H_2O_2, and blocked with 10% serum (Vector), 3% bovine serum albumin (Sigma-Aldrich), and 0.2% gelatin in TBS-Tx.

Double-immunofluorescence analyses were performed utilizing the Tyramide Signal Amplification™-Direct (Red) system (NEN Life Sciences). Specificity of this system was tested by deleting each primary antibody. For the Rab5 studies, sections were double-labeled with monoclonal antibodies against αSYN (1:20,000) (Cell Signaling) and Rab5 (1:75) (Vector), and detected with Tyramide Red and fluorescein isothiocyanate

(FITC)-conjugated secondary antibodies (1:75) (Vector), respectively. For the CKI□ studies, sections were double-labeled with the polyclonal antibodies against αSYN (1:200) (Chemicon) and CKIδ (C-18) (Santa Cruz Biotechnology), and detected with FITC and Tyramid Red-conjugated secondary antibodies (1:75) (Vector), respectively. Sections were imaged with a Zeiss 63X (N.A. 1.4) objective on an Axiovert 35 microscope (Zeiss) with an attached MRC1024 laser scanning confocal microscope (LSCM) system (BioRad). All sections were processed simultaneously under the same conditions and experiments were performed twice for reproducibility.

Construction of RNA interference plasmid & mcherry-tagged proteins

The pSilencer plasmid (gift from Dr. L. Gan, Gladstone Institute of Neurological Disease, San Francisco, CA) was used to construct the RNAi plasmid. Each shRNA insert was designed as a synthetic duplex with 18-22-nucleotide oligonucleotides corresponding to gene-specific sequences of each genetic modifier between an inverted motif that contains the six-nucleotide spacer and five Ts and cloned into the pSilencer plasmid with *EcoR*I and *Xho*1. Four shRNA constructs were generated per gene and sequenced for accuracy. The shRNA constructs that best suppressed gene expressions were used in subsequent experiments. The following nucleotides were used:

Cog6 forward: TTGTACGCAAGAGAACTTTGAC, reverse:
GTCAAAGTTCTCTTGCGTACAA;

Rabgef1 forward: GCAGCAAGCACATCTTCAATGC, reverse:
GCATTGAAGATGTGCTTGCTG;

METHODS

Stx1a forward: AGAACTCATGTCCGACATAAA, reverse:

TTTATGTCGGACATGAGTTCT;

Stx7 forward: TGATGATTCATGAACAAGG, reverse: CCTTGTTCATGAATCATCAC;

Stx12 forward: TTTTCCTTTTCAGATACCCTTC, reverse:

GAAGGGTATCTGAAAAGGAAAA;

Stx16 forward: TTGTCACACCAATCGCTGCTTCTCGA, reverse:

TCGAGAAGCAGCGATTGGTGTGACAA;

Vps24 forward: CTTCCTGATCGTCCATGCTTTC, reverse:

GAAGAAAGCATGGACGATCAGGAAG;

Vps28 forward: GTGAAGTTGTACAAGAACG, reverse: CGTTCTTGTACAACTTCA;

Vps34 forward: TCAACATTGGGTCTTCCAGGACAGC, reverse:

GCTGTCCTGGAAGACCCAATGTTGA;

Vps45 forward: ATACCGCGTGTGATTTATT, reverse: AATAAATCACACGCGGTA;

Vps52 forward: CTAGATAAGAATCCAGGTG, reverse: CACCTGGATTCTTATCTAG;

scrambled forward: TATAAATTACGTAGT, reverse: ACACTACGTAATTTATACACC

Full-length cDNA stx7, Vps24, Vps28, Vps34 and Vps45 plasmids were from Openbiosystems and sub-cloned into pcDNA3.1(-) vector from Invitrogen *Not*I and *Xba*1 or *Not*I and *Xho*1 with mCherry cloned in the *Kpn*I site.

Cell Culture and transfection

SH-SY5Y cells stably transfected with inducible αSYN (gift from Dr. L. Stefanis, Department of Neurology, University of Athens medical school, Athens, Greece) were

cultured in RPMI 1640 (Invitrogen, UCSF Cell Culture Facility), 10% fetal bovine serum (FBS) (Gibco) and 250 μg/mL G418 (Invitrogen) and 50 μg/mL Hygromycin B (UCSF Cell Culture Facility). αSYN expression was switched off with 2 μg/mL doxycycline (UCSF Cell Culture Facility). Cells were differentiated with 20μM all-trans retinoic acid (Invitrogen). Transient transfections on SH-SY5Y cells were carried out using lipofectamine 2000 (Invitrogen).

For primary neuronal survival studies primary cortical neurons were prepared from embryonic day 20-21 timed pregnant rats (Charles River Laboratories), cultured in Neurobasal-A with B27 (Invitrogen) for 5 days and transfected with lipofectamine2000. For the analysis of neuronal survival, images were taken at 12-24 hr intervals using an automated microscope with image acquisition and analysis using Metamorph and custom-designed programs. Transfected neurons were selected for analysis based on fluorescence intensity and morphology, including the presence of extended processes at the start of the experiment. Neuronal death was determined by the changes in neuronal morphology that included cell body fragmention and the ultimate loss of the venus signal. Survival time was determined as the last time point at which the neuron was seen alive. For statistical analysis, StatView software was used to construct Kaplan-Meier curves from the survival data. Survival functions were fit to these curves and used to derive cumulative hazard (or risk of death) curves. Differences in cumulative risk of death curves were analyzed for statistical significance with the log-rank test, and each of the experiments was performed independently 3 times.

METHODS

Toxicity assays

In the case of the LIVE/DEAD assay, cell cultures were exposed to components of the LIVE/DEAD kit (Molecular Probes) for 30 min at room temperature. Fluorescence intensity corresponding to viable and non-viable cells in three separate wells were then assayed using a fluorescent plate reader. In the case of the LDH assay, culture media was replaced by RPMI 1640 containing 1% FBS 24 hours prior to the start of the assay. Cell culture media was collected and exposed to the components of the LDH assay kit (Roche) and absorbance corresponding to cell death was assayed in three separate wells using a fluorescent plate reader. All experiments were repeated in triplicate and reported as mean ± SE.

Cell lysis and immunoblotting

Cells were washed twice with ice-cold PBS and lysed with NP-40 buffer (50mM Tris, pH7.6, 150mM Nacl, 1% Triton X-100, 2mM EDTA, protease inhibitors) on ice for 20 min before centrifugation at 14,000x *g* for 30 min. Protein concentrations of supernatant were determined using the Bradford method (Bio-Rad). Protein samples were resolved on pre-cast SDS-PAGE gels in Bis-Tris glycine buffer (Invitrogen) and transferred to nitrocellulose membrane. Blots were blocked in 5% non-fat dry milk in PBS with 0.1% Tween 20 (PBST) for 30 min. The blots were then incubated with primary antibodies overnight at 4^{o}C or 1 hour at room temperature. The blots were then washed three times with PBST and incubated with HRP-conjugated secondary antibodies for 1 hour at room temperature. The blots were washed with PBST for at least 1 hour and developed with the ECL-Plus chemiluminescence kit (Amersham).

METHODS

Immunocytochemistry

Cells were plated onto poly-D-lysine coated glass coverslips and cultured according to experiment requirements. The cells were fixed with 4% paraformaldehyde (PFA) for 10 min at room temperature and washed 3 times with wash buffer (PBS with 5% FBS and 0.1% Triton 100). The cells were then blocked in wash buffer for 10 min and stained with GM-130 antibody diluted in wash buffer (1:200) for 1 hour at room temperature. After rinsing with wash buffer three times, cells were incubated with AlexaFluor® 488 conjugated secondary antibodies diluted in wash buffer (1:200) for 1 hour at room temperature. The coverslips were then washed three times with wash buffer and once with PBS then mounted with vectashield with DAPI (Vecta Labs). The images were acquired by confocal microscopy (Nikon Eclipse Ti-E Motorized Inverted Microscope) with a 60X Plan-Apochromat oil immersion objective.

Exocytosis and transferrin receptor recycling assays

To monitor release of FM1-43 as a measure of exocytosis, differentiated SH-SY5Y cells were incubated with 15 μM FM1-43 and depolarized with high KCl media (Hank's balanced salts medium with Ca^{2+} and Mg^{2+} plus 90 mM KCl and 63 mM NaCl) for 90s at room temperature. Unbound probe was removed by washing the cells with fresh saline solution for 10 min. Cells were washed twice with Hanks' balanced salts medium and re-incubated with depolarizing solution for 90 s at room temperature. FM1-43 retention is observed only cells with impaired exocytosis. The cells were then washed with Hanks' balanced salts medium, fixed with 4% paraformaldehyde for 10 min at room temperature and imaged by the MC02 Nikon Eclipse TE300 inverted microscope with the

METHODS

40X Plan-Fluor objective.

To monitor transferring receptor recycling, SH-SY5Y cells were plated on poly-D-lysine coated dishes (Mat-tek) and transfected with a plasmid expressing GFP-tagged transferrin receptor (gift from Dr. G.. Yudowski, UCSF, San Francisco). Cells were imaged in OptiMEM (UCSF Cell Culture Facility) without added serum and imaged using a Nikon TE-2000E inverted microscope with a 6 x 1.45 NA TIRF objective, equipped for through-the-objective TIRF illumination using a 488-nm argon laser focused on the periphery of the back focal plane as previously described (30). Data is presented as mean number of events/cell normalized to size of the cell with error bars representing SE of the mean.

Statistical analyses

Statistical analysis was performed using Prism 5 (GraphPad Software). Student's t test were run for pair wise comparisons between groups at a single condition, and ANOVA for repetitive measurements were run for pair wise comparisons between groups throughout multiple treatments or times. Significance P-values were *P< 0.05; **P<0.01; ***P<0.001.

REFERENCES

REFERENCES

Abeliovich A, Schmitz Y, Fariñas I, Choi-Lundberg D, Ho WH, Castillo PE, Shinsky N, Verdugo JM, Armanini M, Ryan A, Hynes M, Phillips H, Sulzer D, Rosenthal A (2000) Mice lacking alpha-synuclein display functional deficits in the nigrostriatal dopamine system. Neuron 25:239-252

Almeida CG, Takahashi RH, Gouras GK (2006) β-Amyloid accumulation impairs multivesicular body sorting by inhibiting the ubiquitin-proteasome system. J Neurosci 26: 4277-7288

Arrasate M, Finkbeiner, S (2005) Automated microscope system for determining factors that predict neuronal fate. Proc Natl Acad Sci USA 102:3840-3845.

Arrasate M, Mitra S, Schweitzer ES, Segal MR, Finkbeiner S (2004) Inclusion body formation reduces levels of mutant huntingtin and the risk of neuronal death. Nature 431:805-810.

Azeredo da Silveira S, Schneider BL, Cifuentes-Diaz C, Sage D, Abbas-Terki T, Iwatsubo T, Unser M, Aebischer P (2009) Phosphorylation does not prompt, nor prevent, the formation of alpha-synuclein toxic species in a rat model of Parkinson's disease. Hum Mol Genet 18: 872-887

Ben Gedalya T, Loeb V, Israeli E, Altschuler Y, Selkoe DJ, Sharon R (2009) Alpha-synuclein and polyunsaturated fatty acids promote clathrin-mediated endocytosis and synaptic vesicle recycling. Traffic 10:218-234

Bennett MK, Miller KG, Scheller RH (1993) Casein kinase II phosphorylates the synaptic vesicle protein p65. J Neurosci 13: 1701-1707

Betarbet R, Sherer TB, Greenamyre JT (2005) Ubiquitin-proteasome system and Parkinson's diseases. Exp Neurol 191 Suppl1:S17-27

Bonangelino CJ, Chavez EM, Bonifacino JS (2002) Genomic screen for vacuolar protein sorting genes in Saccharomyces cerevisiae. Mol Biol Cell 13:1486-2501

Braak H, Braak E (1991) Morphological changes in the human cerebral cortex in dementia. J. Hirnforsch 32: 277-282

Brachmann CB, Davies A, Cost GJ, Caputo E, Li J, Hieter P, Boeke JD (1998) Designer deletion strains derived from Sacchromyces cerevisiae S288C: a useful set of strains and plasmids for PCR-mediated gene disruption and other applications. Yeast 14: 115-132

REFERENCES

Cabin DE, Shimazu K, Murphy D, Cole NB, Gottschalk W, McIlwain KL, Orrison B, Chen A, Ellis CE, Paylor R, Lu B, Nussbaum RL (2002) Synaptic vesicle depletion correlates with attenuated synaptic responses to prolonged repetitive stimulation in mice lacking alpha-synuclein. J. Neurosci 22:8797-8807

Chandra S, Chen X, Rizo J, Jahn R, Sudhof, TC (2003). A broken alpha -helix in folded alpha-synuclein. The Journal of biological chemistry 278, 15313-15318.

Chandra S, Fornai F, Kwon HB, Yazdani U, Atasoy D, Liu X, Hammer RE, Battaglia G, German DC, Castillo PE, Sudhof TC (2004) Double-knockout mice for alpha- and beta-synucleins: effect on synaptic functions. Proc Natl Acad Sci USA 101:14966–14971

Chandra S, Gallardo G, Fernández-Chacón R, Schlüter OM, Südhof TC (2005) Alpha-synuclein cooperates with CSPalpha in preventing neurodegeneration. Cell 123:383-396

Chen DC, Yang BC, Kuo TT (1992) One-step transformation of yeast in stationary phase. Curr Genet 21: 83-84

Chen L, Feany MB (2005) Alpha-synuclein phosphorylation controls neurotoxicity and inclusion formation in a Drosophila model of Parkinson disease. Nat Neurosci 8: 657-663

Chiba-Falek O, Lopez GJ, Nussbaum RL (2006) Levels of alpha-synuclein mRNA in sporadic Parkinson disease patients. Mov Disord 21:1703-1708.

Chartier-Harlin MC, Kachergus J, Roumier C, Mouroux V, Douay X, Lincoln S, Levecque C, Larvor L, Andrieux J, Hulihan M, Waucquier N, Defebvre L, Amouyel P, Farrer M, Destee A (2004) Alpha-synuclein locus duplication as a cause of familiar Parkinson's Disease. Lancet 364: 1197-1169

Chau KY, Ching HL, Schapira AH, Cooper JM (2009) Relationship between alpha synuclein phosphorylation, proteasomal inhibition ad cell death: relevance to Parkinson's disease pathogenesis. J Neurochem 110: 1005-1013

Clayton DF, George JM (1998) The synucleins: a family of proteins involved in synaptic function, plasticity, neurodegeneration and disease. Trends in Neurosci 21:249-254.

Cole NB, Murphy DD, Grider T, Rueter S, Brasaemle D, Nussbaum RL (2002) Lipid droplet biding and oligomerization properties of the Parkinson's disease protein alpha-synuclein. J Biol Chem 277: 6344-6352

REFERENCES

Cookson MR, van der Brug M (2008) Cell systems and the toxic mechanism(s) of alpha-synuclein. Exp Neurol 209:5-11

Cooper AA, Gitler AD, Cashikar A, Haynes CM, Hill KJ, Bhullar B, Liu K, Xu K, Strathearn KE, Liu F, Cao S, Caldwell KA, Caldwell GA, Marsischky G, Kolodner RD, Labaer J, Rochet JC, Bonini NM, Lindquist S (2006) Alpha-synuclein blocks ER-Golgi traffic and Rab1 rescues neuron loss in Parkinson's models. Science 313:324-328

Cullen V, Lindfors M, Ng J, Paetau A, Swinton E, Kolodziej P, Boston H, Saftig P, Woulfe J, Feany MB, Myllykangas L, Schlossmacher MG, Tyynelä J (2009) Cathepsin D expression level affects alpha-synuclein processing, aggregation, and toxicity in vivo. Mol Brain 2:5

Dalfo E, Gomez-Isla T, Rosa JL, Nieto Bodelon M, Cuadrado Tejedor M, Barrachina M, Ambrosio S, Ferrer I (2004) Abnormal alpha-synuclein interactions with Rab proteins in alpha-SYNuclein A30P transgenic mice. J Neuropathol Exp Neurol 63: 302-313

Dalfo E, Ferrer I (2005) Alpha-synuclein binding to rab3a in multiple system atrophy. Neurosci Lett 380: 170-175

Darios F, Ruipérez V, López I, Villanueva J, Gutierrez LM, Davletov B (2010) Alpha-synuclein sequesters arachidonic acid to modulate SNARE-mediated exocytosis. EMBO 11:528-533

Davletov B, Sontag JM, Hata Y, Petrenko AG, Fykse EM, Jahn R, Sudhof TC (1993) Phosphorylation of synaptotagmin I by casein kinase II. J Biol Chem 268: 6816-6822

de Rijk MC, Launer LJ, Berger K, Breteler MM, Dartigues JF, Baldereschi M, Fratiglioni L, Lobo A, Martinez-Lage J, Trenkwalder C. (2000) Prevalence of Parkinson’s disease in Europe: A collaborative study of population-based cohorts. Neurologic diseases in the elderly research group. Neurology 54: S21-23

di Rosa G, Puzzo D, Sant’Angelo A, Trinchese F, Arancio O (2003) Alpha-synuclein: between synaptic function and dysfunction. Histol Histopathol 18: 1257-1266

El-Agnaf OM, Salem SA, Paleologou KE, Cooper LJ, Fullwood NJ, Gibson MJ, Curran MD, Court JA, Mann DM, Ikeda S, Cookson MR, Hardy J, Allsop D (2003) Alpha-synuclein implicated in Parkinson's disease is present in extracellular biological fluids, including human plasma. FASEB J 17:1945–1947.

El-Agnaf OM, Salem SA, Paleologou KE, Curran MD, Gibson MJ, Court JA, Schlossmacher MG, Allsop D (2006) Detection of oligomeric forms of alpha-

synuclein protein in human plasma as a potential biomarker for Parkinson's disease. FASEB J 20:419–425.

Emmanouilidou E, Melachroinou K, Roumeliotis T, Garbis SD, Ntzouni M, Margaritis LH, Stefanis L, Vekrellis K (2010) Cell-produced alpha-synuclein is secreted in a calcium-dependent manner by exosomes and impacts neuronal survival. J Neurosci 30:6838-6851

Faundez VV, Kelly RB (2000) The AP-3 complex required for endosomal synaptic vesicle biogenesis is associated with a casein kinase I alpha-like isoform. Mol Biol Cell 11: 2591-2604

Flower TR, Chesnokova LS, Froelich CA, Dixon C, Witt SN (2005) Heat shock prevents alpha-synuclein-induced apoptosis in a yeast model of Parkinson's disease. J Mol Biol 351: 1081-1100

Flower, T.R., Clark-Dixon, C., Metoyer, C., Yang, H., Shi, R., Zhang, Z. and Witt, S.N. (2007) YGR198w (YPP1) targets A30P alpha-synuclein to the vacuole for degradation. J. Cell Biol., 177, 1091-1104.

Forno LS, Norville RL (1976) Ultrastructure of Lewy bodies in the stellate ganglion. Acta Neuropath 34: 183-197

Fujita Y, Ohama E, Takatama M, Al-Sarraj S, Okamoto K (2006) Fragmentation of Golgi apparatus of nigral neurons with alpha-synuclein-positive inclusions in patients with Parkinson's disease. Acta Neuropathol 112:261-265

Fujiwara H, Hasegawa M, Dohmae N, Kawashima A, Masliah E, Goldberg MS, Shen J, Takio K, Iwatsubo T (2002) alpha-synuclein is phosphorylated in synucleinopathy lesions. Nat Cell Biol 4: 160-164

Garcia-Reitböck P, Anichtchik O, Bellucci A, Iovino M, Ballini C, Fineberg E, Ghetti B, Della Corte L, Spano P, Tofaris GK, Goedert M, Spillantini MG (2010) SNARE protein redistribution and synaptic failure in a transgenic mouse model of Parkinson's disease. Brain 133:2032-2044

Giaever G, Chu Am, Ni L, Connelly, C Riles L, Veronneau S, Dow S, Lucau-Danila A, Anderson K, Andre B et al (2002) Functional profiling of the Saccharomyces cerevisiae genome. Nature 418: 387-391

Giasson BI, Duda JE, Quinn SM, Zhang B, Trojanowski JQ, Lee VM. (2002) Neuronal alpha-synucleinopathy with severe movement disorder in mice expressing A53T human alpha-synuclein. Neuron 34: 521-533

REFERENCES

Gietz RD, Schiestl RH, Willems AR, Woods RA (1995) Studies on the transformation of intact yeast cells by the LiAc/SS-DNA/PEG procedure. Yeast 11: 355-360

Gillooly DJ, Raiborg C, Stenmark H (2003) Phosphatidylinositol 3-phosphate is found in microdomains of early endosomes. Histochem Cell Biol 120: 445-453

Gitler, A.D., Bevis, B.J., Shorter, J., Strathearn, K.E., Hamamichi, S., Su, L.J., Caldwell, K.A., Caldwell, G.A., Rochet, J.C., McCaffery, J.M. et al. (2008) The Parkinson's disease protein alpha-synuclein disrupts cellular Rab homeostasis. Proc. Natl. Acad. Sci. U. S. A., 105, 145-150.

Goedert M (2001) Alpha-synuclein and neurodegenerative diseases. Nat Rev Neurosci 2: 492-501

Goldberg MS, Lansbury PT Jr. (2000) Is there a cause-and-effect relationship between alpha-synuclein fibrillization and Parkinson's disease? Nat Cell Biol 2: E115-119

Gonatas NK, Stieber A, Gonatas JO (2006) Fragmentation of the Golgi apparatus in neurodegenerative diseases and cell death. J Neurol Sci 246:21-30

Gorbatyuk OS, Li S, Sullivan LF, Chen W, Kondrikova G, Manfredsson FP, Mandel RK, Muzyczka N (2008) The phosphorylation state of Ser129 in human alpha-synuclein determines neurodegeneration in a rat model of Parkinson disease. Proc Natl Acad Sci USA 105: 763-768

Gosavi N, Lee HJ, Lee JS, Patel S, Lee SJ (2002) Golgi fragmentation occurs in the cells with prefibrillar alpha-synuclein aggregates and precedes the formation of fibrillar inclusion. J Biol Chem 277:48984-48992

Griffioen G, Duhamel H, van Damme N, Pellens K, Zabrocki P, Pannecouque C, van Leuven F, Winderickx J, Wera S (2006) A yeast-based model of alpha-synucleionopathy identifies compounds with therapeutic potential. Biolchem Biophys Acta 1762: 312-318

Griffith J, Mari M, De Maziere A, Reggiori F (2008) A cryosectioning procedure for the ultrastrutural analysis and the immunogold labeling of yeast Saccharomyces cerevisiae. Traffic 9: 1060-1072

Hamamichi S, Rivas RN, Knight AL, Cao S, Caldwell KA, Caldwell GA (2008) Hypothesis-based RNAi screening identifies neuroprotective genes in a Parkinson's disease model. Proc Natl Acad Sci 105:728-733

Hansen LA, Daniel SE, Wilcock GK, Love S (1998) Frontal cortical synaptophysin in

Lewy body diseases: relation to Alzheimer's disease and dementia. J Neurol Neurosurg Psychiatry 64: 653-656

Hansen LA, Masliah E, Quijada-Fawcett S, Rexin D (1991) Entorhinal neurofibrillary tangles in Alzheimer's disease with Lewy bodies. Neurosci Lett 129: 269-272

Hayashida K, Oyanagi S, Mizutani Y, Yokochi M (1993) An early cytoplasmic change before Lewy body maturation: an ultrastructural study of the substantia nigra from an autopsy case of juvenile parkinsonism. Acta Neuropath 85: 445-448

Hirai Y, Fujita SC, Iwatsubo T , Hasegawa M (2004) Phosphorylated alpha-synuclein in normal mouse brain. FEBS Lett 572: 227-232

Hornykiewicz O (1998) Biochemical aspects of Parkinson's disease. Neurology 51: S2-9

Hurley JH, Emr SD (2006) The ESCRT complexes: structure and mechanism of a membrane-trafficking network. Annu Rev Biophys Biomol Struct 35:277-98

Inglis KJ, Chereau D, Bringham EF, Chiou SS, Schobel S, Frigon NL, Yu M, Caccavello RJ, Nelson S, Motter R, Wright S, Chian D, Santiago P, Soriano F, Ramos C, Powell K, Goldstein JM, Babcock M, Yednock T, Bard F, Basi GS, Sham H, Chilcote TJ, McConlogue L, Griswold-Prenner I, Anderson JP (2009) Polo-like kianse 2 (PLK2) phosphorylates alpha-synuclein at serine 129 in central nervous system. J Biol Chem 284: 2598-2602

Ishii A, Nonaka T, Taniguchi S, Saito T, Arai T, Mann D, Iwatsubo T, Hisanaga S, Goedert M, Hasegawa M (2007) Casein kinase 2 is the major enzyme in the brain that phosphorylates Ser129 of human alpha-synuclein: Implication for alpha-synucleinopathies. FEBS Lett 581: 4711-4717

Itakura E, Kishi C, Inoue K, Mizushima N (2008) Beclin 1 forms two distinct phosphatidylinositol 3-kinase complexes with mammalian Atg14 and UVRAG. Mol Biol Cell 19:5360-5372

Jakes R, Spillantini MG, Goedert M (1994) Identification of two distinct synucleins from human brain. FEBS letters 345: 27-32

Jenco JM, Rawlingson A, Daniels B, Morris AJ (1998). Regulation of phospholipase D2: selective inhibition of mammalian phospholipase D isoenzymes by alpha- and beta-synucleins. Biochemistry 37, 4901-4909.

Johnson EE, Overmeyer JH, Gunning WT, Maltese WA (2006) Gene silencing reveals a specific function of hVPS34 phosphatidylinositol 3-kinase in late versus early endosomes. J Cell Sci 119: 1219-1232

REFERENCES

Katzmann DJ, Stefan CJ, Babst M, Emr SD (2003) Vps27 recruits ESCRT machinery to endosomes during MVB sorting. J Cell BIol 162: 413-423

Kragh CL, Lund LB, Febbraro F, Hansen HD, Gai WP, El-Agnaf O, Richter-Landsberg C, Jensen PH (2009) alpha-synuclein aggregation and ser129 phosphorylation-dependent cell death in oligodendroglial cells. J Biol Chem 284: 10211-10222

Krantz DE, Peter D, Liu Y, Edwards RH (1997) Phosphorylation of a vesicular monoamine transporter by casein kinase II. J Biol Chem 272: 6752-6759

Krüger R, Kuhn W, Müller T, Woitalla D, Graeber D, Graeber M, Kösel S, Przuntek H, Epplen JT, Schöls L, Riess O (1998) Ala30Pro mutation in the gene encoding alpha-synuclein in Parkinson's disease. Nat Genet 18:106-108

Kuusisto E, Parkkinen L, Alafuzoff I (2003) Morphogenesis of Lewy bodies: dissimilar incorporation of alpha-synuclein, ubiquitin, and p62. Journal of neuropathology and experimental neurology 62: 1241-1253

Kuwahara, T., Koyama, A., Koyama, S., Yoshina, S., Ren, C.H., Kato, T., Mitani, S. and Iwatsubo, T. (2008) A systematic RNAi screen reveals involvement of endocytic pathway in neuronal dysfunction in alpha-synuclein transgenic C. elegans. Hum. Mol. Genet., 17, 2997-3009.

Lafourcade C, Galan J-M, Gloor Y, Haguenauer-Tsapis R, Peter M (2004) The GTPase-activating enzyme Gyp1p is required for recycling of internalized membrane material by inactivation of the Rab/Ypt GTPase Ypt1p. Mol Cell Biol 24: 3815-3826

Larsen KE, Schmitz Y, Troyer MD, Mosharov E, Dietrich P, Quazi AZ, Savalle M, Nemani V, Chaudhry FA, Edwards RH, Stefanis L, Sulzer D (2006) Alpha-synuclein overexpression in PC12 and chromaffin cells impairs catecholamine release by interfering with a late step in exocytosis. J Neurosci 26:11915-11922

Lee HJ, Patel S, Lee SJ (2005) Intravesicular localization and exocytosis of alpha-synuclein and its aggregates. J Neurosci 25:6016-6024

Lewis MJ, Nichols BJ, Prescianotto-Baschong C, Riezman H, Pelham HRB (2000) Specific retrieval of exocytic SNARE Snc1p from early yeast endosomes. Mol Biol Cell 11: 23-38

Liang J, Clark-Dixon C, Wang S, Flower TR, Williams-Hart T, Zweig R, Robinson LC, Tatchell K, Witt SN (2008) Novel suppressors of alpha-synuclein toxicity identified using yeast. Hum Mol Genet 17:3784-3795

REFERENCES

Lindersson E, Beedholm R, Højrup P, Moos T, Gai W, Hendil KB, Jensen PH (2004) Proteasomal inhibition by alpha-synuclein filaments and oligomers. J Biol Chem 279:12924-12934

Liu S, Ninan I, Antonova I, Battaglia F, Trinchese F, Narasanna A, Kolodilov N, Dauer W, Hawkins RD, Arancio O (2004) alpha-synuclein produces a long-lasting increase in neurotransmitter release. EMBO 23: 4506-4516

Lotharius J, Brundin P (2002) Pathogenesis of Parkinson's disease: dopamine, vesicles and alpha-synuclein. Nat Rev Neurosci 3: 932-942

Lucking CB, Brice A (2000) Alpha-synuclein and Parkinson's disease. Cell Mol Life Sci 57:1894–1908.

Luo Z, Gallwitz D (2003) Biochemical and genetic evidence for the involvement of yeast Ypt6-GTPase in protein retrieval to different Golgi compartments. J Biol Chem 278: 791-799

Maraganore DM, de Andrade M, Elbaz A, Farrer MJ, Ioannidis JP, Kruger R, Rocca WA, Schneider NK, Lesnick TG, Lincoln SJm HUlihan MM, Aasly JO, Ashizawa T, Chartier-Harlin MC, Checkoway H, Ferrarese C, Hadjigeorgiou G, Hattori N, Kawakami H, Lambert JC, Lynch T, Mellick GD, Papapetropoulos S, Parsian A, Quattrone A, Riess O, Tan EK, Van Broeckhoven C; Genetic Epidemiology of Parkinson's Disease (GEO-PD) Consortium. (2006) Collaborative analysis of alpha-synuclein gene promoter variability and Parkinson's disease. JAMA 296: 661-670

Marchal C, Haguenauer-Tsapis R, Urban-Grimal D (2000) Casein kinase I-dependent phosphorylation within a PEST sequence and ubiquitination at nearby lysines signal endocytosis of yeast uracil permease. J Biol Chem 275: 23608-23614

Marchal C, Dupre S, Urban-Grimal D (2002) Casein kinase I controls a late step in the endocytic trafficking of yeast uracil permease. J Cell Sci 115: 217-226

Mari M, Griffith J, Rieter E, Krisnappa L, Klionsky DJ, Reggiori F (2010) An Atg9-containing compartment functions in the early steps of autophagosome biogenesis. J Cell Biol in press

Masliah E Rockenstein E, Adame A, Alford M, Crews L, Hashimoto M, Seubert P, Lee M, Goldstein J, Chilcote T et al. (2005) Effects of alpha-synuclein immunization in a mouse model of Parkinson's disease. Neuron 46: 857-868

Masliah E, Rockenstein E, Veinbergs I, Mallory M, Hashimoto M, Takeda A, Sagara Y,

Sisk A, Mucke L (2000) Dopaminergic loss and inclusion body formation in alpha-synuclein mice: implications for neurodegenerative disorders. Science 287: 1265-1269

Masliah E, Rockenstein E, Veinbergs I, Sagara Y, Mallory M, Hashimoto M, Mucke L (2001) beta-amyloid peptides enhance alpha-synuclein accumulation and neuronal deficits in a transgenic mouse model linking Alzheimer's disease and Parkinson's disease. Proc Natl Acad Sci USA 98: 12245-12250

McFarland NR, Fan Z, Xu K, Schwarzschild MA, Feany MB, Hyman BT, McLean PJ (2009) Alpha-synuclein S129 phosphorylation mutants do not alter nigrostraiatal toxicity in a rat model of Parkinson disease. J Neuropathol Exp Neurol 68: 515-524

McKeith IG, Galasko D, Kosaka K, Perry EK, Dickson DW, Hansen LA, Salmon DP, Lowe J, Mira SS, Bryne EJ et al. (1996) Consensus guidelines for the clinical and pathological diagnosis of dementia with Lewy bodies (DLB): report of the consortium on DLB international workshop. Neurology 47: 1113-1124

Milne DM, Looby P, Meek DW (2001) Catalyti activity of protein kinase CK1 delta (casein kinase 1delta) is essential for its normal subcellular localization. Exp Cell Res 263: 43-54

Mizuta I, Satake W, Nakabayashi Y, Ito C, Suzuki S, Momose Y, Nagai Y, Oka A, Inoko H, Fukae J, Saito Y, Sawabe M, Murayama S, Yamamoto M, Hattori N, Murata M, Toda T (2006) Multiple candidate gene analysis identifies alpha-synuclein as a susceptibility gene for sporadic Parkinson's disease. Hum Mol Genet 15:1151-1158

Moore DJ, West AB, Dawson VL, Dawson TM (2005) Molecular pathophysiology of Parkinson's Disease. Annu Rev Neurosci 28:57-87

Morsomme P, Riezman H (2002) The Rab GTPase Ypt1p and thethering factors couple protein sorting at the ER to vesicle targeting to the Golgi apparatus. Dev Cell 2: 307-317

Mumberg D, Muller R, Funk M (1994) Regulatable promoters of *Sacchraomyces cerevisiae*: comparison of transcriptional activity and their use for heterologous expression. Nuclei Acids Res 22: 5767-5768

Mumberg D, Muller R, Funk M (1995) Yeast vectors for the controlled expression of heterologous proteins in different genetic backgrounds. Gene 156: 119-122

Murphy DD, Rueter SM, Trojanowski JQ, Lee VM (2000) Synucleins are developmentally expressed and alpha-synuclein regulates the size of presynaptic

vesicular pool in primary hippocampal neurons. J Neurosci 20: 3214-3220

Myhre R, Toft M, Kachergus K, Hulihan MM, Aasly JO, Lungland H, Farrer MJ (2008) Multiple alpha-synuclein gene polymorphisms are associated with Parkinson's disease in a Noregian population. Acta Neurol Scand. 118: 320-327

Okochi M, Walter J, Koyama A, Nakajo S, Baba M, Iwatsubo T, Meijer L, Kahle PJ, Haass C (2000) Constitutive phosphorylation of the Parkinson's disease associated alpha-synuclein. J. Biol Chem 275: 390-397

Olanow CW (2004) The scientific basis for the current treatment of Parkinson's disease. Ann Rev Med 55: 41-60

Nakamura N, Yamamoto A, Wada Y, Futai M (2000) Syntaxin 7 mediates endocytic trafficking to late endosomes. J Biol Chem 275: 6523-6529

Nakamura S, Kawamoto Y, Nakano S, Akiguchi I (2000) Expression of the endocytosis regulatory proteins Rab5 and Rabaptin-5 in glial cytoplamic inclusions from brains with multiple system atrophy. Clin Neuropathol 19: 51-56

Nemani VM, Lu W, Berge V, Nakamura K, Onoa B, Lee MK, Chaudhry FA, Nicoll RA, Edwards RH (2010) Increased expression of alpha-synuclein reduces neurotransmitter release by inhibiting synaptic vesicle reclustering after endocytosis. Neuron 65:66-79

Novik P, Field C, Schekman R (1980) Identification of 23 complementation groups required for post-translational events in the yeast secretory pathway. Cell 21: 205-215

Panek HR, Conibear E, Bryan JD, Colvin RT, Goshorn CD, Robinson LC (2000) Identification of Rgp1p, a novel Golgi recycling factor, as a protein reqired for efficient localization of yeast ceasein kinase 1 to the plama membrane. J Cell Sci 113 pt 24: 4545-4555

Polymeropoulos MH, Lavedan C, Leroy E, Ide SE, Dehejia A, Dutra A, Pike B, Root H, Rubenstein J, Boyer R, Stenroos ES, Chandrasekharappa S, Athanassiadou A, Papapetropoulos T, Johnson WG, Lazzarini AM, Duvoisin RC, Di Iorio G, Golbe LI, Nussbaum RL (1997) Mutation in the alpha-synuclein gene indentified in families with Parkinson's disease. Science 276: 2045-2047

REFERENCES

Presgraves SP, Ahmed T, Borwege S, Joyce JN (2004) Terminally differentiated SH-SY5Y cells provide a model system for studying neuroprotective effects of dopamine agonists. Neurotox Res. 5:579-598

Pronin AN, Morris AJ, Surguchov A, Benovic JL (2000) Synucleins are a novel class of substrates for G protein-coupled receptor kinases. J Biol Chem 387: 149-152

Qing H, Wong W, McGeer EG, McGeer PL (2009) Lrrk2 phosphorylates alpha-synuclein at serine 129: Parkinson disease implications. Biochem Biophys Res Commun 387: 149-152

Ramirez A, Heimbach A, Gründemann J, Stiller B, Hampshire D, Cid LP, Goebe I, Mubaidin AF, Wriekat AL, Roeper J, Al-Din A, Hillmer AM, Karsak M, Liss B, Woods CG, Behrens MI, Kubisch C (2006) Hereditary parkinsonism with dementia is caused by mutations in ATP13A2, encoding a lysosomal type 5 P-type ATPase. Nat Genet 38:1184-1191

Reggiori F, Black MW, Pelham HR (2000) Polar transmembrane domains target proteins to the interior of the yeast vacuole. Mol Biol Cell 11: 3737-3749

Reggiori F, Pelha, HR (2001) Sorting of proteins into multivesicular bodies: ubiquitin-dependent and –independent targeting. EMBO J. 20: 5176-5186

Robinson JS, Klionsky DJ, Banta LM and Emr SD (1988) Protein sorting in Saccharomyces cerevisiae: isolation of mutants defective in the delivery and processing of multiple vacuolar hydrolases. Mol Cell Biol, 8, 4936–4948.

Rockenstein E, Mallory M, Hashimoto M, Song D, Shults CW, Lang I, Masliah E (2002) Differential neuropathological alterations in transgenic mice expressing alpha-synuclein from the platelet-derived growth factor and Thy-1 promoters. J Neurosci Res 68: 568-578

Rockenstein E, Mallory M, Mante M, Sisk A, Masliah E (2001) Early formation of mature amyloid-beta protein deposits in a mutant APP transgenic model depends on levels of Abeta (1042). J Neurosci Res 66: 573-582

Rose K, Rudge SA, Frohman MA, Morris AJ, Engebrecht J (1995) Phospholipase D signaling is essential for meiosis. Proc Natl Acad Sci USA 92: 12151-12155

REFERENCES

Ross GW, Petrovitch H. (2001) Current evidence for neuroprotective effects of nicotine and caffeine against Parkinson's disease. Drugs Aging 18: 797-806

Rothman JH, Howald I, Stevens TH (1989) Characterization of genes required for protein sorting and vacuolar function in the yeast Saccharomyces cerevisiae. EMBO J, 8, 2057–2065.

Ruan Q, Harrington AJ, Caldwell KA, Caldwell GA, Standaert DG (2010) VPS41, a protein involved in lysosomal trafficking, is protective in Caenorhabditis elegans and mammalian cellular models of Parkinson's disease. Neurobiol Dis 37:330-338

Saito T, Guan F, Papolos DF, Rajouria N, Fann CS, Lachman HM (2001) Polymorphism in SNAP29 gene promoter region associated with schizophrenia. Mol Psychiatry 6: 193-201

Sakamoto M, Arawaka S, Hara S, Sato H, Cui C, Machiya Y, Koyama S, Wada M, Kawanami T, Kurita K, Kato T (2009) Contribution of endogenous G-protein-coupled receptor kinases to Ser129 phosphorylation of alpha-synuclein in HEK293 cells. Biochem Biophys Res Commun 384: 378-382

Schmitt-John T, Drepper C, Mussmann A, Hahn P, Kuhlmann M, Thiel C, Hafner M, Lengeling A, Heimann P, Jones JM, Meisler MH, Jockusch H (2005) Mutation of Vps54 causes motor neuron disease and defective spermiogenesis in the wobbler mouse. Nat Genet 37:1213-1215

Scott DA, Tabarean I, Tang Y, Cartier A, Masliah E, Roy S (2010) A pathologic cascade leading to synaptic dysfunction in alpha-synuclein-induced neurodegeneration. J Neurosci 30: 8083-8095

Shin Y, Klucken J, Patterson C, Hyman BT, McLean PJ (2005) The co-chaperone carboxyl terminus of Hsp70-interacting protein (CHIP) mediates alpha-synuclein degradation decisions between proteasomal and lysosomal pathways. J Biol Chem 280:23727-23734

Sidhu A, Wersinger C, Moussa CE, Vernier P (2004) The role of alpha-synuclein in both neuroprotection and neurodegeneration. Ann N Y Acad Sci 1035: 250-270

REFERENCES

Sikorski RS, Hieter P (1989) A system of shuttle vectors and yeast host strains designed for efficient manipulation of DNA in Sacchromyces cerevisiae. Genetics 122: 19-27

Simonsen A, Lippe R, Christoforidis S, Gaullier JM, Brech A, Callaghan J, Toh BH, Murphy C, Zerial M, Stenmark H (1998) EEA1 links PI(3)K function to Rab5 regulation of endosome fusion. Nature 394: 494-498

Singleton AB, Farrer M, Johnson J, Singleton A, Hague S, Kachergus J, Hulihan M, Peuralinna T, Dutra A, Nussbaum R, Lincoln S, Crawley A, Hanson M, Maraganore D, Adler C, Cookson MR, Muenter M, Baptista M, Miller D, Blancato J, Hardy J,Gwinn-Hardy K (2003) alpha-synuclein locus triplication causes Parkinson's disease. Science 302: 841

Skibinski G, Parkinson NJ, Brown JM, Chakrabarti L, Lloyd SL, Hummerich H, Nielsen JE, Hodges JR, Spillantini MG, Thusgaard T, Brandner S, Brun A, Rossor MN, Gade A, Johannsen P, Sorensen SA, Gydesen S, Fisher EMC, Collinge J (2005) Mutations in the endosomal ESCRTIII-complex subunit CHMP2B in frontotemporal dementia. Nat Genet. 37: 806–8

Slot JW, Geuze HK (2007) Cryosectioning and immunolabeling. Nat Protoc 2: 2480-2491

Soper, J.H., Roy, S., Stieber, A., Lee, E., Wilson, R.B., Trojanowski, J.Q., Burd, C.G. and Lee, V.M. (2008) Alpha-SYNuclein-induced aggregation of cytoplasmic vesicles in Saccharomyces cerevisiae. Mol. Biol. Cell, 19, 1093-1103.

Sotiriou S, Gibney G, Baxevanis AD, Nussbaum RL (2009) A single nucleotide polymorphism in the 3'UTR of the SNCA gene encoding alpha-synuclein is a new potential susceptibility locus for Parkinson's disease. Neurosci Lett. 461: 196-201

Spillantini MG, Schmidt ML, Lee VM, Trojanowski JQ, Jakes R, Goedert M (1997) Alpha-synuclein in Lewy bodies. Nature 388: 839-840

Sprecher E, Yamamoto-Ishida A, Mizrahi-Koren M, Rapaport D, Godsher D, Indelman M, Topaz O, Chefetz A, Keren H, O'Brien TJ, Bercovich D, Shalev S, Geiger D, Bergman R, Horowitz M, Mandel H (2005) A mutation in SNAP29, coding for a SNARE protein involved in intracellular trafficking, causes a novel neurocutaneous syndrome characterized by cerebral dysgenesis, neuropathy, ichthyosis, and palmoplantar keratoderma. Am J Hum Genet 77: 242-251

Stenmark H, Olkkonen VM (2001) The Rab GTPase family. Genome biology 2:

REVIEWS3007

Stenmark H, Parton RG, Steele-Mortimer O, Lutcke A, Gruenberg J, Zerial M (1994) Inhibition of Rab5 GTPase activity stimulates membrane fusion in endocytosis. EMBO J 13: 1287-1296

Thayanidhi N, Helm JR, Nycz DC, Bentley M, Liang Y, Hay JC (2010) alpha-synuclein delays endoplasmic reticulum (ER)-to-Golgi transport in mammalian cells by antagonizing ER/Golgi SNAREs. Mol Biol Cell 21:1850-1863

Thomas BJ, Rothstein R (1989) The genetic control of direct-repeat recombination in Saccharomyces: the effect of rad52 and rad1 on mitotic recombination at GAL10, a transcriptionally regulated gene. Genetics 123: 725-738

Tintner R, Jankovic J (2002) Treatment options for Parkinson's disease. Curr Op Neurol 15: 467-476

Tong AH, Evangelista M, Parsons AB, Xu H, Bader GD, Page N, Robinson M, Raghibizadeh S, Hogue CW, Bussey H et al. (2001) Systematic genetic analysis with ordered arrays of yeast deletion mutants. Science 294: 2364-2368

Waxman EA, Giasson BI (2008) Specificity and regulation of casein kinase-mediated phosphorylation of alpha-synuclein. J Neuropathol Exp Neurol 67: 402-416

Willingham S, Outeiro TF, DeVit MJ, Lindquist SL, Muchowski PJ (2003) Yeast genes that enhance the toxicity of a mutant huntingtin fragment or alpha-synuclein. Science 302: 1769-1772

van der Putten H, Wiederhold KH, Probst A, Barbieri S, Mistl C, Danner S, Kauffmann S, Hofele K, Spooren WP, Ruegg MA (2000) Neuropathology in mice expressing human alpha-synuclein. J Neurosci 20: 6021-6029

van der Sluijs P, Hull M, Webster P, Male P, Goud B, Mellman I (1992) The small GTP-binding protein rab4 controls an early sorting event on the endocytic pathway. Cell 70: 729-740

van Ham TJ, Thijssen KL, Breitling R, Hofstra RM, Plasterk RH, Nollen EA (2008) *C. elegans* model identifies genetic modifiers of alpha-SYNuclein inclusion formation during aging. PLoS Genet 4:e1000027

van Niel G, Porto-Carreiro I, Simoes S, Raposo G (2006) Exosomes: A common pathway for a specialized function. J Biochem 140:13-21

Vanitallie TB (2008) Parkinson's disease: primacy of age as a risk factor for

mitochondrial dysfunction. Metabolism 57 Suppl 2:S50-55

Veal EA, Ross SJ, Malakasi P, Peacock E, Morgan BA (2003) Ybp1 is required for the hydrogen peroxide-induced oxidation of the Yap1 transcription factor. J Biol Chem 278: 30896-30904

Vekrellis K, Xilouri M, Emmanouilidou E, Stefanis L (2009) Inducible over-expression of wild type alpha-SYNuclein in human neuronal cells leads to caspase-dependent non-apoptotic death. J Neurochem 109: 1348-1362

Vella LJ, Sharples RA, Nisbet RM, Cappai R, Hill AF (2008) The role of exosomes in the processing of proteins associated with neurodegenerative diseases. Euro Biophys J 37:323-332

Ventruti A, Cuervo AM (2007) Autophagy and neurodegeneration. Curr Neurol Neurosci Rep 7:443-51

Vogiatzi T, Xilouri M, Vekrellis K, Stefanis L (2008) Wild type alpha-SYNuclein is degraded by chaperone-mediated autophagy and macroautophagy in neuronal cells. J Biol Chem 283:23542-23556

Volles MJ, Lee SJ, Rochet JC, Shtilerman MD, Ding TT, Kessler KC, Lansbury PT Jr. (2001) Vesicle permeabilizatino by protofibrillar alpha-ynuclein: implications for the pathogenesis and treatment of Parkinson's disease. Biochem 40: 7812-7819

Volles MJ, Lansbury PT Jr. (2002) Vesicle permeabilization by protofibrillar alpha-synuclein is sensitive to Parkinson's disease-linked mutations and occurs by a pore-like mechanism. Biochem 41: 4595-4602

Watanabe E, Vachal E, Tomita T (1977) Dense core vesciles around the Lewy body in incidental Parkinson's disease: an electron microscopic study. Acta Neuropath 2" 173-175

Watanabe I, Vachal E, Tomita T (1977) Dense core vesicles around the Lewy body in incidental Parkinson's disease: an electron microscopic study. Acta Neuropathol 39: 173-175

Witt SN, Flower TR (2006) alpha-synuclein, oxidative stress and apoptosis from the perspective of a yeast model of Parkinson's disease. FEMS Yeast Res 6: 1107-

1116

Yasojima K, Kuret J, DeMaggio AJ, McGreer E, McGeer PL (2000) Casein kinase 1 delta mRNA is upregulated in Alzheimer disease brain. Brain Res. 865: 116-120

Yu S, Roth MG (2002) Casein kinase I regulates membrane binding by ARF GAP1. Mol Biol Cell 13: 2559-2570

Yudowski GA, Puthenveedu MA, von Zastrow M (2006) Distinct modes of regulated receptor insertion to the somatodendritic plasma membrane. Nat Neurosci 9:622-627

Zabrocki, P., Bastiaens, I., Delay, C., Bammens, T., Ghillebert, R., Pellens, K., De Virgilio, C., Van Leuven, F. and Winderickx, J. (2008) Phosphorylation, lipid raft interaction and traffic of alpha-synuclein in a yeast model for Parkinson. Biochim. Biophys. Acta, 1783, 1767-1780.

Zarranz JJ, Alegre J, Gomez-Esteban KC, Lezcano E, Ros R, Ampuero I, Vidal L, Hoenicka J, Rodriguez O, Atares B (2004) The new mutation, E46K, of alpha-SYNuclein causes Parkinson and Lewy body dementia. Ann Neurol ff: 164-173

Zhang Y, Zolov SN, Chow CY, Slutsky SG, Richardson SC, Piper RC, Yang B, Nau KK, Westrick RJ, Morrison SJ, Meisler MH, Weisman LS (2007) Loss of Vac14, a regulator of the signaling lipid phosphatidylinositol 3,5-bisphosphate, results in neurodegeneration in mice. Proc Natl Acad Sci 104: 17518-17523

Zhou X, Wang L, Hasegawa H, Amin P, Han BX, Kaneko S, He Y, Wang F. (2010) Deletion of PIK3C3/Vps34 in sensory neurons causes rapid neurodegeneration by disrupting the endosomal but not the autophagic pathway. Proc Natl Acad Sci 107:9424-9429

PUBLISHING AGREEMENT

I hereby grant permission to the Graduate Division of the University of California, San Francisco to release copies of my thesis, dissertation, or manuscript to the Campus Library to provide access and preservation, in whole or in part, in perpetuity.

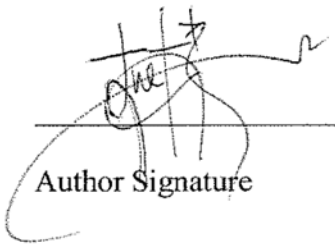

Author Signature

9/7/10

Date